ABSTRACT

Dendritic Cell Targeting Vaccines for HPV-Associated Malignancies and Prostate Cancer

Wenjie Yin, Ph.D.

Mentor: SangKon Oh, Ph.D.

Dendritic cells (DCs) are major antigen-presenting cells (APCs) that are able to capture, process and cross-present antigens to $CD8^+$ T cells. $CD8^+$ T cells play key roles in host immunity to cancers by efficiently killing tumor cells. DC-based immunotherapeutic strategies against cancers have thus been well rationalized. The first generation of DC vaccine, reinfusion of tumor-associated antigen (TAA)-loaded autologous *in vitro* generated DCs, is safe, but the clinical efficacy of this type of vaccine has been limited. In addition to cost, most importantly, *in vitro* generated DCs are not the same as the DCs *in vivo*. We have thus employed a DC-targeting vaccine strategy, in the form of recombinant fusion proteins composed of TAA and monoclonal antibody (mAb) specific to DC surface receptors. However, critical questions have remained for the rational design of DC targeting vaccines against cancers. First, we need to determine which targeted receptors can result in the greatest $CD8^+$ T cell responses. Second, we have to demonstrate that prototype vaccines designed to target selected receptors meet the requirements to be tested in patients.

In this study, we compared antigen-specific $CD4^+$ and $CD8^+$ T cell responses elicited by DCs targeted with mAb-antigen fusion proteins via 11 different DC surface receptors. We found that targeting antigens to DCs via CD40 primed and activated the greatest levels of antigen-specific naïve and memory $CD8^+$ T cells, respectively. We then generated prototype DC-targeting vaccines for human papilloma virus (HPV)-associated cancer, αCD40-HPV16.E6/7, and for prostate cancer, αCD40-PSA (prostate-specific antigen). We demonstrated that αCD40-HPV16.E6/7 could activate HPV16.E6/7-specific $CD4^+$ and $CD8^+$ T cells from $HPV16^+$ head-and-neck cancer patients. αCD40-HPV16.E6/7 was also immunogenic in human CD40 transgenic (hCD40Tg) mice and could thus prevent and suppress the growth of TC-1 tumor cells expressing HPV16.E6/7 protein. In addition, αCD40-PSA was also able to prime and activate PSA-specific T cells from prostate cancer patients. We demonstrated that αCD40-PSA could induce PSA-specific $CD4^+$ and $CD8^+$ T cell responses in hCD40Tg mice. Therefore, this dissertation offers a proof-of-concept that tumor antigen delivery to DCs through CD40 can be an effective immunotherapeutic strategy for cancer patients.

Dendritic Cell Targeting Vaccines for HPV-Associated Malignancies and Prostate Cancer

by

Wenjie Yin, B.S., M.S.

A Dissertation

Approved by the Institute of Biomedical Studies

_____

Robert R. Kane, Ph.D., Director

Submitted to the Graduate Faculty of Baylor University in Partial Fulfillment of the Requirements for the Degree of

Doctor of Philosophy

Approved by the Dissertation Committee

_____

SangKon Oh, Ph.D., Chairperson

_____

HyeMee Joo, Ph.D.

_____

Robert R. Kane, Ph.D.

_____

Christopher M. Kearney, Ph.D.

_____

Joseph H. Taube, Ph.D.

_____

Gerard Zurawski, Ph.D.

Accepted by the Graduate School

December 2015

_____

J. Larry Lyon, Ph.D., Dean

Page bearing signatures is kept on file in the Graduate School.

TABLE OF CONTENTS

LIST OF FIGURES

LIST OF TABLES

LIST OF ABBREVIATIONS

ANOVA	analysis of variance
APC	antigen-presenting cell
CaP	prostate cancer
CCL	chemokine C-C motif ligand
CCR	chemokine C-C motif receptor
CD	cluster of differentiation
CD40L	CD40 ligand
cDC	classical/conventional dendritic cell
CFSE	carboxyfluorescein succinimidyl ester
CHO	Chinese hamster ovary
CLEC	C-type lectin
Coh	cohesin
CRPC	castration-resistant prostate cancer
CTL	cytotoxic T lymphocyte
CTLA-4	cytotoxic T-lymphocyte-associated protein 4
DC	dendritic cell
DC-ASGPR	DC-asialoglycoprotein receptor
DC-SIGN/L	DC-/lymph node-specific ICAM3-grabbing non-integrin
DCIR	dendritic cell inhibitory receptor
dDC	dermal dendritic cell
Dectin-1	dendritic-cell-associated C-type lectin-1

Doc	dockerin
EEA1	early endosome antigen 1
ELISA	enzyme-linked immunosorbent assay
ELISpot	enzyme-linked immunospot
EpCAM	epithelial cell adhesion molecule
ER	endoplasmic reticulum
ESAM	endothelial cell-specific adhesion molecule
Fc	fragment crystallizable
FcγR	Fc receptor for immunoglobulin G
FDA	Food and Drug Administration
Flt3	Fms-like tyrosine kinase 3
Flt3L	Flt3 ligand
Flu.HA1	influenza type A virus hemagglutinin subunit 1
Flu.M1	influenza type A virus matrix protein
Flu.NP	influenza type A virus nucleoprotein
GM-CSF	granulocyte macrophage colony-stimulating factor
GMP	good manufacturing practice
HLA	human leukocyte antigen
HPV	human papillomavirus
HRP	horseradish peroxidase
i.m.	intramuscular(ly)
i.p.	intraperitoneal(ly)
IFN	interferon

IL	interleukin
JaCoP	Just another Colocalization Plugin
LAMP-1	lysosomal-associated membrane protein 1
LC	Langerhan cell
LN	lymph node
LOX-1	lectin-like oxidized low-density lipoprotein receptor 1
M-CSF	macrophage colony-stimulating factor
mAb	monoclonal antibody
MARCO	macrophage receptor with collagenous structure
MART-1	melanoma-associated antigen recognized by T cells 1
mDC	myeloid dendritic cell
MHC	major histocompatibility complex
MIIC	MHC class II compartment
Mo-DC	monocyte-derived dendritic cell
MyD88	myeloid differentiation primary response 88
NHP	non-human primate
OD	optical density
PAMP	pathogen-associated molecular pattern
PAP	prostatic acid phosphatase
PBMC	peripheral blood mononuclear cell
PBS	phosphate-buffered saline
PD-1	programmed cell death protein 1
pDC	plasmacytoid dendritic cell

PHA	phytohemagglutinin
PMA	phorbol 12-myristate 13-acetate
Poly(I:C)	polyinosinic:polycytidylic acid
pRB	retinoblastoma protein
PRR	pattern recognition receptor
PSA	prostate-specific antigen
RIG-I	retinoic acid-inducible gene
s.c.	subcutaneous(ly)
SD	standard deviation
SSC	squamous cell carcinoma
TAA	tumor-associated antigen
TAP	transporter associated with antigen processing
TCR	T cell receptor
TDLN	tissue-draining lymph node
Tfh	follicular helper T cell
Th1/2/17	type 1/2/17 helper T cell
TMB	3,3',5,5'-tetramethylbenzidine
TNF	tumor necrosis factor
TNFR Cys	tumor necrosis factor receptor cysteine-rich region
WT	wild type
XCL	chemokine X-C motif ligand
XCR	chemokine X-C motif receptor

ACKNOWLEDGMENTS

It has finally come to this moment. I want to, first and foremost, thank my mentor, Dr. SangKon Oh, for providing all the mentorship and encouragement throughout my four years' laboratory life in pursuit of the Ph.D. It really has been a wonderful time doing research with him. I have seen and learned many qualities that a good scientist should have by working with him. I believe that I will benefit from those good qualities in my future career, regardless of what I actually will be doing.

I would also like to thank my committee members, Drs. HyeMee Joo, Robert R. Kane, Christopher M. Kearney, Joseph H. Taube and Gerard Zurawski, for all their sincere guidance and insightful comments and suggestions.

My thanks also go to all of the current and past Oh laboratory members. Thank you to Dr. Dorothée Duluc for showing me how to efficiently design and execute work plans. It was a fun time working on mouse projects together. Thank you to Dr. HyeMee Joo again, for teaching me basically all the mouse-related experiment techniques. Thank you to Drs. Ling Ni and Dapeng Li for teaching me the basic experiment techniques and helping me adapt to the new laboratory life when I first joined. Thank you to Yaming Xue for the all-year long technical and mental support. Thank you to Chao Gu, Dr. Richard Ouedraogo and Lei Wang for the help in mouse-related projects and the often excellent discussions on research projects. Thank you to Katherine C. Upchurch and Sandra Clayton for carefully reading my manuscripts and dissertation and providing critical comments and suggestions. Thank you to Jerome Ellis for the assistance in Luminex.

I also want to thank Zhiqing Wang, Dr. Xiao-Hua, Li and Sandy Zurawski for constantly providing fusion proteins and protein conjugates. Thank you to Dr. LuAnn Thompson-Snipes for meticulously screening and maintaining the transgenic mice. Thank you to Dr. Clay Beauregard for coordinating research projects. Thank you to Drs. Anne-Laure Flamar and Monica Montes for demonstrating experiment techniques in non-human primate samples. Thank you to Shiying Bian and Dr. Luz S. Muniz for the help in recruiting patients and procuring blood samples. Thank you to Drs. Andrew Sikora and Lance Oxford for acquiring patient samples. Thank you to Kay Kayembe and Elizabeth M. Lavecchio of the Flow Cytometry SRL for providing assistance in cell sorting. Thank you to Dr. Carson Harrod for the general guidance in Journal Club. Thank you to Cindy Samuelson, Angela M. Plata, Pamela W. Jennings and Hermila Crear of Baylor Institute for Immunology Research, and Rhonda S, Bellert of Baylor University for the administrative support throughout. Thank you to Drs. Te-Chia Wu, Kangling Xu and Yuanyuan Wang for providing help in various stages of my life as a Ph.D. student.

Last but not least, I want to express my sincere appreciation to my parents. Without their continued support, encouragement and love, I would not have achieved what I have today. I hope that my parents are proud of me, and I am eternally grateful to them.

It has been an eventful and meaningful time with all the people I have worked with at Baylor. I thank everyone that has helped me.

CHAPTER ONE

Introduction

The Biology of Dendritic Cells

Dendritic cells (DCs) are major antigen-presenting cells (APCs) that are highly capable of processing and presenting both extracellular and intracellular antigens to T cells in the form of major histocompatibility complex (MHC) class I- or II-peptide complex, initiating antigen-specific immune responses. DCs also sense environmental danger signals, including pathogen-associated molecular patterns (PAMPs), through various pattern-recognition receptors (PRRs), and alert the innate immune system. The multifaceted nature of DCs effectively puts them at the interface of innate and adaptive immunity. However, due to the inherent complexity of DCs, including their origin, development, migration pattern, activation status, and their intricate surrounding microenvironment, these particular APCs subsets are composed of distinct subsets that are able to function differentially, resulting in immune responses of different quality and magnitudes. Studies on mouse models have led to a far deeper understanding of mouse DC network than that of their human counterparts. Although discrepancies in the DC systems between the two species exist, specific human and mouse DC subsets share similarities in many of the key functional aspects. This part of the introduction focuses on several the well-characterized human and mouse DC subsets and their specialized functions.

Plasmacytoid Dendritic Cells and Classical Dendritic Cells

Plasmacytoid dendritic cells. Plasmacytoid dendritic cells (pDCs) are a unique DC subset which are the major source of type I interferons (IFNs) (Cella et al., 1999; Siegal et al., 1999). They are present in the blood and lymphoid tissues and are a main driver of the innate antiviral immunity by responding to viruses through the recognition of nucleic acids with Toll-like receptor (TLR7) and TLR9 (Blasius and Beutler, 2010; Gilliet et al., 2008). It has been also reported that pDCs promote NK cell activation through the secretion of pro-inflammatory cytokines (Conry et al., 2009). However, pDCs can also promote a plethora of adaptive immune responses, including antigen presentation (Villadangos and Young, 2008), immune regulation (Guéry and Hugues, 2013), T-cell polarization and immune cell recruitment (Cervantes-Barragan et al., 2012; Persson and Chambers, 2010), and B-cell immunity (Jego et al., 2003). In general, human and mouse pDCs share a lot phenotypic and functional similarities (Hochrein et al., 2002).

Classical dendritic cells. Classical dendritic cells (cDCs), previously known as myeloid DCs (mDCs), encompass all DCs other than pDCs. cDCs are a group of highly heterogenous DCs that differ in their localization, phenotype, and functions. Nonetheless, cDCs populate most lymphoid and non-lymphoid tissues and possess an enhanced ability to constantly acquire blood and tissue antigens. By presenting processed exogenous or autologous antigens to T cells in the lymph node (LNs), cDCs can efficiently prime and activate antigen-specific $CD4^+$ and/or $CD8^+$ T cells. So far, at least five major human cDC subsets have been identified and extensively studied. Along with pDCs, major

human cDCs and their phenotypic markers, PRRs expressed, mouse equivalent, and general locations are shown in Figure 1 (Merad et al., 2013).

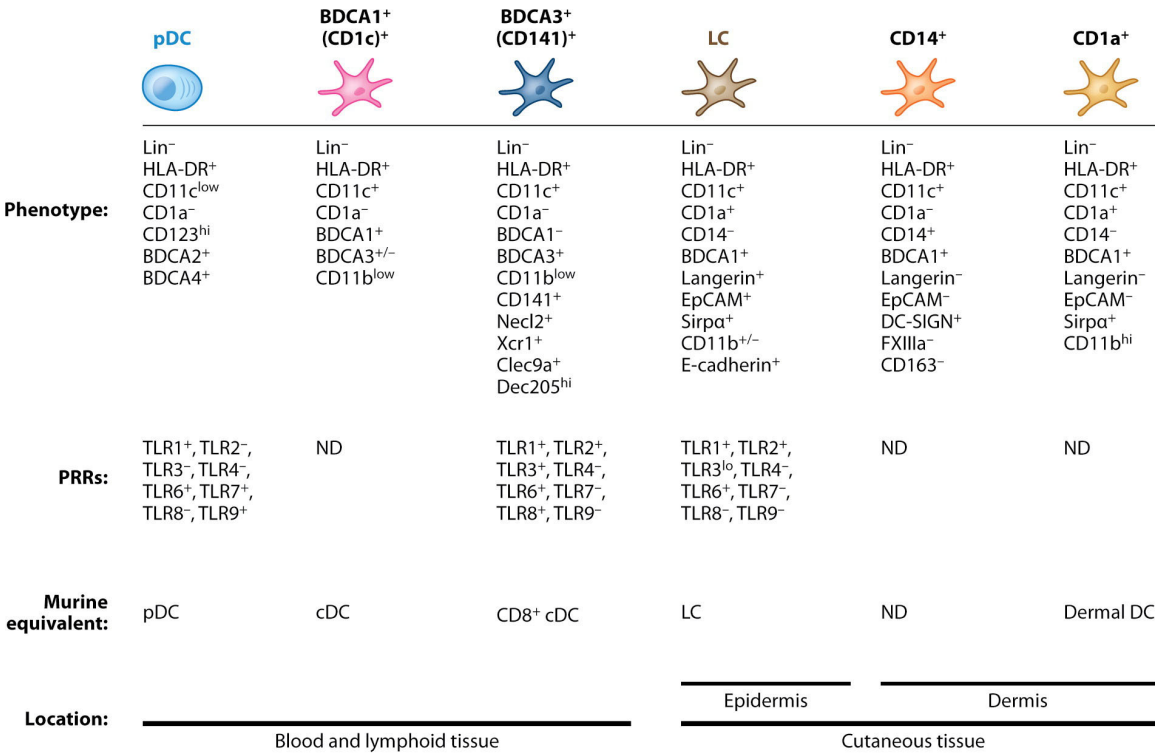

Figure 1. Major human DC subsets, their phenotypes, PRRs expressed, murine equivalents and locations. Adapted from Merad et al., 2013.

Subsets of Mouse Classical Dendritic Cells and Their Specialized Functions

The main mouse cDC subsets consist of lymphoid tissue cDCs, including $CD8^+$ and $CD11b^+$ cDCs, non-lymphoid tissue cDCs, including $CD103^+CD11b^-$, $CD103^-$ $CD11b^+$, and $CD103^+CD11b^+$ intestinal cDC, and Langerhans cells (LCs).

Lymphoid resident cDCs. Lymphoid resident cDCs include $CD8^+$ cDCs and $CD11b^+$ cDCs. $CD8^+$ cDCs express $CD8\alpha^+$, but no or low levels of CD11b. In addition, $CD8\alpha^+$ cDCs differentially express lectins receptors, including CD205, Clec9A, and

langerin (Crowley et al., 1989; Jiang et al., 1995). $CD8^+$ cDCs have been known to efficiently cross-present antigen and stimulate $CD8^+$ T cell-mediated immunity (Zelenay et al., 2012), as well as secrete high levels of interleukin (IL)-12, promoting type 1 T helper (Th1) cell differentiation (Edelson et al., 2010; Hildner et al., 2008; Mashayekhi et al., 2011). $CD11b^+$ cDCs, on the other hand, do not express $CD8\alpha^+$, and are the dominant lymphoid-resident cDC population in all lymphoid organs, except the thymus. $CD11b^+$ cDCs in the spleen can be further divided into two subpopulations based on the expression of endothelial cell-specific adhesion molecule (ESAM). The two $CD11b^+$ splenic cDC subpopulations are thought to have different precursors, with $ESAM^{hi}CD11b^+$ cDCs derived from DC-restricted precursors, and $ESAM^{lo}CD11b^+$ cDCs from circulating monocytes (Lewis et al., 2011). Both $CD8^+$ cDCs and $CD11b^+$ cDCs are dependent on the receptor Fms-like tyrosine kinase 3 (Flt3) and proliferate in response to Flt3-Flt3 ligand (Flt3L) ligation (Hieronymus et al., 2005; Karsunky et al., 2003). Contrary to $CD8^+$ cDCs, $CD11b^+$ cDCs are potent drivers of $CD4^+$ T-cell proliferation and express a wide range of TLRs, including TLRs 5, 6, 7, 9, and 13 (Dudziak et al., 2007). Additionally, $CD11b^+$ cDCs express an intracellular PRR, retinoic acid-inducible gene 1 (RIG-I), that recognizes double-stranded and single-stranded RNA and triggers antiviral responses (Merad et al., 2013).

Non-lymphoid cDCs. $CD103^+CD11b^-$ cDCs resemble lymphoid $CD8^+$ cDCs in terms of their origin and functions (Del Rio et al., 2010; Helft et al., 2010). $CD103^+CD11b^-$ cDCs also express $CD8\alpha^+$, and proliferate in response to Flt3L (Ginhoux et al., 2009). In addition to their ability to cross-present antigens to $CD8^+$ T cells and

initiate T cell-mediated immunity (Helft et al., 2012), non-lymphoid $CD103^{+}CD11b^{-}$ cDCs are strong mediators of immune tolerance (Annacker et al., 2005). $CD103^{+}CD11b^{-}$ cDCs are reported to capture and present apoptotic antigens during steady state and induce cross-tolerance (Desch et al., 2011). $CD103^{-}CD11b^{+}$ cDCs in non-lymphoid tissues are a heterogenous collection due to the lack of defining markers for each subpopulation. Similar to the lymphoid $CD11b^{+}$ cDCs, $CD103^{-}CD11b^{+}$ cDCs in non-lymphoid tissues are thought to derive from different precursors, further complicating the difficulty in understanding these subsets (Miller et al., 2012). $CD103^{-}CD11b^{+}$ cDCs in lung have been shown to induce type 2 helper (Th2) cell-mediated immunity in response to house dust mite (Plantinga et al., 2013). However, in *Aspergillus fumigatus* infection, $CD103^{-}CD11b^{+}$ cDCs are reported to induce type 17 helper (Th17) cell responses (Schlitzer et al., 2013). Among the intestinal $CD11b^{+}$ cDCs, it has been know that there exists one particular subpopulation that expresses both CD103 and CD11b. $CD103^{+}CD11b^{+}$ cDCs contribute to the mucosal Th17 immunity through the expression of IL-6 and IL-23, which are the main Th17-inducing and maintain cytokines, respectively (Cerovic et al., 2013; Kinnebrew et al., 2012).

Tissue-migratory cDCs. Tissue-migratory cDCs are non-lymphoid tissue cDCs that have migrated to the tissue-draining lymph nodes (TDLNs) through the lymphatics. Migration of cDCs is controlled by the c-c chemokine receptor type 7 (CCR7) (Ohl et al., 2004), which binds chemokine (C-C) motif ligand 19 (CCL19) and (C-C) motif ligand 21 (CCL21) (Forster et al., 2008). Migratory DCs in steady state express high levels of MHC class II and low levels of CD11c. DC Maturation, represented by upregulation with

MHC class II complexes and costimulatory molecules, including CD80, CD83, and CD86, normally happens during migration during the steady state or upon inflammation (Reis e Sousa, 2006).

Langerhans cells. LCs are DCs that populate the epidermis of the skin (Merad et al., 2008). LCs are a unique self-renewing DC subset that derive from embryonic precursors (Ginhoux and Merad, 2010). LCs express the epithelial cell adhesion molecule (EpCAM) and langerin, a C-type lectin within LC-specific organelles called Birbeck granules. Compared to other skin cDCs, LCs express lower levels of MHC class II. The development of LCs relies on macrophage colony-stimulator factor (M-CSF) (Schlitzer et al., 2013), not Flt3-Flt3L (Ginhoux et al., 2009). LCs efficiently drive $CD4^+$ T cell-mediated immunity upon skin infection (Igyártó et al., 2011). In steady state, LCs present antigen to $CD4^+$ T cells, inducing anergy and promoting peripheral tolerance (Nakajima et al., 2012). Overall, LC-induced immune responses are highly dependent on the environmental and pathogenic cues, rather than pre-imprinted functional specialties.

Subsets of Human Dendritic Cells and Their Specialized Functions

Human cDCs are composed of $CD1c^+$ and $CD141^+$ DCs in blood and lymphoid tissues, epidermal LCs, dermal $CD14^+$ and $CD1a^+$ DCs.

Blood and lymphoid cDCs. $CD1c^+$ DCs are the major DC subset in blood, spleen, LNs and non-lymphoid tissues. $CD1c^+$ DCs express the majority of TLRs, as well as the fungal uptake receptors Dectin-1 and Dectin-2 (Harman et al., 2013; Lundberg et al.,

2013). Similar to mouse CD11b$^+$ DCs, human CD1c$^+$ DCs are the main inducers of CD4$^+$ T cell-mediated immunity (Penel-Sotirakis et al., 2012; Rydnert et al., 2014; Schlitzer et al., 2013), although they are also able to potently prime CD8$^+$ T cells (Nizzoli et al., 2013; Yu et al., 2013). CD141$^+$ DCs, similar to CD1c$^+$ DCs, are present in blood, LNs, and some non-lymphoid tissues. CD141$^+$ DCs, while being the minor population in blood, efficiently cross-present antigens to CD8$^+$ T cells (Jongbloed et al., 2010; Silk et al., 2012). Such superior cross-presentation capacities of CD141$^+$ DCs closely resemble those of the mouse CD8$^+$ and CD103$^+$CD11b$^-$ DCs (Bachem et al., 2010; Haniffa et al., 2012).

Skin DCs. Dermal CD14$^+$ cDCs are a DC subset unique to the human DC system. CD14$^+$ cDCs can be also found in LNs and some non-lymphoid tissues. According to transcriptome studies, CD14$^+$ DCs are phenotypically close to blood CD14$^+$ monocytes (McGovern et al., 2014). CD14$^+$ DCs are considered to be strong activators of follicular helper T cells (Tfh) and B cells (Angel et al., 2006; Klechevsky et al., 2008; Matthews et al., 2012). CD1a$^+$ DCs are the other dermal DC subset that display an activated and migratory phenotype under steady-conditions and may aid in maintaining immune tolerance (Santegoets et al., 2008). LCs, similar to their mouse homologues, are self-renewing DCs in the epidermis (Kanitakis et al., 2011). Human LCs are also characterized by the high expression of EpCAM and langerin (Valladeau et al., 1999). In addition, human, but not mouse, LCs express high levels of CD1a$^+$ (Fithian et al., 1981). Functionally, human LCs are able to induce potent Th17 response upon *Candida albicans*

infection, and are known to be efficient at cross-presenting antigens to $CD8^+$ T cells (Segura et al., 2012).

Alignment of Mouse and Human Dendritic Cells

Although human DCs are less characterized, the alignment of human and mouse DC subsets is being made with recent progress the studies on the transcriptomes and functions of distinct DC subsets (Lundberg et al., 2013; Miller et al., 2012). It has been shown that mouse LCs and pDCs share high levels of similarities with their human counterparts (Hochrein et al., 2002; Mestas and Hughes, 2004), while mouse $CD11b^+$ cDCs display functional resemblances to human $CD1c^+$ DCs (Schlitzer and Ginhoux, 2014). Mouse $CD8^+$ and $CD103^+CD11b^-$ DCs are considered to be the equivalent of human $CD141^+$ cDCs, due to their superior capacities to cross-present antigens to $CD8^+$ T cells (Villadangos and Shortman, 2010). Moreover, mouse $CD8^+$ and $CD103^+CD11b^-$ DCs and human $CD141^+$ cDCs share similarities in cytokines required for differentiation from their respective precursors (Hieronymus et al., 2005; Karsunky et al., 2003), further suggesting that the these DC subsets are developmentally related. This close relationship is particularly important for the rational design of DC-based vaccines that induce antigen-specific $CD8^+$ T cell-mediated immunity against virus and tumors, especially since preclinical tests in mouse models will provide more clinically related interpretations on the efficacies of these vaccines.

Dendritic Cell-Based Immunotherapies

The superior capacities of DCs to capture, process and cross-present antigens have been perceived by many as a golden opportunity to make more effective vaccines against intracellular pathogens and cancers. This part of the introduction focuses on the principles of current DC-based immunotherapies and explores the advantages and disadvantages of the ever-evolving DC-targeting strategies. Finally, the important factors of designing and improving DC-targeting vaccines are discussed.

The Principles of DC-Based Immunotherapies

DCs have been recognized as key initiators of immune responses since their discovery. Following the discovery of *in vitro* generation of DCs from isolated monocytes, there have been numerous attempts to harness the functional specialties of DCs in immunotherapies against cancer. One type of the early DC-based vaccines included the use of *ex vivo* antigen-loaded DCs. With the advances in understanding the biology of DCs, recent DC-based immunotherapies have shifted from *ex vivo* loading to *in vivo* targeting by delivering antigens to specific *in vivo* DC subsets.

Immunotherapies using ex vivo antigen-loaded DCs. In the early trials of immunotherapies against cancers, DCs were generated from isolated monocytes or $CD34^+$ precursors from patient blood by apheresis. The differentiation from monocytes or other precursors to mature or immature DCs include the use of a mixture of cytokines similar to those found in the *in vivo* system, including granulocyte-macrophage colony-stimulating factor (GM-CSF) and IL-4. In order to generate effective DC vaccines, MHC

class I and II molecules on the DC surface must be loaded with appropriate antigenic cargo. Common antigens include tumor lysate, peptides, apoptotic cells, and recombinant proteins, and even RNA-encoding tumor antigens, which make DCs themselves express tumor antigen. *Ex vivo* antigen-loaded DCs are then delivered back to the patient intradermally with the addition of inflammatory cytokines to promote DC migration to TDLNs, initiating antigen-specific immune responses.

Immunotherapies targeting in vivo dendritic cells. DCs are known to express numerous surface receptors, which have been utilized in approaches to deliver antigens to DCs by linking the relevant antigens to antibodies or ligands. As shown in Figure 2, when a DC-targeting vaccine is delivered to the sites where desired DC subsets are present, the antibody/ligand-antigen complexes bind to target DC surface receptor and are internalized. In most cases, the complexes enter the DCs by the endocytic pathway. Small quantities of antigens escape from the complex-containing endosome to the cytosol and gain access to the MHC class I antigen-processing pathway. Escaped antigens are then broken into short peptides by the cytosolic immunoproteasome and transported to the endoplasmic reticulum (ER) through transporter associated with antigen processing (TAP). The peptides are further modified and loaded on the MHC class I molecules. The cognate $CD8^+$ T cells. However, which receptor(s) to choose as the best candidate(s) to induce potent $CD8^+$ T cell-mediate immunity against cancers or intracellular remains unanswered. Figure 3 lists the current knowledge on DC-targeting studies, both *in vivo* and *in vitro*, on a variety of DC surface receptors (Kastenmuller et al., 2014).

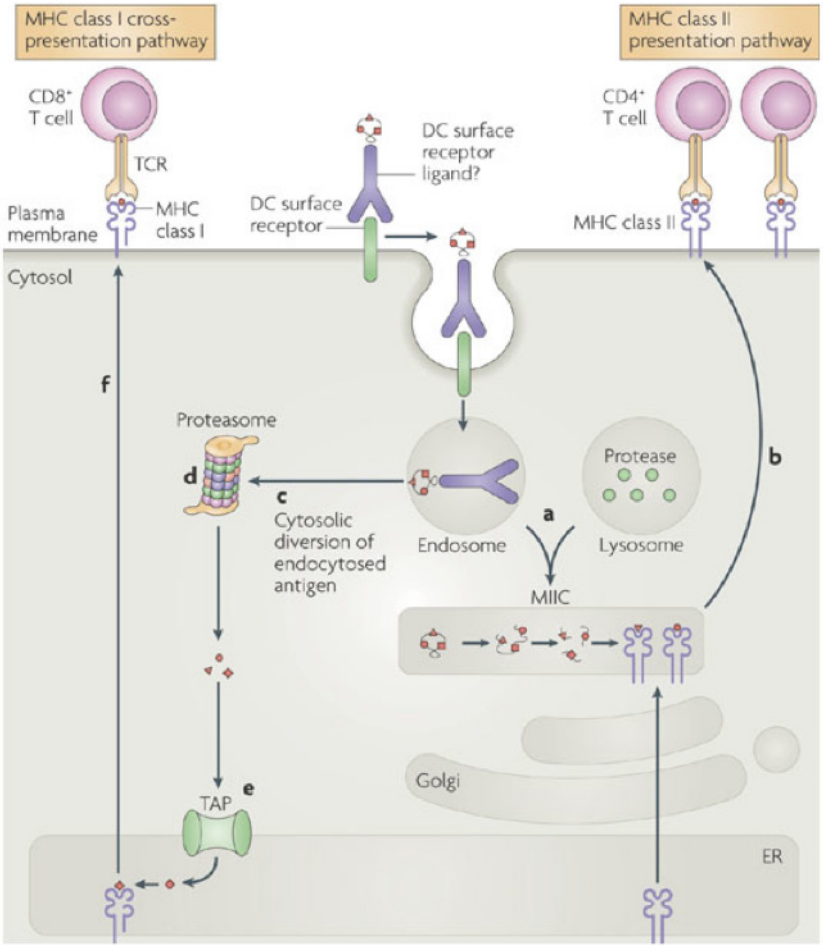

Figure 2. Intracellular fate of antigen targeted to DC surface receptors. (a) Targeting vectors bind to DC surface receptors and are internalized through the endocytic pathway. Targeted protein and antigen remain in the endosome and are fused with protease-containing lysosomes, resulting smaller peptides of the antigen. (b) Generated peptides are loaded onto MHC class II molecules residing in the MHC class II compartment (MIIC), and are presented at the cell surface to $CD4^+$ T cells. (c–e) Some endocytosed antigens were processed by proteasome and the resulting peptides are loaded onto MHC class I molecules by transporter associated with antigen processing (TAP) protein. (f) The loaded MHC Class I molecules are transported to the cell surface, where the peptides are presented to $CD8^+$ T cells. TCR, T-cell receptor; ER, endoplasmic reticulum. Reprint by permission from Macmillan Publishers Ltd: Nature Reviews Immunology, copyright 2007. (Tacken et al., 2007)

The Pros and Cons of Dendritic Cell-Based Immunotherapies

The two major types of DC-based immunotherapies are promising strategies in the treatment of cancers and viruses. However, there exist advantages and disadvantages

for each of the immunotherapies. It is essential to understand every aspect of the DC-based vaccines to further improve their efficacies.

Immunotherapies using ex vivo antigen-loaded dendritic cells. The maturation and activation of *ex vivo* loaded DCs can be tightly controlled due to the standardized DC differentiation protocol and closed culture system. In addition, the DC vaccine specificity is highly controlled and only the *ex vivo* DCs are activated, thus limiting bystander activation of other cell types. However, because each vaccine is tailor-made to each patient, the production procedure is extremely labor-intensive and costly. Furthermore, DCs used in the final vaccine need to be quality-checked at different differentiation stages, which also differ per production site. Most importantly, as the *ex vivo* DCsresemble only a small fraction of *in vivo* DC populations, the range of immune responses that can be elicited may be limited (Palucka and Banchereau, 2012; Tacken et al., 2007).

Immunotherapies targeting in vivo dendritic cells. In vivo DC-targeting vaccines are much easier and less expensive in manufacture. Meanwhile, the mass production of DC-targeting vaccines needs only one specialized good manufacturing practice (GMP) manufacturer with fewer checkpoints for quality control. Since DC-targeting vaccines are not tailor-made to a specific patient, it is thus more accessible to a large number of patients. Most importantly, DC-targeting vaccines are delivered to *in vivo* DCs whose environment is not artificially modified, and multiple DC subsets expressing the same receptors can be targeted simultaneously, eliciting more potent and/or several immune

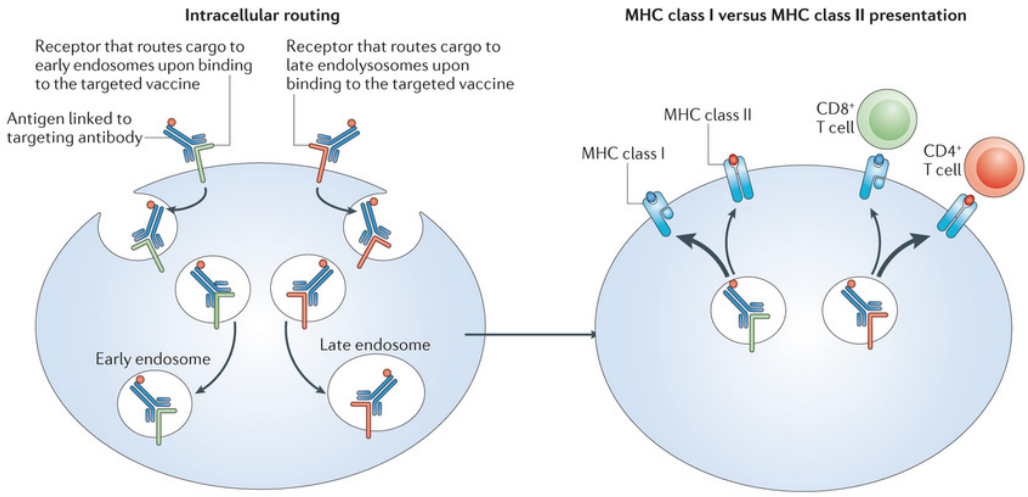

Receptor	Early endosomal compartment	Late endosomal compartment	Stimulates CD4+ T cells		Stimulates CD8+ T cells	
			In vitro	*In vivo*	*In vitro*	*In vivo*
CD205	No	Yes	+	+	+	++ +/– (human)
CD207	Yes	No	+	+	+	++
Mannose receptor 1	Yes	No	+	+	+	+
DC-SIGN	Yes (ligand dependent)	Yes (ligand dependent)	+	+	+	+
CLEC9A	Yes	No	+	+	+	++
DCIR2	No	Yes	+	++	+	+
CLEC12A	Not investigated	Not investigated	+	++	+	+/–
DC-ASGPR	No	Yes	+	++	+	+/–
Dectin 1	No	Yes	+	++	+	+
CD11c	Not investigated	Not investigated	+	+	+	++
CD11b	Not investigated	Not investigated	+	++	+	+
MHC class II	No	Yes	+	+	+	+/–
CD40	Yes	No	++ (human)	+	++ (human)	+
FcγR	No	Yes	+	+	+	+
XCR1 or XCL1	Not investigated	Not investigated	+	+	+	++

Figure 3. Antigen presentation and intracellular routing. Targeting antigens via DC surface receptors leads to internalization of the receptor and its cargo. Most receptors are routed to late endolysosomes where antigen is quickly degraded and presented on MHC Class II molecules to $CD4^+$ T cells. Some receptors transfer their cargo to early endosomes where antigen undergoes a slow degradation and leads to a prolonged MHC Class I presentation to $CD8^+$ T cells. +, intermediate stimulation of T cells; ++, strong stimulation of T cells; +/−, low stimulation of T cells; CLEC, C-type lectin domain family member; DC-ASGPR, DC-asialoglycoprotein receptor; DCIR2, dendritic cell inhibitory receptor 2; DC-SIGN, DC-specific ICAM3-grabbing non-integrin; FcγR, Fc receptor for IgG; XCL1, XC-chemokine ligand 1; XCR1, XC-chemokine receptor 1. Reprint by permission from Macmillan Publishers Ltd: Nature Reviews Immunology, copyright 2014. (Kastenmuller et al., 2014)

responses. However, due to the uncertainty of the fate of injected vaccines, the clinical efficacies cannot be controlled and oftentimes adjuvants are required with vaccine

injection to ensure optimal DC activation and maturation (Palucka and Banchereau, 2012; Tacken et al., 2007).

Improving the Dendritic Cell-Targeting Vaccines Against Cancers

DC-targeting vaccines have been considered a much more accessible and versatile immunotherapy against cancer. To achieve an even better outcome, the following factors need to be taken into account in designing and improving DC-targeting vaccines.

Target receptor and DC subsets. DC surface receptors differ in terms of expression levels, signaling pathways, and intracellular trafficking pathways. Studies on targeting to CD207 (langerin) and CLEC9A have shown to induce strong $CD8^+$ T cell responses (Kastenmuller et al., 2014). Interestingly, both receptors localize to the early endosomal compartment when internalized. This is a good indicator for choosing the ideal receptor as a target, as localization to the early endosomal compartment is likely associated with cross-presentation (Cohn et al., 2013). However, the outcome of targeting different receptors is not merely dictated by the receptor alone, as different DC subsets express different sets of receptors and the expression level of the same receptor can differ. Certain DC subsets are known to be efficient at cross-priming $CD8^+$ T cells, including $CD141^+$ DCs and LCs. Targeting antigens to such DC subsets also requires different immunization routes due to the DC frequency differences at the sites of injection (Figdor et al., 2004).

DC maturation and activation status. Signaling between DCs and T cells is one of the key factors that decide the quality of the ensuing immune response. It has been shown that non-activated DCs can cause T-cell tolerance rather than productive immunity (Steinman and Nussenzweig, 2002). TLRs and CD40 ligand are common DC activators that have been used in *ex-vivo* antigen-loaded DCs (Krug et al., 2001). Recent preclinical trials in non-human primates using polyinosinic:polycytidylic acid [poly(I:C)], and its derivative, poly-ICLC, have shown promising agonistic effects on DCs that can significantly expand antigen-specific T-cell immunity (Thompson et al., 2015). The inclusion of activating molecules in DC immunotherapies has been therefore considered necessary to improve the efficacy of DC-targeting vaccines.

Combination therapy. Tumor microenvironment, established jointly by tumor cells and by resident and infiltrating non-tumor cells and their metabolic products, promotes tumor progression (Witz, 2009). Several immune checkpoints, including cytotoxic T-lymphocyte-associated protein 4 (CTLA-4) and programmed cell death protein 1 (PD-1), expressed on tumor-specific T cells lead to compromised activation and suppressed effector functions (Lote et al., 2015; Ville et al., 2015). Clinical studies using monoclonal antibody (mAb) specific to CTLA-4 or PD-1, in addition to DC-targeting vaccines, have shown striking therapeutic results in inducing antitumor activity (Le et al., 2015; Sangro et al., 2013). The combination therapy that elicits strong $CD8^+$ T cell responses and blocks inhibitory checkpoints represents a new and promising strategy that can further control, and even eradicate, the tumors.

CHAPTER TWO

Objectives

The development of safe and effective vaccines against viral infections and cancers become a focal point in the field of vaccinology. Meanwhile, the concept of DC-targeting vaccines has emerged as an effective way to evoke strong antigen-specific immune responses, particularly $CD8^+$ T cell responses, as DCs are able to cross-present antigens to $CD8^+$ T cells. However, DCs express a plethora of surface receptors. The question then becomes which receptor to target to elicit strong $CD8^+$ T cell responses. Herein, we give a preliminary answer to this question through a series of staged investigations from the basic immunology study of DC-targeting to the *in vivo* assessment of our CD40-targeting prototype vaccines against human papillomavirus (HPV)-related malignancies and prostate cancer (CaP).

Aim 1: Determine the functional specialties of DC surface receptors at cross-presenting antigen to $CD8^+$or $CD4^+$ T cells

a) Compare the ability of selected DC surface receptors in priming naïve $CD8^+$ T cells

b) Compare the ability of selected DC surface receptors in activating memory $CD8^+$ and $CD4^+$ T cells

c) Identify the fate of the receptor-bound antibodies through intracellular trafficking

In Chapter Three, nine different human DC surface receptors were compared for their ability to promote antigen cross-presentation to $CD8^+$ T cells. The functionality of the resulting $CD8^+$ T cells was also tested. The subcellular and intracellular trafficking of receptor-bound antibodies against CD40, LOX-1 and Dectin-1 was also determined.

Aim 2: Assess the preclinical efficacy of αCD40-HPV16.E6/7 against HPV-related malignancies

a) Study the in vitro immunogenicity of αCD40-HPV16.E6/7

b) Test the in vivo immunogenicity of αCD40-HPV16.E6/7

c) Compare the in vivo immune response profiles between αCD40-HPV16.E6/7 and αLangerin-HPV16.E6/7

d) Test the in vivo efficacy of αCD40-HPV16.E6/7 in tumor prevention and tumor rejection models

In Chapter Four, a recombinant fusion protein of αCD40 antibody and HPV16.E6/7 (αCD40-HPV16.E6/7) was generated. The *in vitro* immunogenicity test was performed to confirm whether αCD40-HPV16.E6/7 was able to expand pre-existing HPV16.E6/7-specific $CD8^+$ T cells in head and neck cancer patients. Next, the immunogenicity of αCD40-HPV16.E6/7 and αLangerin-HPV16.E6/7 was assessed in the human CD40 transgenic mice. Lastly, the *in vivo* efficacy of αCD40-HPV16.E6/7 was determined in tumor prevention and rejection models.

Aim 3: Investigate the immunogenicity of αCD40-PSA

a) Study the agonistic effect of αCD40-PSA

b) Test the in vitro immunogenicity of αCD40-PSA

c) Determine the in vivo immunogenicity of αCD40-PSA

In Chapter Five, a recombinant fusion protein of αCD40 antibody and PSA (αCD40-PSA) was generated. *In vitro* immunogenicity of αCD40-PSA was assessed in the blood of healthy donors and CaP patients. Human CD40 transgenic mice were used to test the *in vivo* immunogenicity of αCD40-PSA.

CHAPTER THREE

Specialized Functions of Human Dendritic Cell Surface Receptors that Enhance Antigen Cross-Presentation to Either $CD8^+$ or $CD4^+$ T Cells

Abstract

Dendritic cells (DCs) are major antigen-presenting cells that can efficiently cross-prime antigen-specific T cells. Delivering antigen to DCs via surface receptors is thus an appealing strategy to evoke cellular immunity. Nonetheless, which targeted receptor results in optimal $CD8^+$ and $CD4^+$ T cell responses remains elusive. Herein, we report the superiority of CD40 over eight different lectins and scavenger receptors at evoking antigen-specific human $CD8^+$ T cell responses. However, lectins (e.g., LOX-1 and Dectin-1) were significantly more efficient than CD40 at eliciting $CD4^+$ T cell responses. Common and distinct patterns of subcellular and intracellular localization of receptor-bound αCD40, αLOX-1 and αDectin-1 further support their functional specialization at enhancing antigen presentation to either $CD8^+$ or $CD4^+$ T cells. This study provides fundamental information for the biology of human DC surface receptors and for the rational design of vaccines against cancers and viral infections.

Introduction

Dendritic cells (DCs) are professional antigen presenting cells (APCs) that can efficiently prime T cells. Both endogenous and exogenous antigens are efficiently presented by DCs in the context of major histocompatibility class I and II (MHC I and II)/peptide complexes. Among various types of APCs, DCs are the most efficient at

cross-presenting antigens to T cells (Delamarre and Mellman, 2011; Jung et al., 2002; Segura and Villadangos, 2009), although the types and magnitude of T cell responses largely rely on the functional specialty and plasticity of DC subsets.

T cell-mediated immunity plays crucial roles in therapeutic immunity against cancers and viral infections. The potent ability of DCs to cross-prime T cells, particularly $CD8^+$ T cells, positions them as novel cellular targets for the rational design of vaccines. In line with this premise, Bonifaz *et al.* (Bonifaz et al., 2002; Bonifaz et al., 2004) demonstrated that the efficiency of antigen cross-presentation by DCs, assessed by measuring the magnitude of $CD8^+$ T cell responses, could be improved over 100-fold by targeting antigens to DEC205 in mice. This seminal observation has led many scientists to further study the biology of DC surface receptors and the use of the "DC-targeting vaccines" against cancers and viral infections.

For more than a decade, researchers have been attempting to optimize DC-targeting vaccines by delivering antigens to different DC surface receptors. These receptors include c-type lectins (e.g., DEC205, DC-SIGN, CD207, LOX-1, DC-ASGPR, Dectin-1, DCIR, DCIR2, CLEC6, CLEC9A, and CLEC12A) (Bonifaz et al., 2004; Caminschi et al., 2008; Carter et al., 2006; Delneste et al., 2002; Dudziak et al., 2007; Duluc et al., 2014; Flacher et al., 2014b; Flamar et al., 2013; Idoyaga et al., 2008; Idoyaga et al., 2011; Kastenmuller et al., 2014; Lahoud et al., 2009; Li et al., 2012; Meyer-Wentrup et al., 2008; Ni et al., 2010; Sancho et al., 2008; Tacken et al., 2005; Tacken et al., 2007; Tacken et al., 2011; Weck et al., 2008), as well as non-lectin receptors, including CD40 (Chatterjee et al., 2012; Cohn et al., 2013; Flamar et al., 2013), mannose receptor (Tsuji et al., 2011), and integrins (Castro et al., 2008). Antigens

delivered to DCs via each of these receptors have been reported to elicit certain levels of antigen-specific $CD8^+$ T cell responses *in vitro* in humans and *in vivo* in mice or non-human primates (NHPs). However, it still remains unclear which targeted receptors are the most efficient at priming and boosting antigen-specific $CD8^+$ and $CD4^+$ T cell responses. Finding a specific DC surface receptor that permits us to efficiently evoke potent $CD8^+$ and $CD4^+$ T cell responses will be fundamental for the rational design of effective DC-targeting vaccines against cancers and viral infections. Recent preclinical (in NHPs) and clinical data of DEC205-targeting vaccines also suggest that efficient priming and activation of antigen-specific $CD8^+$ CTLs are still major challenges for the success of DC-targeting vaccines for cancer immunotherapy (Kastenmuller et al., 2014). However, it is also important to note that $CD4^+$ T cells are crucial for the longevity of memory $CD8^+$ CTL-mediated immunity (Janssen et al., 2003), which will determine the efficacy of vaccines in many circumstances.

In this study, we first compared nine different human DC surface receptors for their ability to promote antigen cross-presentation to $CD8^+$ T cells. We found that CD40 was the most efficient at priming and boosting antigen-specific $CD8^+$ CTLs that were functional. We then compared CD40 with the two best DC lectins, LOX-1 and Dectin-1, for their ability to present antigens to $CD4^+$ T cells. Interestingly, both LOX-1 and Dectin-1 were superior to CD40 at evoking antigen-specific $CD4^+$ T cell responses. To understand this functional dichotomy of CD40 versus lectins (LOX-1 and Dectin-1) in antigen presentation to $CD8^+$ and $CD4^+$ T cells, we have also studied subcellular and intracellular trafficking of the three different receptor-bound antibodies in DCs.

Materials and Methods

Antibodies, Peptides, Tetramers and Other Reagents

αCD4, αCD8, αCD11c, αCD80, αCD83, αCD86, αPerforin and αIFNγ mAbs were purchased from BioLegend. αCD3, αCD19, αCD123, Lin-1, αHLA-DR, αIFNγ, αCD45RA, and αCD45RO mAbs were purchased from BD Biosciences. αCD14 and αHLA-ABC were purchased from eBioscience. LIVE/DEAD fixable dead cell stain kit and αGranzyme B mAb were from Invitrogen. HLA-A*0201-Flu.M1$_{58\text{-}66}$ and -MART-1$_{26\text{-}35}$ tetramers were from Beckman Coulter. Flu.M1$_{58\text{-}66}$ and MART-1$_{26\text{-}35\ (27L)}$ peptides were synthesized by Bio-Synthesis. Overlapping 15-mer peptides (staggered by 11 amino acids) spanning the entire nucleoprotein (NP) (A/environment/Viet Nam/1203/2004 H5N1) and hemagglutinin subunit 1 (HA1) (A/PR/8/34 H1N1) were purchased from Mimotopes. CFSE (Invitrogen) was used for measuring $CD8^+$ T cell proliferation. Human GM-CSF was purchased from the Baylor University Medical Center Investigational Pharmacy. IL-2, IL-4, IL-7, and IL-15 were purchased from PeproTech.

DC-Targeting mAbs

mAbs specific for the ectodomains of human receptors (αLOX-1 (15C4) (Li et al., 2012), αDC-ASGPR (49C11) (Li et al., 2012), αDCIR (9E8) (Klechevsky et al., 2010), αCD40 (12E12) (Flamar et al., 2013), αDectin-1 (15E2) (Ni et al., 2010), and αDEC205 (MG38) (Bonifaz et al., 2002) were previously described. mAbs specific for the ectodomains of human MARCO (11A8), CLEC6 (9B9), and DC-SIGN/L (16E7) were generated using receptor ectodomain.hIgG (human IgG1 Fc) and human placental alkaline phosphatase (AP), as previously described (Ni et al., 2010). Cloned mAbs were

purified by HPLC using MabSelect resin (GE Healthcare). The specificities of mAbs were verified by their specific binding to corresponding receptors expressed on 293F cells transfected with the full-length receptors. The specificities of the mAbs were also confirmed by ELISA by comparing them to the recombinant receptor-Fc and hIgG-Fc fusion proteins (Ni et al., 2010). Chimeric mAbs containing human IgG4 heavy chain with two site mutations (S228P and L235E) (Reddy et al., 2000) were made to further abolish non-specific binding to Fc receptors.

Recombinant Fusion Proteins of mAb-Doc, Coh-Antigen, and Their Conjugates

Recombinant fusion proteins of mAb-Doc, Coh-Flu.M1$_{58-66}$, and Coh-MART-1$_{26-35\ (27L)}$ were previously described (Flamar et al., 2012; Ni et al., 2010). Recombinant mAb-antigen conjugates were formed by mixing one molar equivalent of mAb-Doc fusion proteins with two molar equivalents of Coh-antigen fusion proteins in 1X PBS with Ca^{2+} and Mg^{2+} (Biosources). The Doc and Coh domains self-associate, forming a stable and specific complex.

Recombinant Fusion Proteins of mAb-Flu.M1$_{58-66}$ peptide, -Flu.NP, and -Flu.HA

Production of mAb-Flu.NP and mAb-Flu.HA1 recombinant proteins was as previously described (Li et al., 2012; Skinner et al., 2014). Fusion proteins bearing the Flu.M1$_{58-66}$ were made using the same method.

Cells

All healthy (cancer-free) blood donors provided a written informed consent prior to inclusion in the study in accordance with the approval by the Institutional Review Boards at Baylor Research Institute. Mo-DCs were prepared by culturing purified blood monocytes from healthy individuals. Briefly, monocytes enriched from fresh PBMCs or frozen elutriated cell fractions were cultured in DC culture medium (CellGenix) in the presence of 100 ng/mL human GM-CSF and 50 ng/mL IL-4 for 6 days. On day 3, culture medium was replaced with fresh medium containing the same concentrations of GM-CSF and IL-4. PBMCs of HLA-A*0201$^+$ healthy donors were fractionated by elutriation. Total CD4$^+$ and CD8$^+$ T cells were enriched using enrichment kits (StemCell Technologies). Naïve CD8$^+$ T cells (CD45RA$^+$CD45RO$^-$) (purity > 99.2%) were further sorted on a FACSAria II (BD Biosciences). Monocytes and total B cells were purified using enrichment kits (StemCell Technologies). Blood myeloid DCs (mDCs, Lin-1$^-$HLA-DR$^+$CD11c$^+$CD123$^-$) and plasmacytoid DCs (pDCs, Lin-1$^-$HLA-DR$^+$CD11c$^-$CD123$^+$) were pre-enriched using a pan-DC enrichment kit (StemCell Technologies) and then sorted. All flow cytometry data were collected on a FACSCanto II (BD Biosciences) and analyzed with FlowJo v9 (Tree Star).

T Cell Assays

A total of 5 x 10^3 Mo-DCs were loaded with the indicated amounts of recombinant proteins or antigens and co-cultured with 2 x 10^5 purified autologous CFSE-labeled CD8$^+$ T cells for nine days in the presence of 20 units/mL IL-2 and 10 units/mL IL-7. In experiments using PBMCs, 50 units/mL IL-15 was added to the cultures on day

2. RPMI 1640 medium (Gibco), supplemented with 10% heat-inactivated human AB serum (Gemini), 50 unit/mL penicillin, 50 μg/mL streptomycin, 2 mM L-glutamate, non-essential amino acids (Sigma), 25 mM HEPES (Life Technologies), and 1 mM sodium pyruvate (Sigma), was used. $CD8^+$ T cells were then stained with tetramer and αCD8 mAb. In some experiments, $CD8^+$ T cells were stained with tetramer, αGranzyme B and αPerforin mAbs at the same time. To assess intracellular IFNγ expression, T cells were restimulated with the indicated peptides for 6 h in the presence of brefeldin A (BD Biosciences), as per the manufacturer's protocols. To measure cytotoxicity of $CD8^+$ T cells, a 5-h ^{51}Cr-release assay was performed using T2 cells loaded with the indicated peptides. The cytotoxicity of MART-1_{26-35}-specific $CD8^+$ T cells was also measured using cell lines (MEL290 and K562) that were grown in complete RPMI 1640 medium containing 10% FCS (Gemini).

Immunofluorescence

Mo-DCs (2 x 10^5/well) were plated in 24-well culture plates. αCD40 (12E12), αLOX-1 (15C4), or αDectin-1 (15E2) mAbs conjugated with Alexa Fluor 647 were added at 1 μg/mL followed by a 1-h incubation on ice. For internalization assays, cells were incubated for 1 h in a CO_2 incubator at 37°C. Cells were prefixed with 3% paraformaldehyde (Polysciences) for 30 min on ice and then fixed for 20 min at room temperature. Cells were then stained with Alexa Fluor 488-coupled rabbit anti-human EEA1 or anti-human LAMP-1 in PBS containing 0.1% saponin. Each optical slice was 0.5 μm thick. Images were acquired on a Leica DMI16000 confocal microscope (Nanterre, France). Image-J software was used to perform image analysis, channel

imaging, and surface plotting (3D presentation). For each donor (n=9) and each labeling antibody (αCD40, αLOX-1, and αDectin-1 mAbs), at least 10 pictures each with more than 10 cells were taken and analyzed. Just another Colocalization Plugin (JaCoP) software was used to calculate Mander's coefficients.

Statistics

Statistical significance was determined using the analysis of variance (ANOVA) and Student's *t* test with Prism 6 software (GraphPad Software). Significance was set at $P < 0.05$.

Results

The Superiority of CD40 over Eight Other Receptors for CD8$^+$ T Cell Cross-Priming

Herein, we compared the levels of MART-$1_{26\text{-}35}$-specific CD8$^+$ T cell responses primed with monocyte-derived DCs (Mo-DCs) loaded with different monoclonal antibody (mAb)-MART-$1_{26\text{-}35\ (27L)}$ conjugates. We used nine mAbs that were specific to different DC surface receptors. All mAbs were engineered as chimeras containing the mouse V-region and human IgG4 Fc with two mutations (S228P and L235E) to further abolish their non-specific binding to Fc receptors (Reddy et al., 2000). mAb-antigen conjugates were made through non-covalent stable interactions between Cohesin (Coh)-antigen and mAb-Dockerin (Doc), and they were well suited for targeting antigens to DCs via surface receptors (Flamar et al., 2013; Ni et al., 2010). Mo-DCs generated in serum-free DC culture medium containing GM-CSF and IL-4 expressed CD11c, CD14, costimulatory molecules (CD80, CD83, CD86) and high levels of HLA-ABC and HLA-

DR (Figure 4A). However, the expression levels of such surface molecules were variable among Mo-DCs generated with monocytes from different donors (Figure 4B).

Figure 5A shows that DCs loaded with any of the eight different mAb-MART-$1_{26\text{-}35\ (27L)}$ conjugates were able to prime various levels of MART-$1_{26\text{-}35}$-specific $CD8^+$ T cell responses, as measured by tetramer staining. DCs loaded with conjugates made with αLOX-1 and αDEC205 resulted in similar levels of MART-$1_{26\text{-}35}$-specific $CD8^+$ T cell responses, but they were more efficient at priming MART-$1_{26\text{-}35}$-specific $CD8^+$ CTLs than conjugates made with other mAbs (αDC-ASGPR, αCLEC6, αMARCO, and control IgG4). Thus, we selected the αLOX-1 conjugate and compared it to αCD40 and αDectin-1 conjugates in the second experiments (Figure 5B). The αCD40 conjugate was more efficient than the other two at priming MART-$1_{26\text{-}35}$-specific naïve $CD8^+$ T cells. Representative tetramer staining data for Figures 5A and 5B are presented in Figures 6A and 6B, respectively.

Figure 5C shows that DCs expressed higher levels of CD40 and DCIR than other receptors tested, although the αDCIR conjugate was less efficient than the αLOX-1 conjugate at priming MART-$1_{26\text{-}35}$-specific naïve $CD8^+$ T cells. DCs also expressed slightly higher levels of DC-SIGN/L, DEC205, and DC-ASGPR than LOX-1, CLEC6, and Dectin-1. These data suggested that the magnitude of antigen-specific $CD8^+$ T cell responses elicited with different mAb-MART-$1_{26\text{-}35\ (27L)}$ conjugates (Figures 5A and 5B) does not necessarily correlate with the surface expression levels of the receptors targeted or consequently with antigen loads (Reuter et al., 2015). We thus concluded that the αCD40-MART-$1_{26\text{-}35\ (27L)}$ conjugate was more efficient than eight other mAb conjugates at priming MART-$1_{26\text{-}35}$-specific $CD8^+$ T cells.

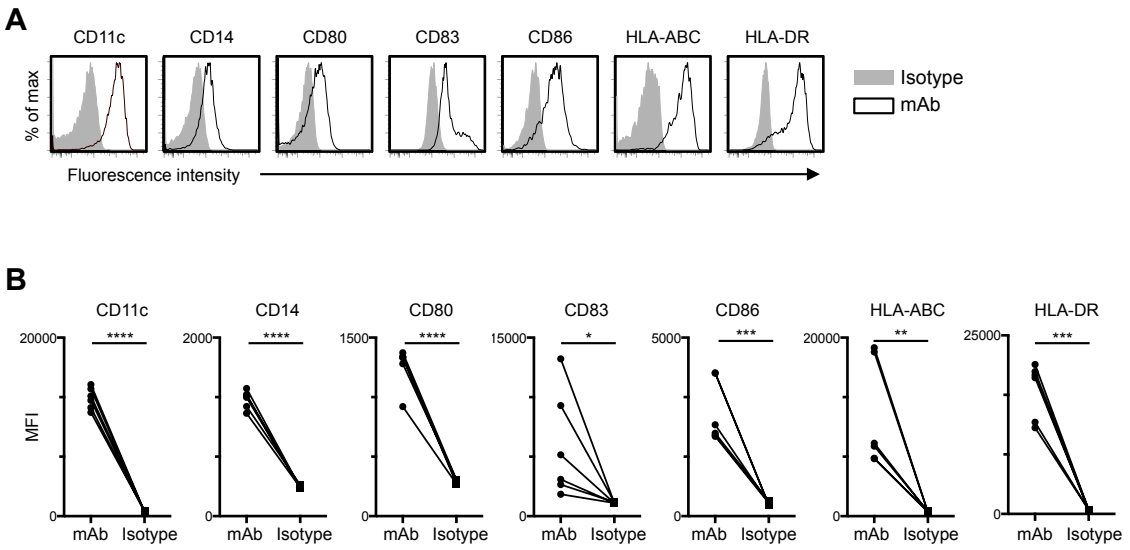

Figure 4. Surface phenotype of Mo-DCs. (A and B) Mo-DCs were stained with fluorescence-labeled mAbs specific to the indicated surface markers or with their isotype-matching controls. (A) Representative flow cytometric data and (B) summarized data on mean fluorescence intensities (MFIs) of each marker are shown. Dots represent data generated with cells from individual healthy donors (n=6). Significance was determined using a paired *t* test. *, $P < 0.05$; **, $P < 0.01$; ***, $P < 0.005$; ****, $P < 0.001$.

$CD8^+$ CTLs Primed with CD40-Targeted DCs Are Functional

Next, we tested whether αCD40-MART-$1_{26\text{-}35\ (27L)}$ conjugate could target CD40 expressed on DCs. DCs were loaded with two different concentrations of αCD40-MART-$1_{26\text{-}35\ (27L)}$ conjugate and then co-cultured for nine days with autologous naïve $CD8^+$ T cells. As shown in Figure 7A, DCs loaded with αCD40 conjugate primed MART-$1_{26\text{-}35}$-specific $CD8^+$ T cells at both 5 and 1 μg/mL; whereas DCs loaded with 5 μg/mL IgG4 conjugate only resulted in a minimal level of $CD8^+$ T cell priming. Summarized data from 13 independent experiments using cells from different healthy donors are presented (right, Figure 7A). In addition, DCs loaded with 5 nM (1 μg/mL) αCD40-MART-$1_{26\text{-}35(27L)}$, which contains 10 nM MART-$1_{26\text{-}35\ (27L)}$, were far more efficient than DCs loaded

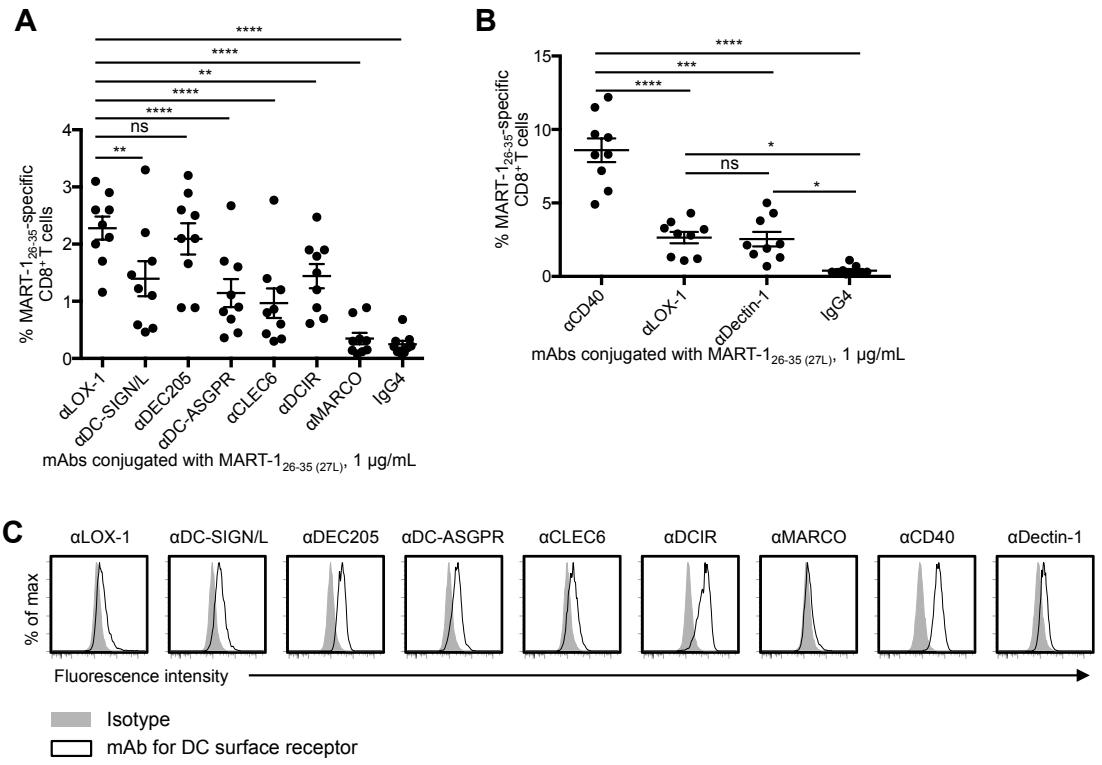

Figure 5. The superiority of CD40 over eight other receptors for $CD8^+$ T cell cross-priming. (A and B) Purified naïve $CD8^+$ T cells were co-cultured with Mo-DCs loaded with 1 µg/mL mAb-MART-$1_{26-35(27L)}$ for 9 days. $CD8^+$ T cells were then stained with HLA-A*A0201-MART-1_{26-35} tetramer. Dots represent data generated with cells from individual healthy donors (n=9). Data are presented as mean ± SD, and significance was determined using an ANOVA test. (C) Mo-DCs were stained with 1 µg/mL of the indicated fluorescence-labeled mAbs and analyzed by flow cytometry. Representative flow cytometric data out of three experiments are shown. *, $P < 0.05$; **, $P < 0.01$; ***, $P < 0.005$; ****, $P < 0.001$; ns, not significant.

with 10 nM MART-$1_{26-35\ (27L)}$ peptide (Figure 7B). Targeting MART-$1_{26-35\ (27L)}$ to DCs via CD40 was at least 1000 times more efficient at priming MART-1_{26-35}-specific $CD8^+$ T cells than the non-targeted loading of MART-$1_{26-35\ (27L)}$ onto DCs (Figure 7B). Summarized data generated with cells from six different donors are presented (right, Figure 7B).

Fractions of MART-1_{26-35}-specific $CD8^+$ T cells primed with DCs loaded with αCD40-MART-$1_{26-35\ (27L)}$ expressed both granzyme B and perforin (Figure 8A). They

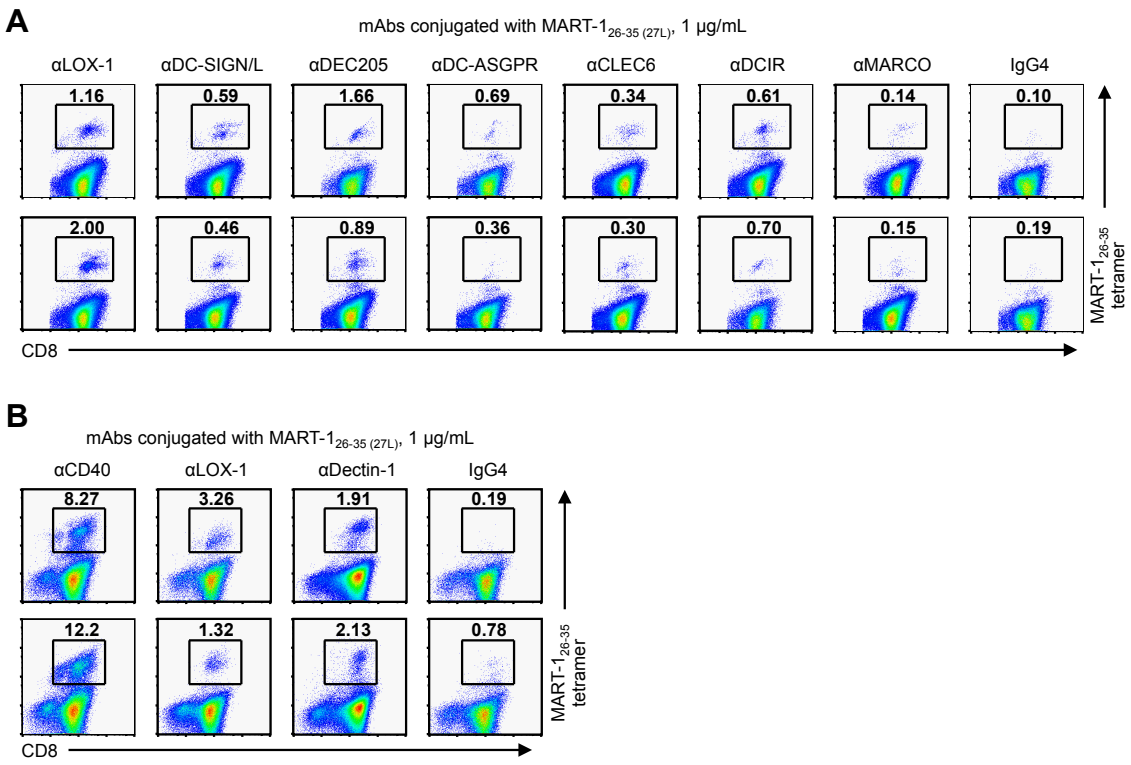

Figure 6. Targeting antigen to DCs via CD40 can efficiently prime $CD8^+$ CTLs. (A and B) Purified naïve $CD8^+$ T cells were co-cultured for 9 days with Mo-DCs loaded with 1 µg/mL of the indicated mAb-MART-$1_{26\text{-}35\ (27L)}$ conjugates. $CD8^+$ T cells were then stained with HLA-A*A0201-MART-$1_{26\text{-}35}$ tetramer. Representative flow cytometric data from duplicate assays (top and bottom panels) are shown.

were also able to lyse T2 cells loaded with 10 mM MART-$1_{26\text{-}35}$. $CD8^+$ CTLs that were primed with IgG4-MART-$1_{26\text{-}35\ (27L)}$-loaded DCs showed minimal killing activity (Figure 8B). As shown in Figure 8C, MART-$1_{26\text{-}35}$-specific $CD8^+$ CTLs that were primed with αCD40-MART-$1_{26\text{-}35\ (27L)}$-loaded DCs could also lyse MEL290 cells (HLA-A*0201^+ and MART-1^+) but not the control cell line K562 (left, Figure 8C). $CD8^+$ T cells primed with IgG4-MART-$1_{26\text{-}35\ (27L)}$-loaded DCs could not specifically lyse MEL290 (right, Figure 8C).

The functional activities of $CD8^+$ CTLs primed with αCD40-MART-$1_{26\text{-}35\ (27L)}$-loaded DCs were further compared with those primed with four other mAb-MART-$1_{26\text{-}35}$

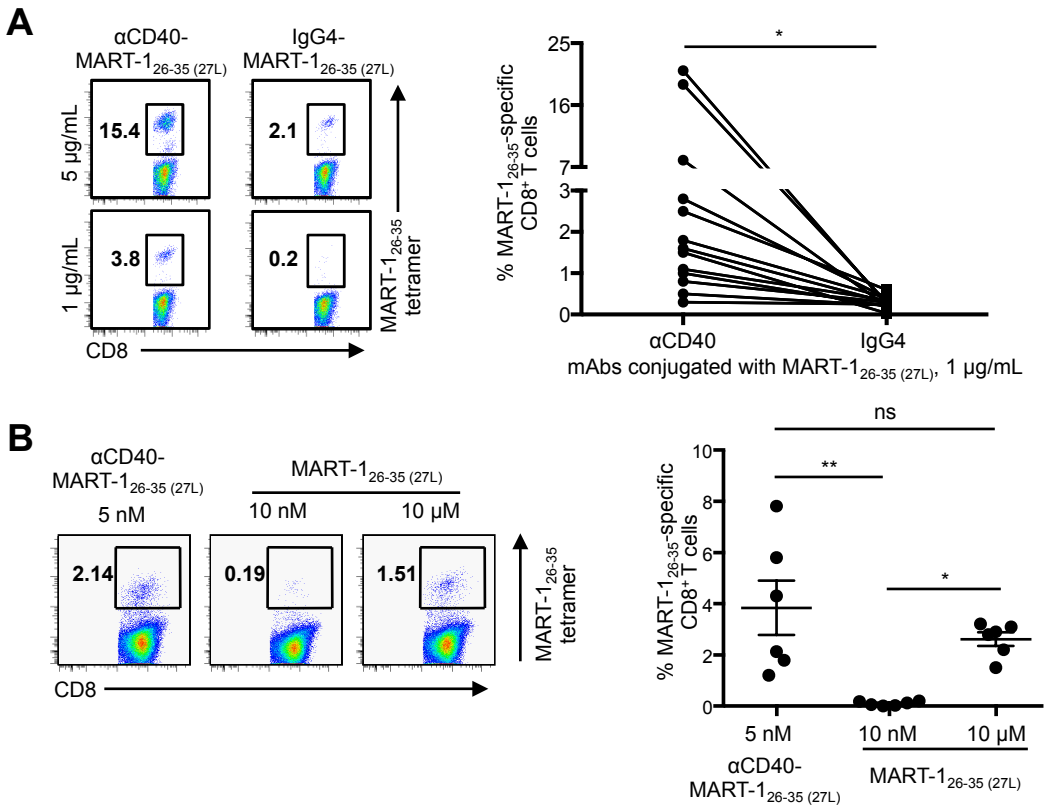

Figure 7. $CD8^+$ T cells can be primed with CD40-targted DCs. (A) Purified naïve CD8 T cells were co-cultured with Mo-DCs loaded with the indicated amounts of αCD40-MART-$1_{26\text{-}35\ (27L)}$ or IgG4-MART-$1_{26\text{-}35\ (27L)}$ conjugates for 9 days. $CD8^+$ T cells were then stained with HLA-A*A0201-MART-$1_{26\text{-}35}$ tetramer. Representative flow cytometric data (left) and donor-matched frequencies of MART-$1_{26\text{-}35}$-specific $CD8^+$ T cells induced with αCD40-MART-$1_{26\text{-}35\ (27L)}$- or IgG4-MART-$1_{26\text{-}35\ (27L)}$-loaded Mo-DCs are shown (right). Dots represent data generated with cells from individual healthy donors (n=13). Significance was determined using a paired *t*-test. (B) As in (A), purified naïve $CD8^+$ T cells were co-cultured with Mo-DCs loaded with the indicated amounts of αCD40-MART-$1_{26\text{-}35\ (27L)}$ conjugate or MART-$1_{26\text{-}35\ (27L)}$ peptide. $CD8^+$ T cells were stained with HLA-A*A0201-MART-$1_{26\text{-}35}$ tetramer. Representative flow cytometric data (left) and summarized data (right). Dots represent data generated with cells from individual healthy donors (n=6). Data are presented as mean ± SD. Significance was determined using an ANOVA test. *, $P < 0.05$; **, $P < 0.01$; ns, not significant.

$_{(27L)}$ conjugates. DCs loaded with αCD40-MART-$1_{26\text{-}35\ (27L)}$ induced a greater frequency of $IFN\gamma^+$ and $TNF\alpha^+CD8^+$ T cell responses than the other four (Figure 9). This was further supported by the data in Figure 10, showing that $CD8^+$ CTLs primed with αCD40-MART-$1_{26\text{-}35\ (27L)}$-loaded DCs were more efficient than those primed with other mAb-

MART-$1_{26\text{-}35\ (27L)}$-loaded DCs at lysing T2 cells. We therefore concluded that αCD40-MART-$1_{26\text{-}35\ (27L)}$ targeted CD40 and could thus efficiently prime functional MART-$1_{26\text{-}35}$-specific $CD8^+$ CTLs.

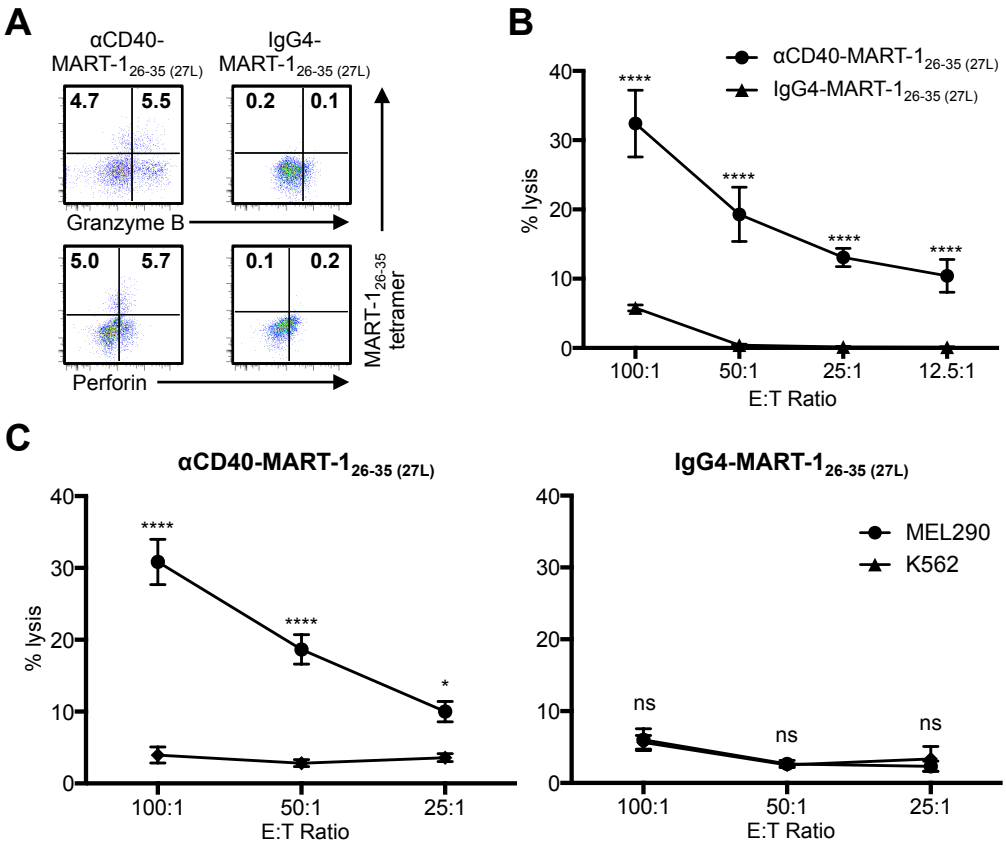

Figure 8. $CD8^+$ CTLs primed with CD40-targted DCs are functional. (A) $CD8^+$ T cells primed with Mo-DCs loaded with 1 μg/mL mAb-MART-$1_{26\text{-}35\ (27L)}$ were stained for granzyme B and perforin. (B) A 5-h ^{51}Cr release assay using T2 cells loaded with 10 μM MART-$1_{26\text{-}35}$ peptide were used as target cells. $CD8^+$ T cells primed with Mo-DCs loaded with 1 μg/mL αCD40-MART-$1_{26\text{-}35\ (27L)}$ or IgG4-MART-$1_{26\text{-}35\ (27L)}$ were used as effector cells. (C) A 5-h ^{51}Cr release assay using MEL290 and control K562 cell lines as target cells. $CD8^+$ T cells primed with Mo-DCs loaded with 1 μg/mL αCD40-MART-$1_{26\text{-}35\ (27L)}$ (left) or IgG4-MART-$1_{26\text{-}35\ (27L)}$ (right) were used as effector cells. Error bars indicate SD of triplicate assays. Significance was determined using an ANOVA test. Two independent experiments resulted in similar data. *, $P < 0.05$; ****, $P < 0.001$; ns, not significant.

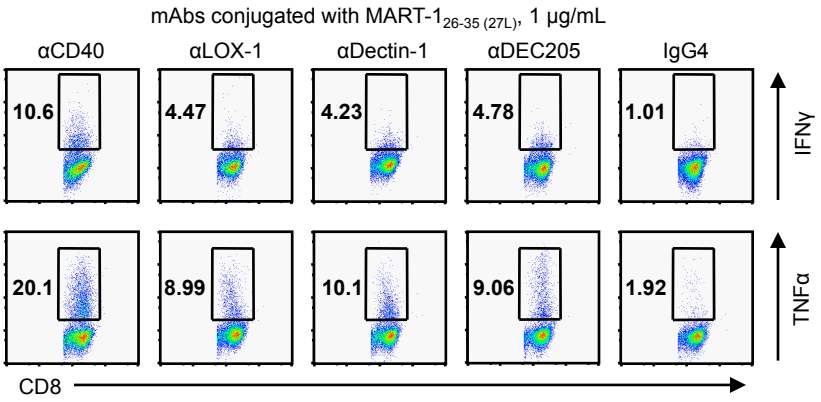

Figure 9. $CD8^+$ T cells primed with CD40-targted DCs express the highest levels of IFNγ and TNFα. Purified naïve $CD8^+$ T cells were co-cultured with Mo-DCs loaded with 1 µg/mL mAb-MART-$1_{26\text{-}35\ (27L)}$ conjugates for 9 days. $CD8^+$ T cells were then restimulated with 1 µM MART-$1_{26\text{-}35}$ and stained for intracellular IFNγ and TNFα expression. Two independent experiments showed similar results. Representative flow cytometric data are shown.

The Superiority of CD40 over LOX-1 and Dectin-1 for Boosting Memory $CD8^+$ CTLs

We compared the levels of Flu.$M1_{58\text{-}66}$-specific memory $CD8^+$ T cell responses elicited by DCs loaded with αCD40 conjugates with those elicited by αDectin-1 and αLOX-1 conjugates. These mAbs (αDectin-1 and αLOX-1) were selected based on the data in Figures 5A and 5B. Figure 11A shows that DCs loaded with 0.1 µg/mL αCD40-Flu.$M1_{58\text{-}66}$ were more efficient than DCs loaded with the same concentration of αLOX-1- or αDectin-1-Flu.$M1_{58\text{-}66}$ at activating Flu.$M1_{58\text{-}66}$-specific $CD8^+$ T cells, as measured by tetramer staining. Similarly, when compared with six other mAb-Flu.$M1_{58\text{-}66}$ conjugates, DCs loaded with αCD40-Flu.$M1_{58\text{-}66}$ resulted in the greatest level of Flu.$M1_{58\text{-}66}$-specific $CD8^+$ T cell activation (Figures 13A and 13B). Figure 11B (left) further demonstrates that DCs loaded with αCD40-Flu.$M1_{58\text{-}66}$ are far more efficient than DCs loaded with the equimolar amounts of Flu.$M1_{58\text{-}66}$. Data from five independent

experiments using cells from different healthy donors (n=6) are shown in Figure 11B (right).

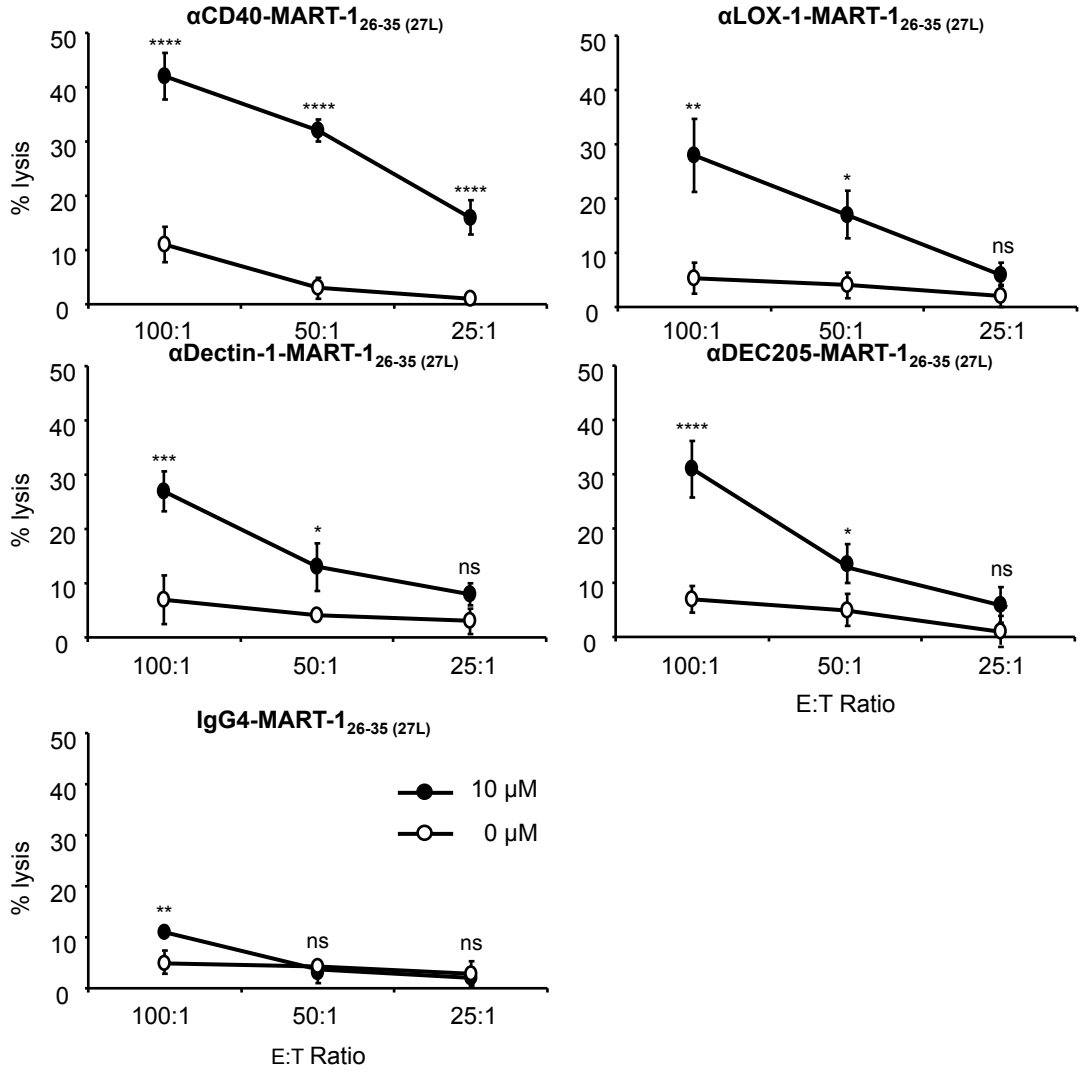

Figure 10. $CD8^+$ T cells primed with CD40-targted DCs are the most functional. A 5-h ^{51}Cr release assay using T2 cells loaded with 0 or 10 μM MART-1_{26-35} peptide. MART-1_{26-35}-specific $CD8^+$ T cells in Figure 9 were used as effector cells. Data are presented as mean ± SD of triplicate assays, and significance was determined using an ANOVA test. Two independent experiments resulted in similar data. *, $P < 0.05$; **, $P < 0.01$; ***, $P < 0.005$; ****, $P < 0.001$; ns, not significant.

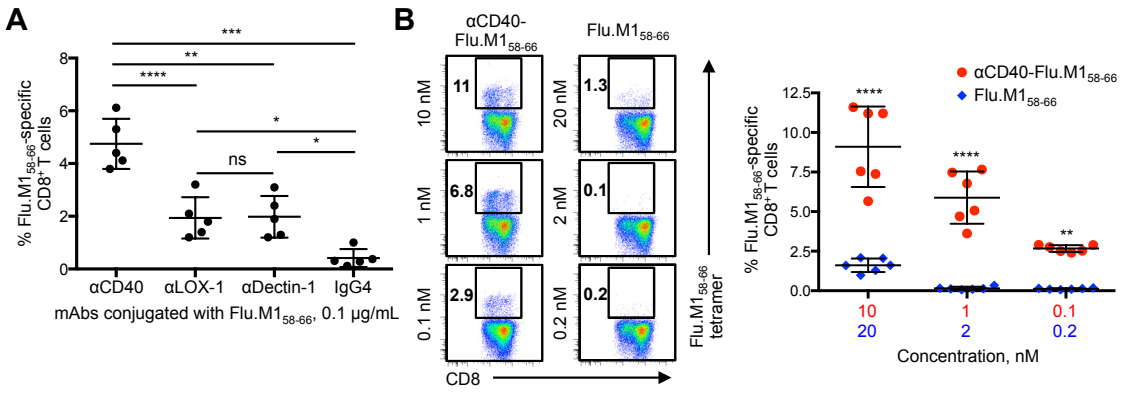

Figure 11. The superiority of CD40 over LOX-1 and Dectin-1 for boosting memory CD8$^+$ CTLs. (A–B) Purified CD8$^+$ T cells were co-cultured with Mo-DCs loaded with the indicated amounts of mAb-Flu.M1$_{58\text{-}66}$ conjugates or Flu.M1$_{58\text{-}66}$ peptide. CD8$^+$ T cells were then stained with HLA-A*A0201-Flu.M1$_{58\text{-}66}$ tetramer. (A) Frequencies of Flu.M1$_{58\text{-}66}$-specific CD8$^+$ T cells activated by Mo-DCs loaded with 0.1 μg/mL mAb-Flu.M1$_{58\text{-}66}$ conjugates. Dots represent data generated with cells from healthy donors (n=5). (B) Frequencies of Flu.M1$_{58\text{-}66}$-specific CD8$^+$ T cells elicited by Mo-DCs loaded with αCD40-Flu.M1$_{58\text{-}66}$ at 10, 1, 0.1 nM, or with Flu.M1$_{58\text{-}66}$ peptide at 20, 2, 0.2 nM. Each Flu.M1$_{58\text{-}66}$ conjugate molecule contains two molecules of Flu.M1$_{58\text{-}66}$ antigen. Representative flow cytometric data (left) and summarized data (mean ± SD) from five independent experiments (n=6) are presented. Significance was determined using an ANOVA test. *, $P < 0.05$; **, $P < 0.01$; ***, $P < 0.005$; ****, $P < 0.001$; ns, not significant.

Fractions of Flu.M1$_{58\text{-}66}$-specific CD8$^+$ CTLs elicited by DCs loaded with αCD40-Flu.M1$_{58\text{-}66}$ expressed granzyme B and perforin (Figure 12A) as well as IFNγ (Figure 12B). In line with this, they were also able to lyse T2 cells loaded with Flu.M1$_{58\text{-}66}$ peptide at both 10 and 1 nM (left, Figure 12C), while CD8$^+$ CTLs elicited with IgG4-Flu.M1$_{58\text{-}66}$ only lysed target cells loaded with 10 nM Flu.M1$_{58\text{-}66}$ peptide (right, Figure 12C). Taken together, we concluded that αCD40-Flu.M1$_{58\text{-}66}$ targeted CD40 and could thus efficiently activate Flu.M1$_{58\text{-}66}$-specific memory CD8$^+$ CTLs. In addition, targeting Flu.M1$_{58\text{-}66}$ to DCs via CD40 is more efficient at boosting Flu.M1$_{58\text{-}66}$-specific CD8$^+$ T cell responses than targeting Flu.M1$_{58\text{-}66}$ to other receptors (Figure 13), including LOX-1 or Dectin-1.

To further confirm the specialized function of CD40 for enhancing antigen cross-presentation to CD8$^+$ T cells, we used recombinant fusion proteins of mAbs and influenza

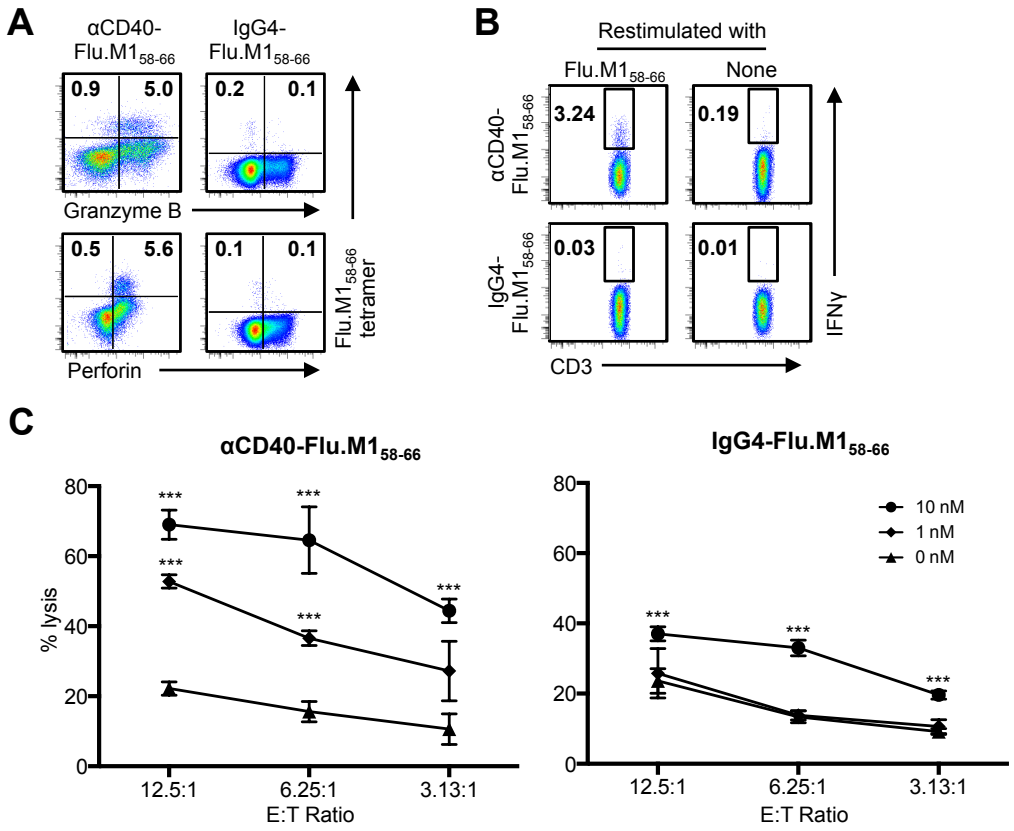

Figure 12. The superiority of CD40 over LOX-1 and Dectin-1 for boosting functional memory $CD8^+$ CTLs. (A) $CD8^+$ T cells activated with Mo-DCs loaded with αCD40-Flu.$M1_{58-66}$ or IgG4-Flu.$M1_{58-66}$ in Figure 11C were further stained for intracellularly granzyme B and perforin. Three independent experiments showed similar results. Representative flow cytometric data on the frequencies of Flu.$M1_{58-66}$-specific granzyme B^+ or perforin$^+CD8^+$ T cells are shown. (B) $CD8^+$ T cells activated with Mo-DCs loaded with αCD40-Flu.$M1_{58-66}$ or IgG4-Flu.$M1_{58-66}$ in (A) were restimulated with 1 μM Flu.M1 peptide, and intracellular IFNγ expression was assessed. Three independent experiments showed similar results. Representative flow cytometric data on the frequencies of Flu.$M1_{58-66}$-specific IFNγ^+CD8^+ T cells are shown. (C) A 5-h ^{51}Cr release assay using T2 cells loaded with the indicated amounts of Flu.$M1_{58-66}$ peptide. $CD8^+$ T cells activated with Mo-DCs loaded with 0.1 μg/mL αCD40-Flu.$M1_{58-66}$ or IgG4-Flu.$M1_{58-66}$ were used as effector cells. Error bars indicate SD of triplicate assays. Three independent experiments resulted in similar data. Significance in (C) was determined using an ANOVA test. *, $P < 0.05$; **, $P < 0.01$; ***, $P < 0.005$; ****, $P < 0.001$; ns, not significant.

viral nucleoprotein (Flu.NP). Experiments performed with recombinant fusion proteins of

mAbs and whole protein antigens (e.g., Flu.NP) are thought to be a more biologically

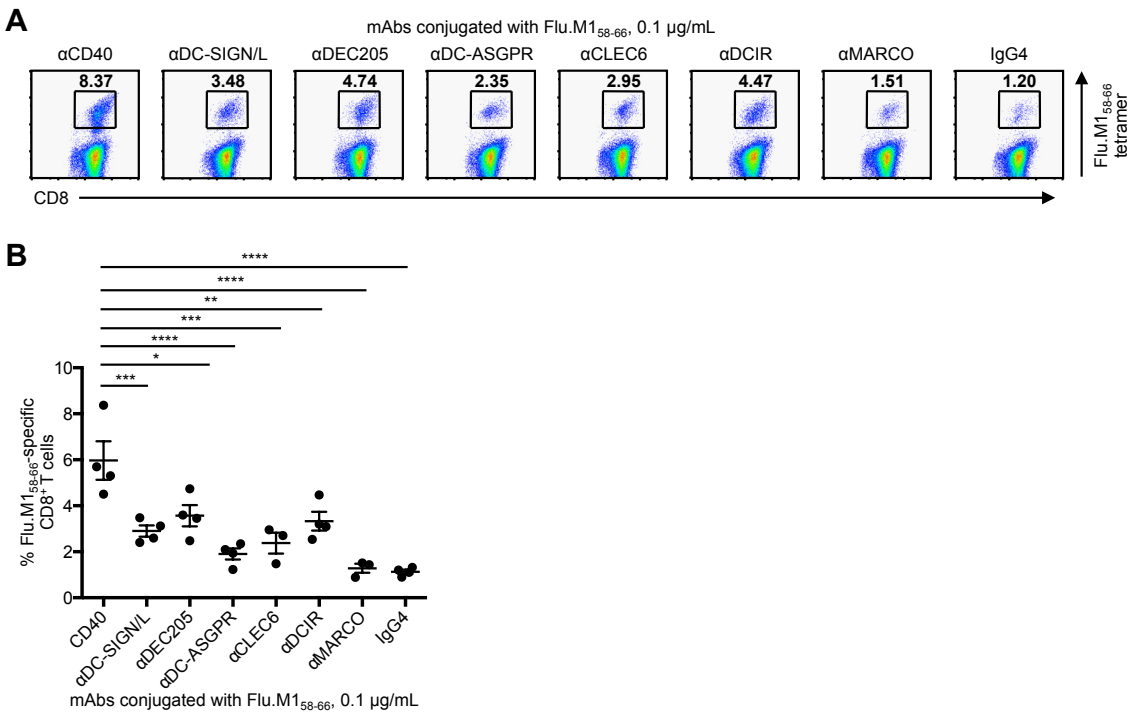

Figure 13. Targeting antigen to DCs via CD40 can efficiently activate antigen-specific memory $CD8^+$ CTLs. (A–B) Purified $CD8^+$ T cells were co-cultured for 8 days with Mo-DCs loaded with 0.1 µg/mL of the indicated mAb-Flu.$M1_{58-66}$ conjugates. $CD8^+$ T cells were stained with HLA-A*A0201-Flu.$M1_{58-66}$ tetramer. (A) Representative flow cytometric data and (B) summarized data (mean ± SD) from healthy donors (n=4) are presented. Significance was determined using an ANOVA test. *, $P < 0.05$; **, $P < 0.01$; ***, $P < 0.005$; ****, $P < 0.001$.

relevant way to assess the ability of DCs to cross-present antigens and subsequently should be utilized for the rational design of vaccines against cancers and microbial infections. It also allows us to assess the multiple repertoires of antigen-specific $CD8^+$ as well as $CD4^+$ T cell responses. CFSE-labeled PBMCs were cultured for eight days with αCD40-Flu.NP, αLOX-1-Flu.NP or αDectin-1-Flu.NP. They were then restimulated with a Flu.NP peptide pool to measure intracellular IFNγ expression. As shown in Figure 14A (left), αCD40-Flu.NP was more efficient than αLOX-1-Flu.NP or αDectin-1-Flu.NP at activating Flu.NP-specific $IFN\gamma^+CD8^+$ T cells. Data from nine independent experiments

using cells from different healthy donors are summarized in Figure 14A (right). Interestingly, however, αCD40-Flu.NP was significantly less efficient than αLOX-1-

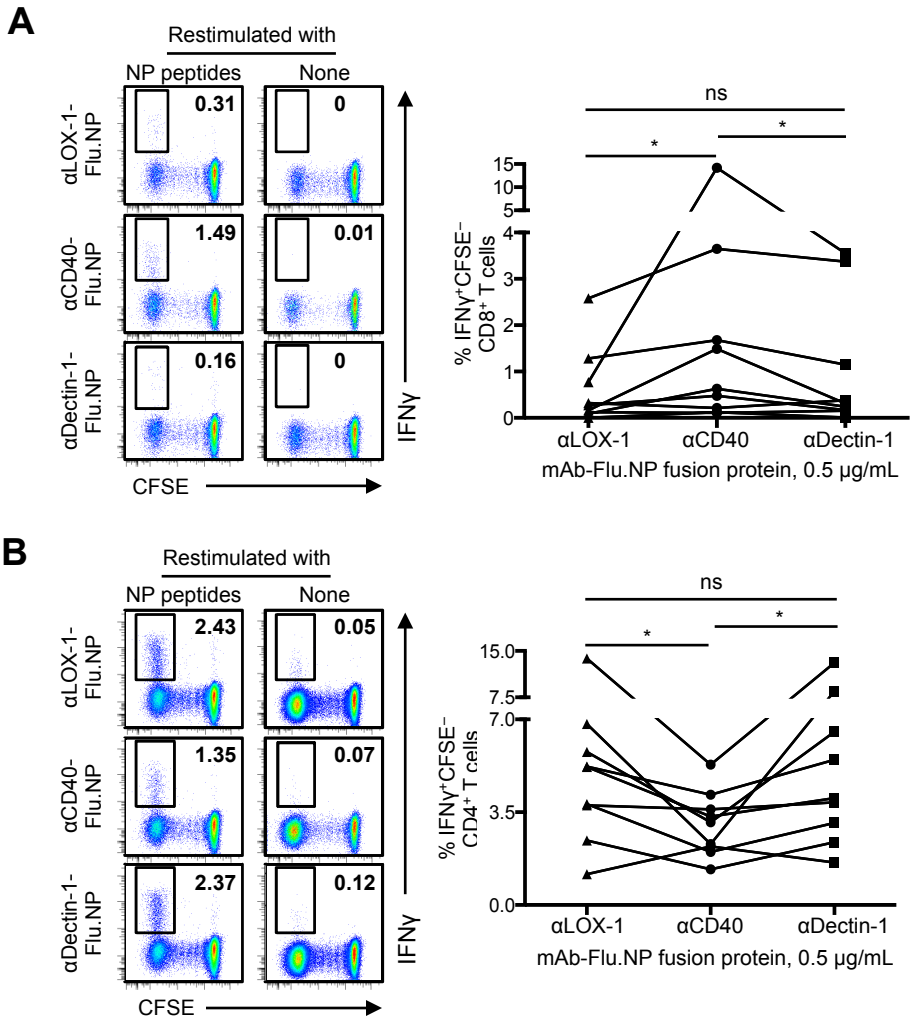

Figure 14. Functional specialty of CD40 and lectins (e.g., LOX-1 and Dectin-1) in enhancing Flu.NP-specific $CD8^+$ and $CD4^+$ T cell responses, respectively. (A–C) CFSE-labeled PBMCs from healthy donors (n=9) were cultured in the presence of 0.5 μg/mL of the indicated mAb-Flu.NP recombinant fusion proteins for 8 days. Cells were restimulated with a Flu.NP peptide pool at 1 μM (of each peptide), and intracellular IFNγ expression in live (A) $CD8^+$ and (B) $CD4^+$ T cells was assessed. Representative flow cytometric data on the frequencies of $CFSE^-IFN\gamma^+$ (A) $CD8^+$ or (B) $CD4^+$ T cells (left) and donor-matched frequencies of $CFSE^-IFN\gamma^+$ (A) $CD8^+$ and (B) $CD4^+$ T cells (right) are shown. Dots represent data generated with cells from individual donors, and significance was determined using a paired *t* test. *, $P < 0.05$; ns, not significant.

Flu.NP or αDectin-1-Flu.NP at activating Flu.NP-specific IFNγ$^+$CD4$^+$ T cells (left, Figure 14B). Data from nine independent experiments further confirmed this (right,

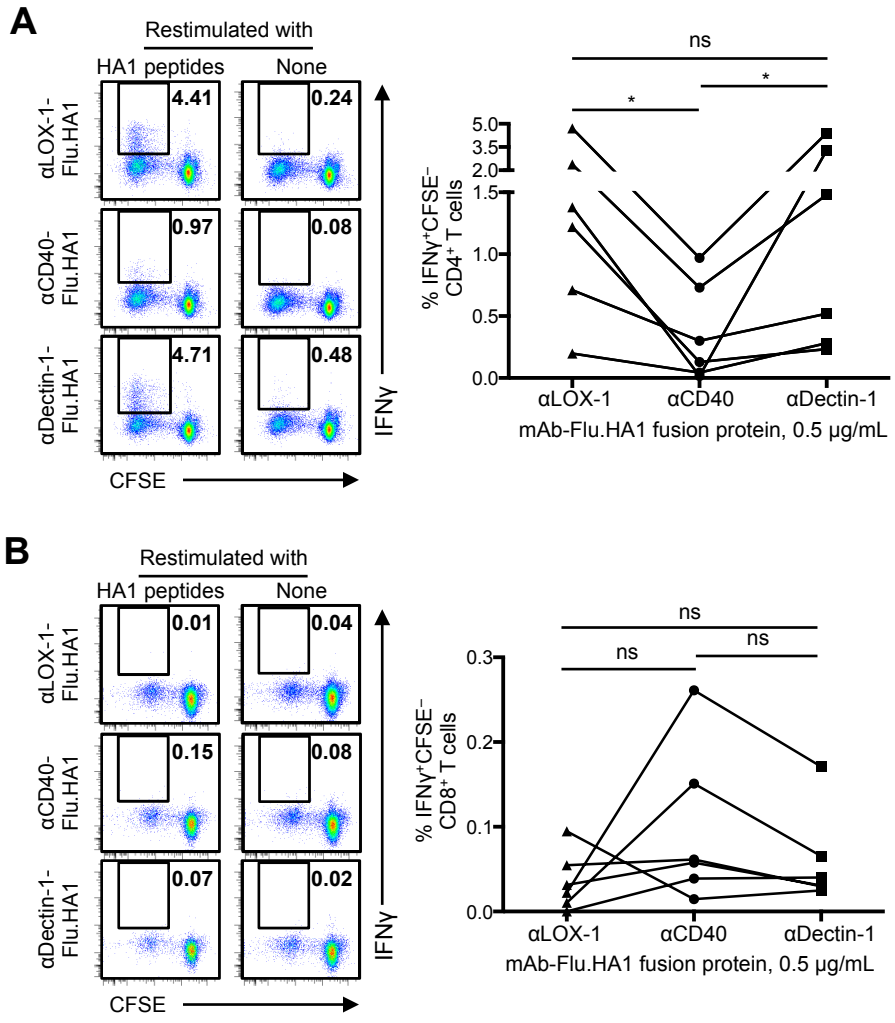

Figure 15. Functional specialty of CD40 and lectins (e.g., LOX-1 and Dectin-1) in enhancing Flu.HA1-specific CD8$^+$ and CD4$^+$ T cell responses, respectively. (A–B) CFSE-labeled PBMCs from healthy donors (n=6) were cultured in the presence of 0.5 μg/mL of the indicated mAb-Flu.HA1 recombinant fusion proteins for 8 days. Cells were restimulated with a Flu.HA1 peptide pool at 1 μM (of each peptide), and intracellular IFNγ expression in live (A) CD4$^+$ and (B) CD8$^+$ T cells was assessed. Representative flow cytometric data on the frequencies of CFSE$^-$IFNγ$^+$ (A) CD4$^+$ or (B) CD8$^+$ T cells (left) and donor-matched frequencies of CFSE$^-$IFNγ$^+$ (A) CD4$^+$ and (B) CD8$^+$ T cells (right) are shown. Dots represent data generated with cells from individual donors, and significance was determined using a paired *t* test. *, $P < 0.05$; ns, not significant.

Figure 14B). αLOX-1-Flu.NP and αDectin-1-Flu.NP resulted in similar levels of Flu.NP-specific $CD8^+$ (Figure 14A) and $CD4^+$ T cell responses (Figure 14B). The difference

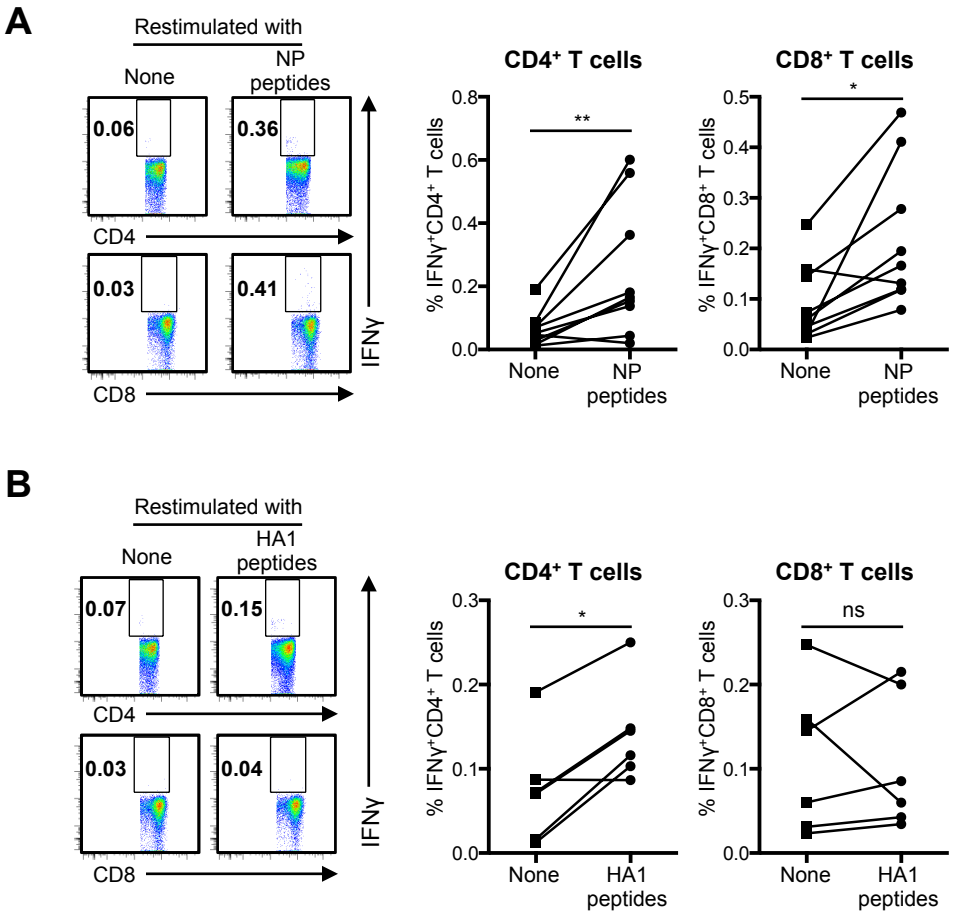

Figure 16. Frequencies of Flu.HA1- and Flu.NP-specific memory $CD4^+$ and $CD8^+$ T cells in healthy individuals. (A and B) PBMCs from healthy donors ($n \geq 6$) were stimulated with (A) Flu.NP or (B) Flu.HA1 peptide pools at 1 μM (each peptide) for 6 h. $CD4^+$ and $CD8^+$ T cells were stained for intracellular IFNγ expression. Representative flow cytometric data (left) and summarized data (right) are shown. Dots represent data generated with cells from individual healthy donors. Significance was determined using a paired *t* test. *, $P < 0.05$; **, $P < 0.01$; ns, not significant.

between CD40 and the other two receptors at eliciting $CD4^+$ T cell responses was further confirmed by assessing influenza hemagglutinin subunit 1 (Flu.HA1)-specific $IFN\gamma^+CD4^+$ T cell responses elicited with Flu.HA1 fusion proteins of the three mAbs

(Figure 15A). αCD40-Flu.HA1 was less efficient than αLOX-1-Flu.HA1 or αDectin-1-Flu.HA1 at eliciting Flu.HA1-specific $CD4^+$ T cell responses. We also measured

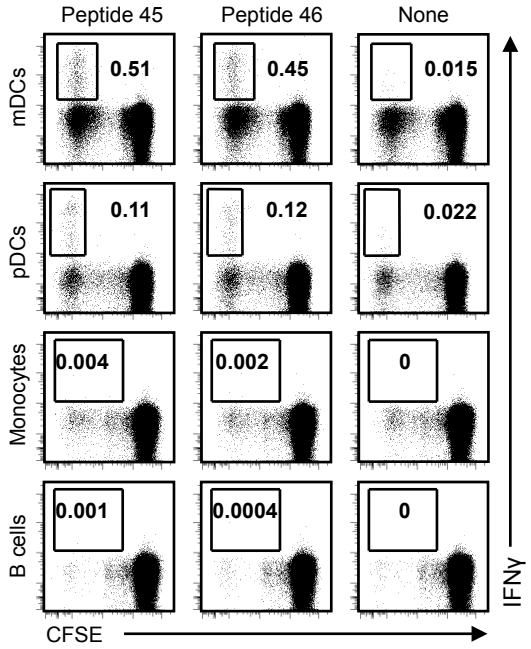

Figure 17. DCs, particularly mDCs, are the major antigen-presenting cells to elicit Flu.HA1-specific $CD4^+$ T cell responses. Blood mDCs, pDCs, $CD14^+$ monocytes, and $CD19^+$ B cells purified from the same donor were loaded with αDectin-1-HA1 at 1 μg/mL. They were then cultured for 7 days with CFSE-labeled purified autologous $CD4^+$ T cells. T cells were restimulated for 6 h with pre-determined Flu.HA1-derived peptides, GNLIAPWYAFALSRGFG (peptide 45) and WYAFALSRGFGSGIITS (peptide 46). Intracellular IFNγ expression was assessed. Two independent experiments showed similar data.

Flu.HA1-specific $CD8^+$ T cell responses (Figure 15B), but there was no significant level of Flu.HA1-specific $CD8^+$ T cell responses to the three mAb-Flu.HA1 fusion proteins. Previous studies (Lee et al., 2008; McMichael et al., 1986; Townsend and Skehel, 1982) have shown that influenza-specific $CD8^+$ memory T cells mostly target internal proteins, including Flu.NP, but not outer membrane proteins, such as Flu.HA1. Figures 16A and 16B demonstrate that the variability of the magnitude of Flu.NP- and Flu.HA1-specific T

cell responses among donors (as observed in Figures 14 and 15) was mainly due to the variability of the frequencies of pre-existing Flu.NP- and Flu.HA1-specific memory T cells of the donors. PBMCs from nine healthy donors were stimulated with Flu.NP or Flu.HA1 peptide pools. The frequencies of Flu.NP- and Flu.HA1-specific $CD4^+$ and

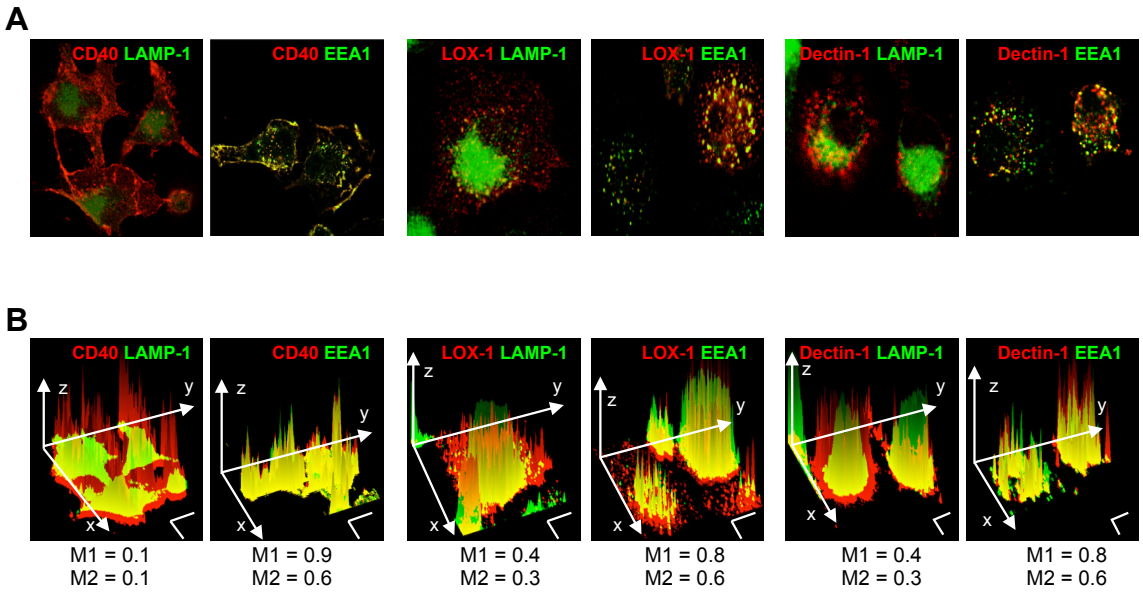

Figure 18. Distinct patterns of subcellular and intracellular localization of αCD40, αLOX-1 and αDectin-1 mAbs. (A–B) Mo-DCs were incubated with fluorescent αCD40, αLOX-1, and αDectin-1 mAbs at 1 μg/mL. DCs were further stained with αLAMP-1 and αEEA1 antibodies. Images were acquired on a Leica DMI16000 confocal microscope (100X). (A) Representative merged images of CD40, LOX-1 or Dectin-1 (red) staining and LAMP-1 or EEA-1 (green) staining are shown. Scale bar indicates 10 mm. (B) Representative three-dimensional graphs were plotted based on the fluorescence intensity (z-axis) and merged images in (A). Scale bars indicate 10 mm on both x-axis and y-axis. Mander's coefficients, M1 and M2, were calculated using the Just Another Colocalization Plugin Software (JaCoP). M1 represents the percentage of αEEA1 or αLAMP-1 mAb that overlaps with αCD40, αLOX-1, or αDectin-1 mAb. M2 represents the percentage of αCD40, αLOX-1, or αDectin-1 that overlaps with αEEA1 or αLAMP-1 mAb.

$CD8^+$ T cells were measured by intracellular IFNγ staining. Taken together, we concluded that CD40 has a specialized function to promote antigen cross-presentation to

$CD8^+$ but not $CD4^+$ T cells, in contrast to LOX-1 and Dectin-1, which promoted $CD4^+$ but not $CD8^+$ T cells.

Not only DCs, but also monocytes and B cells express CD40 (Flamar et al., 2013), LOX-1 (Li et al., 2012), and Dectin-1 (Ni et al., 2010). Therefore, both monocytes

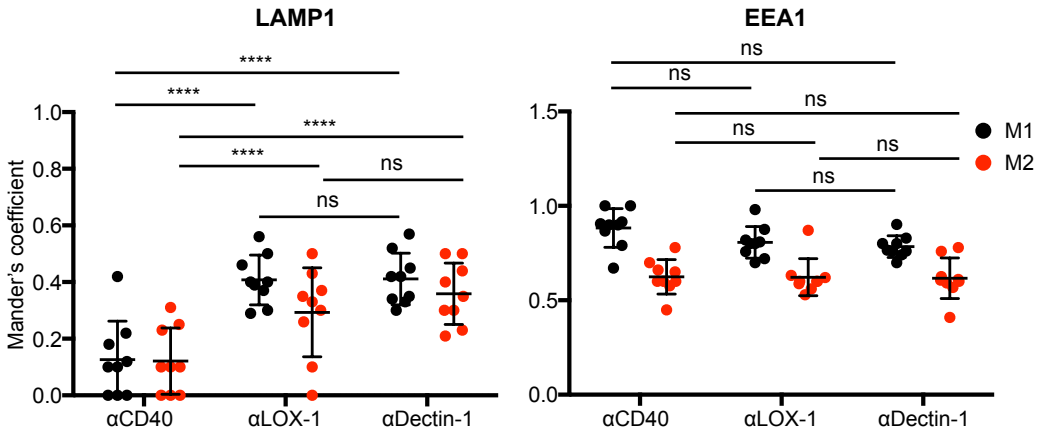

Figure 19. Distinct patterns of subcellular and intracellular localization of αCD40, αLOX-1 and αDectin-1 mAbs (summary). Summarized data represent M1 and M2 from 9 donors. For each donor, at least 100 cells from 10 pictures were acquired to calculate the colocalization values. Dots represent individual donors and error bars indicate SD. Significance was determined using an ANOVA test. ****, $P < 0.001$; ns, not significant.

and B cells targeted with antigens could also contribute to the $CD4^+$ and $CD8^+$ T cell responses observed in Figures 14 and 15. However, we have previously reported that the majority of antigen-specific T cell responses elicited by targeting antigens to CD40 and LOX-1 were due to the roles of DCs (Flamar et al., 2013; Li et al., 2012). Figure 17 further demonstrates that DCs, particularly myeloid DCs (mDCs), loaded with aDectin-1-Flu.HA1 are far more efficient than loaded plasmacytoid DCs (pDCs), monocytes, or B cells at eliciting Flu.HA1-specific T cell responses.

Distinct Patterns of mAb-Bound Receptor Localization in Subcellular and Intracellular Compartments

The cellular compartments where antigens are delivered can impact the outcome of antigen cross-presentation by DCs (Belizaire and Unanue, 2009; Burgdorf et al., 2007; Burgdorf et al., 2008; Chatterjee et al., 2012; Cohn et al., 2013; Harding et al., 1991; Zehner et al., 2011). To further understand the functional specialties of CD40, LOX-1, and Dectin-1 that have been observed in this study, we examined subcellular and intracellular localization of receptor-bound αCD40, αLOX-1, and αDectin-1 mAbs in DCs (Figure 18). We found two major differences between αCD40 and the other two mAbs. First, a large fraction of αCD40 mAb stayed at the plasma membrane of DCs (left, Figure 18A). In contrast, the majority of αLOX-1 and αDectin-1 mAbs were internalized into the cell cytoplasm (middle and right, Figure 18A). Second, αCD40 mAb that did internalize into the cytosolic compartment mainly accumulated in the early endosomes, as it co-localized with anti-early endosome antigen 1 mAb (αEEA1) (left, Figure 18A). In contrast, significant fractions of αLOX-1 (middle, Figure 18A) and αDectin-1 mAbs (right, Figure 18A) localized into both the early and late endosomes, as they co-localized with αEEA1 as well as anti-lysosomal-associated membrane protein 1 mAb (αLAMP-1, targeting the late endosome). These observations were further confirmed by the Mander's coefficients acquired by using the Image-J software (Figures 18B and 19). M1 represents the fraction of αEEA1 or αLAMP-1 mAb that overlaps with αCD40, αLOX-1, or αDectin-1 mAb; while M2 represents the fraction of αCD40, αLOX-1, or αDectin-1 that overlaps with αEEA1 or αLAMP-1 mAb. Only ~10% of DCs showed co-localization of αCD40 and αLAMP-1 mAbs, while more than 75% of DCs showed co-localization of αCD40 and αEEA-1 mAbs. In contrast to αCD40 mAb, 35-45% of DCs showed co-

localization of αLOX-1 and αLAMP-1 mAbs. αDectin-1 mAb showed patterns of subcellular localization that were similar to what were observed with αLOX-1 mAb. Summarized data from nine donors, each with analyses done on at least 100 cells are shown in Figure 19. Taken together, the patterns of subcellular and intracellular localization of CD40-bound αCD40 mAb were distinct from those of αLOX-1 and αDectin-1 mAbs, which showed a high similarity.

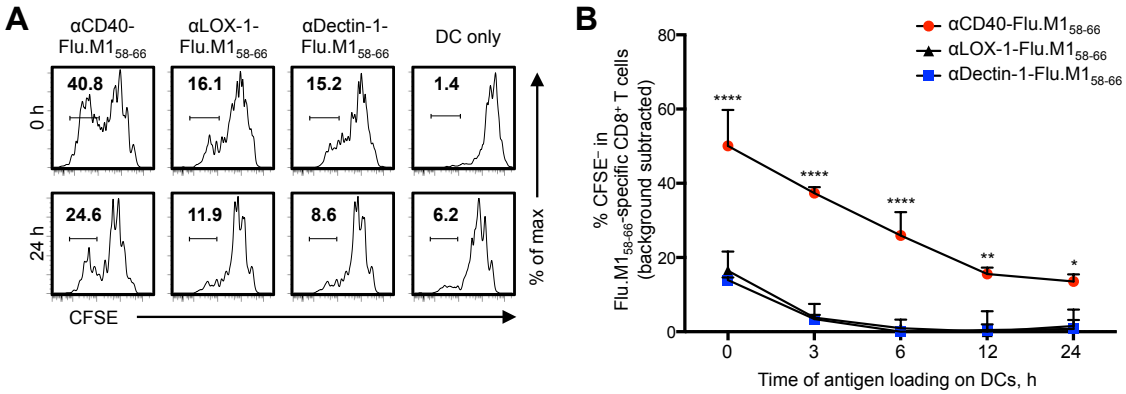

Figure 20. Kinetics of antigen cross-presentation of DCs targeted via CD40, LOX-1, or Dectin-1. (A and B) CFSE-labeled Flu.M1$_{58-66}$-specific CD8$^+$ T cell lines were co-cultured with Mo-DCs pre-incubated for the indicated time periods with 1 nM (0.1 μg/mL) mAb-Flu.M1$_{58-66}$ fusion proteins. On day 6, CD8$^+$ T cell proliferation was assessed by flow cytometry. (A) Representative flow cytometric data from 0 and 24 h. (B) Summarized data are presented as mean ± SD of triplicate assays. Significance was determined using an ANOVA test. Two independent experiments resulted in similar data. *, $P < 0.05$; ***, $P < 0.005$; ****, $P < 0.001$.

To further investigate the kinetics of antigen presentation of DCs targeted with different conjugates, CFSE-labeled Flu.M1$_{58-66}$-specific CD8$^+$ T cell lines were co-cultured with DCs incubated for different time periods (0, 3, 6, 12, and 24 h) with the three different mAb-Flu.M1$_{58-66}$ (Figure 20). After six days, CD8$^+$ T cell proliferation was assessed by measuring CFSE dilution. As shown in Figures 20A and 20B, DCs loaded with αCD40-Flu.M1$_{58-66}$ were more efficient than DCs loaded with the other two

mAb-Flu.M1$_{58-66}$ conjugates or Flu.M1$_{58-66}$ peptide at all time points tested. This suggests that CD40-targeted antigens could be more efficiently cross-presented via MHC class I than LOX-1- or Dectin-1-targeted antigens. It also indicates that DCs targeted with antigens via CD40 are able to present antigens for a longer time period than DCs targeted with antigens via Dectin-1 or LOX-1.

Discussion

Understanding the biology of human DC surface receptors and the functional consequences of the actions of individual receptors is fundamental for the rational design of medicines for cancers, inflammatory diseases (including autoimmune diseases) and microbial infections. Of the many different receptors expressed on the surface of DCs, lectin-like receptors have been generally considered as the main pattern-recognition receptors. Some of these receptors, Dectin-1 (Duluc et al., 2014; Joo et al., 2015; LeibundGut-Landmann et al., 2007), DCIR (Fujikado et al., 2008), DC-SIGN (Geijtenbeek and Gringhuis, 2009), LOX-1 (Joo et al., 2014), and DC-ASGPR (Li et al., 2012), are known to play important roles in shaping the quality and quantity of host immune responses. These receptors can also capture foreign antigens, as well as act as scavenger receptors for self-antigens. The ability of these receptors to capture antigens and deliver them to intracellular compartments makes them novel targets for DC antigen delivery to enhance antigen cross-presentation to T cells. However, one major question still remains: "Which targeted receptor results in optimal antigen cross-presentation to T cells?" This study has demonstrated that CD40 is superior to eight other lectins and scavenger receptors at cross-presenting antigen to $CD8^+$ T cells. This was confirmed with

both a tumor-associated self antigen and two different forms of viral antigens (peptide epitope and whole protein antigens). However, this was not the case for antigen presentation to $CD4^+$ T cells. DC lectins (e.g., LOX-1 and Dectin-1) were superior to CD40 at presenting antigens to $CD4^+$ T cells. This superiority of lectins (e.g., LOX-1 and Dectin-1) over CD40 was demonstrated by assessing the whole repertoires of T cell responses specific to Flu.NP and Flu.HA1) in nine independent experiments using cells from different healthy donors.

To further understand the functional specialization of CD40 and lectins (LOX-1 and Dectin-1), we examined the subcellular and intracellular localization of receptor-bound mAbs in DCs. Previous studies (Burgdorf et al., 2007; Burgdorf et al., 2008) showed that early endosomes are essential for the cross-presentation of antigens. Recently, Cohn (Cohn et al., 2013) and Chatterjee (Chatterjee et al., 2012) also showed that antigen delivery to early endosomes could result in enhanced antigen cross-presentation to $CD8^+$ T cells. In this study, however, we found that significant fractions of receptor-bound αLOX-1 and αDectin-1 mAbs also localized to the early endosomes, although targeting CD40 was far more efficient at eliciting $CD8^+$ T cell responses than targeting LOX-1 or Dectin-1. Quantitative analysis of the intracellular compartments across nine different donors further revealed that αCD40 mAb localized mainly to the early endosomes, but αLOX-1 and αDectin-1 localized to both the early and late endosomes. This suggested that there could be other critical factors, in addition to the roles of early endosomes, that can further influence the efficiency of antigen cross-presentation by DCs via MHC class I molecules. Accordingly, we showed that a large fraction of αCD40 mAb remained at the plasma membrane even after a 1-h incubation at

37°C, whereas the majority of both αLOX-1 and αDectin-1 mAbs were internalized into the cytoplasm. Slow internalization to early endosomes or rapid antigen recycling, as speculated previously (Chatterjee et al., 2012; Cohn et al., 2013), could result in increased antigen stability, followed by prolonged antigen presentation and enhanced $CD8^+$ T cell responses, as shown in Figure 20. However, this entire process has yet to be fully demonstrated. The activating signals through CD40 do not promote antigen cross-presentation by DCs (Chatterjee et al., 2012), although DC maturation caused by αCD40 enhances antigen cross-presentation by mouse DCs (Bonifaz et al., 2004; Delamarre et al., 2003). In addition, LOX-1 endocytoses heat shock proteins independently of TLR2/4 pathways, but may require activating signals to promote antigen presentation (Delneste et al., 2002; Jeannin et al., 2005). However, CD40 signaling does not promote LOX-1-mediated antigen presentation (Delneste, 2004).

In summary, this study reports novel and specialized functions of CD40 versus lectins (Dectin-1 and LOX-1) expressed on the surface of human DCs. Data from this study also provide fundamental information for the rational design of vaccines against cancers and viral infections. In spite of recent success with the inhibitors of immune checkpoints (e.g., αCTLA4, αPD-1, and αPD-L1 antibodies), particularly in cancer immunotherapy, there is still a need for boosting tumor-specific immunity in patients for better treatment outcomes.

CHAPTER FOUR

Preclinical Assessment of CD40 Targeting Vaccines for HPV16-Associated Malignancies

Abstract

Human papillomavirus (HPV) infection, particularly by HPV16, can cause cancer in various types of mucosa. Therefore, development of safe and effective vaccines that can prevent and cure this cancer is highly desirable. Herein, we report a new vaccine model, a recombinant fusion protein of humanized αCD40 monoclonal antibody with HPV16.E6/7 (αCD40-HPV16.E6/7). αCD40-HPV16.E6/7 was able to target human CD40 expressed on dendritic cells (DCs) and could thus activate HPV16.E6/7-specific $CD8^+$ and $CD4^+$ T cells from the blood of $HPV16^+$ head and neck cancer patients. Next, we demonstrated that the combination of αCD40-HPV16.E6/7 and poly(I:C) primed and activated HPV16.E6/7-specific T cells, especially $CD8^+$ T cells, in human CD40 transgenic mice (C57BL/6 background). This was further confirmed when the immune responses elicited by αCD40-HPV16.E6/7 were compared with those generated by αLangerin-HPV16.E6/7. αCD40-HPV16.E6/7 was efficient at stimulating $CD8^+$ T cell responses, while αLangerin-HPV16.E6/7 was efficient at eliciting $CD4^+$ T cell responses, including IL-10-producing $CD4^+$ T cell responses. Lastly, we demonstrated that αCD40-HPV16.E6/7 plus poly(I:C) could efficiently prevent TC-1 tumor growth, mount therapeutic immunity, and could thus suppress and reject pre-established TC-1 tumors. This study will aid in the design of preventive and therapeutic vaccines against HPV-associated mucosal malignancies.

Introduction

Squamous cell carcinomas (SCCs) account for more than 90% of tumors in the head-and-neck cancer cases and have been a major cause of morbidity and mortality worldwide(Sanderson and Ironside, 2002). Risk factors, including smoking tobacco and alcohol consumption, were considered to be the main environmental causes for the incidence of head and neck cancers(Blot et al., 1996). However, during the past 30 years, the incidence and epidemiology of head-and-neck cancers has changed drastically, with the cause shifting from environmental risk factors to human papillomavirus (HPV) infection. By January 2014, the prevalence of HPV-related oropharyngeal squamous cell carcinomas had reached 50% in Europe and 65% in the United States (Stein et al., 2015; Young et al., 2015). In addition to head and neck cancer, studies have shown that around 40 HPV types are known to infect the mucosal surface of the genital tract, 14 of which are detectable in nearly all biopsies of invasive cervical cancer (Kreimer et al., 2005). It has also been estimated that the worldwide HPV prevalence in cervical carcinomas has reached 99.7% (Stein et al., 2015; Walboomers et al., 1999). Among all the HPV-related squamous cell carcinomas, HPV16 is responsible for 86.7% of HPV^+ oropharyngeal SCCs (Kreimer et al., 2005), and over 50% of HPV^+ cervical carcinomas (Walboomers et al., 1999).

The carcinogenic mechanism of HPV-related SCCs also differs from those associated with environmental factors. It is primarily driven by the expression of oncoproteins E6 and E7, which bind and inactivate p53 and pRB (a retinoblastoma tumor suppressor gene product), respectively, and thus deregulate cell cycle with loss of control of crucial cellular events, including DNA replication, DNA repair and apoptosis (Munger

et al., 1992; Tommasino and Crawford, 1995). Up to 22% of adults are HPV16-seropositive, but most primary infections are cleared without sequelae (de Sanjose et al., 2007; Dunne et al., 2006; Newall et al., 2008; Woodman et al., 2001). However, in a small proportion of individuals, their immune systems fail to eradicate the virus despite continual expression of viral oncoproteins E6 and E7 in infected cells. Such persistent infection can lead to cancers. Currently available vaccines, Gardasil (U.S. FDA, 2006) and Cervarix (U.S. FDA, 2009), are not effective at eliminating pre-existing HPV infection and related malignancies (Schiller et al., 2008). It is therefore important to develop an effective therapeutic vaccine against HPV16-associated malignancies. In line with these findings, several therapeutic vaccine models have been designed and tested in preclinical and clinical settings. These include E6- and/or E7-derived peptides (de Vos van Steenwijk et al., 2012; Kenter et al., 2009; Steller et al., 1998; Voskens et al., 2012), proteins (Fausch et al., 2003; Gerard et al., 2001), DNA plasmids (Lin et al., 2010; Peng et al., 2013) and live vector vaccines (Gunn et al., 2001; Jabbar et al., 2000; Lin et al., 2002; Maciag et al., 2009). However, none of these vaccine models have been approved. Some of these current vaccine models might also confront significant safety issues, especially in immune-compromised individuals who have HPV-associated malignancies. Most importantly, eliciting robust therapeutic immune responses against E6 and/or E7 in patients with HPV-associated cancers still remains a major challenge (Kenter et al., 2008; Stanley, 2008; Welters et al., 2008). Recent compelling evidence also indicates that the lack of significant clinical improvements with the current vaccine models is strongly associated with an immune suppressive microenvironment in tumors.

Dendritic cells (DCs) are major antigen-presenting cells (APCs) that are able to efficiently prime $CD8^+$ T cells. Both endogenous and exogenous antigens can be presented by DCs in the context of major histocompatibility class I (MHC I)- peptide complex. Among various types of APCs, DCs are the most efficient at cross-presenting antigens to prime and boost naïve and memory $CD8^+$ T cells, respectively (Delamarre and Mellman, 2011; Jung et al., 2002; Segura and Villadangos, 2009). Both effector and memory $CD8^+$ T cells play a crucial role in therapeutic immunity against cancers and viral infections. Thus, the potent ability of DCs to cross-present antigens to $CD8^+$ T cells makes them ideal cellular targets for the rational design of cancer vaccines (Bonifaz et al., 2002; Bonifaz et al., 2004).

In this study, we generated recombinant fusion protein of αCD40 antibody and HPV16.E6/7 (αCD40-HPV16.E6/7). We then validated that αCD40-HPV16.E6/7 targeted CD40 expressed on DCs and could thus activate E6/7-specific $CD4^+$ and $CD8^+$ T cells in the blood of head-and-neck cancer patients. We also assessed the immunogenicity and efficacy of αCD40-HPV16.E6/7 in human CD40 transgenic mice.

Materials and Methods

Antibodies, Peptides, Tetramers and Other Reagents

Fluorescent dye-labeled αCD8, αCD4, and αIFNγ were purchased from BioLegend. αCD3 was purchased from BD Biosciences. Live/Dead fixable dead cell stain kit was from Invitrogen. Overlapping 15-mer peptides (staggered by 11 amino acids) spanning the entire HPV16.E6 and HPV16.E7 proteins, and human prostate specific antigen (PSA) were purchased from Mimotopes. IL-2, IL-7, and IL-15

(PeproTech) were used PBMC cultures. In mouse experiments, αB220 (BD Biosciences), αCD3 (BD Biosciences), αCD4 (eBioscience), αCD8 (BD Biosciences), αCD11c (BD Biosciences), αIL-10 (BioLegend), and H-2D^{b}-HPV16.E7$_{RAHYNIVTF}$ tetramer labeled with fluorescent dye (MBL International) were used. Poly(I:C) was purchased from Invivogen. Phytohemagglutinin (PHA) was purchased from Sigma. Mouse CD8^{+} T cell (negative) enrichment kit and CD4^{+} T cell (positive) enrichment kit were both purchased from StemCell. DC-targeting antibodies are described below.

DC-Targeting mAbs

αCD40 (12E12) specific for ectodomains of human CD40, was previously described (Flamar et al., 2013). αLangerin (4C7) specific for ectodomains of human Langerin (4C7) was generated using receptor ectodomain.hIgG (human IgG1 Fc) and AP (human placental alkaline phosphatase), as previously described (Ni et al., 2010). Cloned mAbs were purified by HPLC using MabSelect resin (GE Healthcare). The specificities of mAbs were verified by their specific binding to corresponding receptors expressed on 293F cells transfected with the full-length receptors. The specificities of the mAbs were also confirmed with ELISA by comparing with their corresponding recombinant receptor-Fc and hIgG-Fc fusion proteins (Ni et al., 2010). Chimeric mAbs containing human IgG4 heavy chain with two site mutations (S228P and L235E) were made (Reddy et al., 2000).

Recombinant Fusion Proteins of mAb-HPV16.E6/7

Fusion proteins bearing the HPV16.E6 and E7 proteins fused to the heavy chain C-terminus were produced using methods previously described and are exemplified in the GenBank sequences of a humanized αCD40 (12E12) derivative αCD40VH2-HPV16.E6/7 (GenBank KP684039) paired with the corresponding light chain αCD40VK2-hIgGK sequence within KM660792.

Human Cells, Cell Culture Medium, and In Vitro Experiments

All human samples were from donors who provided a written informed consent prior to inclusion in the study in accordance to the approval by the Institutional Review Boards at Baylor Research Institute, Baylor University Medical Center, and Icahn School of Medicine at Mount Sinai. PBMCs were enriched from peripheral blood of $HPV16^+$ head and neck cancer patients by density gradient centrifugation with Ficoll Paque PLUS (GE Healthcare). RPMI 1640 medium (Gibco), supplemented with 10% heat-inactivated human AB serum (Gemini), 50 unit/mL penicillin, 50 μg/mL streptomycin, 2 mM L-glutamate, 1X non-essential amino acids (Sigma), 25 mM HEPES (Life Technologies), and 1 mM sodium pyruvate (Sigma), was used as cell culture medium for human in vitro experiments. A total of 5 x 10^5 PBMCs were incubated in the presence of αCD40-HPV16.E6/7 at 0.2 μg/mL, or whole E6/7 protein, E6/7 peptide pool at same final molar mass concentration as HPV16.E6/7 in αCD40-HPV16.E6/7 for 9 days in a 37°C incubator with 5% CO_2. IL-2 (50 units/mL), IL-7 (50 units/mL), and IL-15 (50 ng/mL) were supplemented on day 2. Cells were recovered on day 9 and restimulated with HPV16.E6/7 peptide clusters and peptide pool, PSA peptide pool, at 1 μM, or PHA at 5

μg/mL for either 48 h for quantification of IFNγ in the supernatant by Luminex, or for 6 h in the presence of brefeldin A for intracellular staining of IFNγ expression by $CD4^+$ and $CD8^+$ T cells. Mouse splenic $CD4^+$ T cells were similarly intracelluarly stained for IL-4 when restimulated the indicated stimuli. For binding test of αCD40-HPV16.E6/7 on human PBMCs or mouse splenocytes, cells were loaded with the indicated amounts of fusion proteins and incubated on ice in the dark for 25 min, followed by washing with PBS. All flow cytometry data were collected on FACSCanto II (BD Biosciences) and analyzed with FlowJo v9 (Tree Star).

Mice, Immunization, Tumor Implantation and Sample Collection

hCD40Tg mice (ImmuRx) used were 6-to-10-week-old females. Mouse experiments were conducted with the approval of the Institutional Animal Care and Use Committee at Baylor Research Institute. In experiments testing the immunogenicity of HPV16.E6/7 recombinant fusion proteins, hCD40Tg or wild-type mice were immunized either s.c. or i.p., as indicated, on days 0, 14 and 28, with 100 μL of vaccine composed of 30 μg αCD40-HPV16.E6/7 or αLangerin-HPV16.E6/7, and 50 μg poly(I:C) in 100 μL PBS. In tumor treatment experiments, a total of 2×10^4 TC-1 cells were injected s.c. in the left flank of the mice after shaving (marked as day 0). Mice with tumor cells were then randomized into four groups at 10 per group. A dose of vaccine composed of 30 μg αCD40-HPV16.E6/7 and 50 μg poly(I:C) in 100 μL PBS was given to each mouse, in three of the four groups, s.c., i.p., or i.m., as indicated, on days 6, 12, 18, 24, 30, and 36 post tumor implantation. The last group was left unimmunized. In one tumor treatment experiment, hCD40Tg mice were implanted with TC-1 cells and were injected with

vaccine on days 6, 12, and 18. In tumor protection experiments, hCD40Tg mice were immunized with the indicated vaccine on days 0, 14, 28. On day 35, immunized mice and unimmunized controls were injected with TC-1 cells. In all TC-1 cell-related experiments, tumor volumes were measured twice every 7 days from day 0. Flow cytometric analysis of the tumor-infiltrating tetramer^{+}CD8^{+} T cells was performed on single-cell suspensions of tumors processed with mouse tumor dissociation kit (Miltenyi Biotec) from tumor-bearing mice. Peripheral blood from mice was collected from the retro-orbital sinus into tubes coated with heparin (Baylor University Medical Center). Spleen was also collected from all the mice and processed into single-cell suspension with frosted-end glass slides (Fisher Scientific).

ELISpot Assays

Mouse IFNγ ELISpot^{Plus} pre-coated plates and reagents were obtained from Mabtech. Briefly, purified splenic CD4^{+} and CD8^{+} T cells from immunized mice were stimulated with γ-irradiated wild-type splenocytes loaded with the indicated peptide pools (1 mM). After 40-h incubation, plates were washed and incubated with biotinylated rat anti-mouse IFNγ for 2 h. After washing plates, streptavidin-horseradish peroxidase (HRP) was added and incubated for 1 h. IFNγ was detected using 3,3',5,5'-tetramethylbenzidine (TMB). The reaction was terminated once the formation of discrete purple-colored spots was detected. Spots were counted using ELISpot services (Zellnet Consulting).

Statistical Analysis

Primary methods of data analysis included descriptive statistics (mean and SD). Differences between two groups were detected using Student's t test or analysis of variance, as indicated in figure legends. Significance was set at $P < 0.05$. Data are presented as the mean ± SD. All data sets were calculated and analyzed with Prism 6 (GraphPad Software).

Results

Generation of αCD40-HPV16.E6/7 Protein

Recombinant fusion protein of humanized αCD40 antibody (12E12) and HPV16.E6/7 (αCD40-HPV16.E6/7) were generated as previously described (Flamar et al., 2013; Joo et al., 2014; Li et al., 2012). As shown in Figure 21A, αCD40-HPV16.E6/7 carries $E6_{1-120}$ and $E7_{1-60}$. HPV16.E6 and E7 sequences were associated with αCD40 through a linker sequence. Figure 21B (left) further illustrates the structure of αCD40-HPV16.E6/7 protein generated. Results from SDS-PAGE analysis of the parental humanized αCD40 antibody, αCD40-HPV16.E6/7, and control IgG4-HPV16.E6/7 are shown in Figure 21B (right).

We next tested whether αCD40-HPV16.E6/7 bound to human CD40. Human CD40 transfected CHO cell line was stained with different amounts (0.01 to 10 μg/mL) of αCD40-HPV16.E6/7 and IgG4-HPV16.E6/7. As shown in Figure 22A, αCD40-HPV16.E6/7 bound to CHO-hCD40 in a dose-dependent manner, while IgG4-HPV16.E6/7 showed no binding capacity. Neither αCD40-HPV16.E6/7 nor IgG4-HPV16.E6/7 bound to CHO cells transfected with a mock plasmid. αCD40-HPV16.E6/7

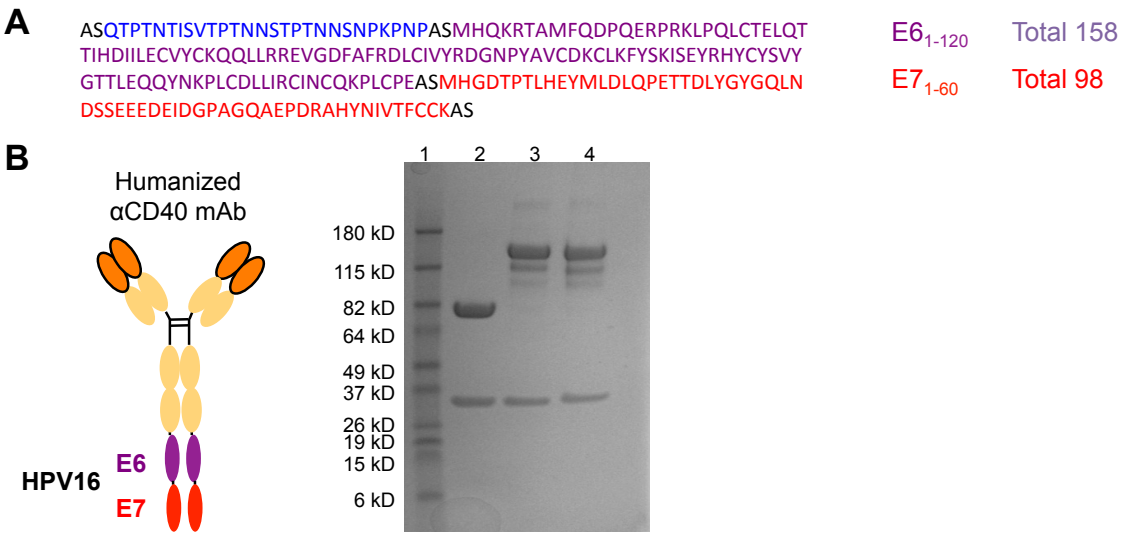

Figure 21. Composition of recombinant fusion protein αCD40-HPV16.E6/7. (A) Amino acid sequence of HPV16.E6/7. Linker (blue), E6 (magenta), and E7 (red) are shown. (B) Left, schematic representation of αCD40-HPV16.E6/7. Right, reducing SDS-PAGE analysis of purified recombinant fusion proteins. Lane 1, molecular weight ladder; Lane 2, αCD40; Lane 3, αCD40-HPV16.E6/7; Lane 4, control IgG4-HPV16.E6/7.

was also able to efficiently bind to $CD11c^+$ myeloid DCs (mDCs) in the blood even at a concentration of 0.002 μg/mL (Figure 22B, left), while IgG4-HPV16.E6/7 did not. Summarized data from two experiments are shown in (Figure 22D, right). Similarly, αCD40-HPV16.E6/7 was able to bind to blood B cells and plasmacytoid DCs (pDCs) (Figure 23, left), but not T cells or monocytes (Figure 23, right). Taken together, we conclude that αCD40-HPV16.E6/7 could efficiently bind to CD40 and could thus target CD40-expressing APCs, especially DCs.

αCD40-HPV16.E6/7 Can Activate HPV16.E6/7-Specific $CD8^+$ and $CD4^+$ T Cells from Head-and-Neck Cancer Patients

We tested whether αCD40-HPV16.E6/7 could activate HPV16.E6/7-specific T cells from $HPV16^+$ head and neck cancer patients. Peripheral blood mononuclear cells (PBMCs) were cultured for 7 days in the presence of 0.2 μg/mL αCD40-HPV16.E6/7 or

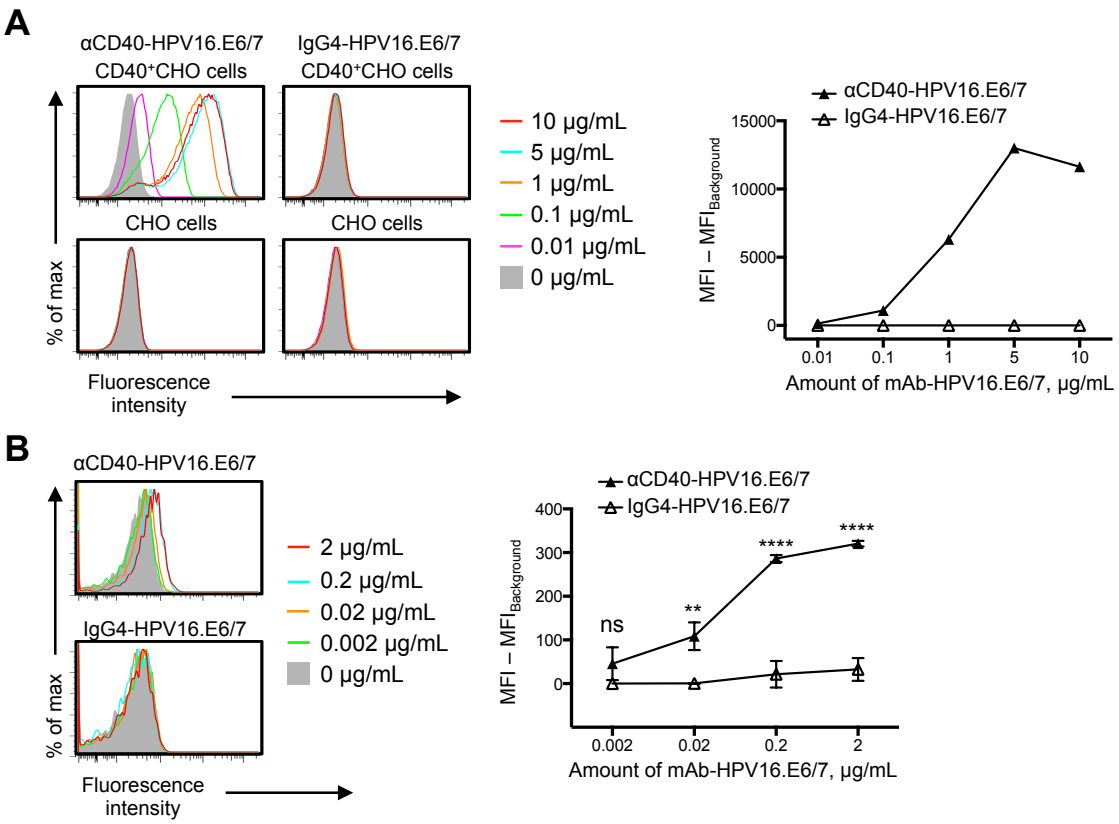

Figure 22. αCD40-HPV16.E6/7 can bind human DCs. (A) Binding of αCD40-HPV16.E6/7 or control IgG4-HPV16.E6/7 to CD40-expressing or control CHO cells. Left, histogram overlays showing distributions of fluorescence intensities (MFIs) of fusion proteins at 10, 5, 1, 0.1, 0.01 and 0 µg/mL. Right, MFI comparisons between fusion proteins on CD40-expressing CHO cells. (B) Binding of αCD40-HPV16.E6/7 or control IgG4-HPV16.E6/7 to Lin 1^{-}HLA-$DR^{+}CD11c^{+}$ mDCs. (D) Left, histogram overlays showing distributions of MFIs of fusion proteins at 2, 0.2, 0.02, 0.002 and 0 µg/mL. Right, MFI comparison between fusion proteins. Results are representative of two independent experiments. Data are presented as mean ± SD and significance was calculated using an ANOVA test. *, $P < 0.05$; **, $P < 0.01$; ****, $P < 0.001$; ns, not significant.

HPV16.E6/7 peptide pool as a control. Cells were then restimulated for 48 h with HPV16.E6/7 peptide pool or control peptides. The supernatants were collected for quantification of IFNγ. Figure 24A shows that both αCD40-HPV16.E6/7 and HPV16.E6/7 peptide pool were able to expand HPV16.E6/7-specific IFNγ-producing T cells. They produced significant amount of IFNγ in response to HPV16.E6/7 peptide

pool, but not control peptides. Interestingly, αCD40-HPV16.E6/7 protein was more efficient than HPV16.E6/7 peptide pools at eliciting IFNγ-producing HPV16.E6/7-specific T cell responses in the experiments performed with certain patients, such as patient 1. Data from experiments performed with PBMCs from nine patients are summarized in Figure 24B.

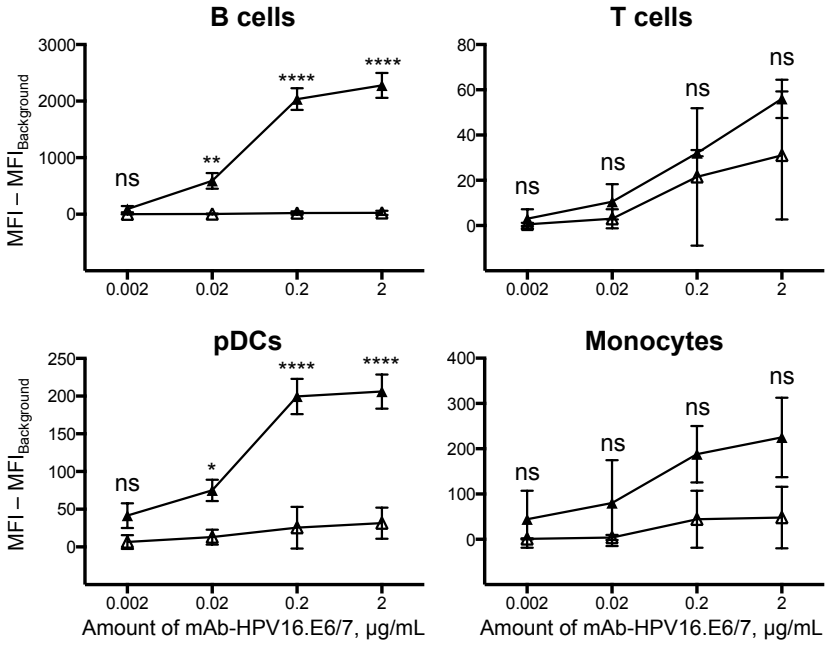

Figure 23. αCD40-HPV16.E6/7 can bind human B cells and pDCs. Binding of αCD40-HPV16.E6/7 or control IgG4-HPV16.E6/7 to B cells, T cells, Lin 1^{-}HLA-$DR^{+}CD123^{+}$ pDCs, and monocytes in human PBMCs. MFI comparisons between fusion proteins on indicated cell populations at 2, 0.2, 0.02, 0.002 and 0 µg/mL. Results are representative of two independent experiments. Data are presented as mean ± SD and significance was calculated using an ANOVA test. *, $P < 0.05$; **, $P < 0.01$; ****, $P < 0.001$; ns, not significant.

We next examined E6/7-specific $CD4^{+}$ and $CD8^{+}$ T cell responses by intracellular IFNγ staining (Figure 25). In addition to αCD40-HPV16.E6/7 and HPV16.E6/7 peptide pool, we also included HPV16.E6/7 whole protein as a control for non-targeted antigen

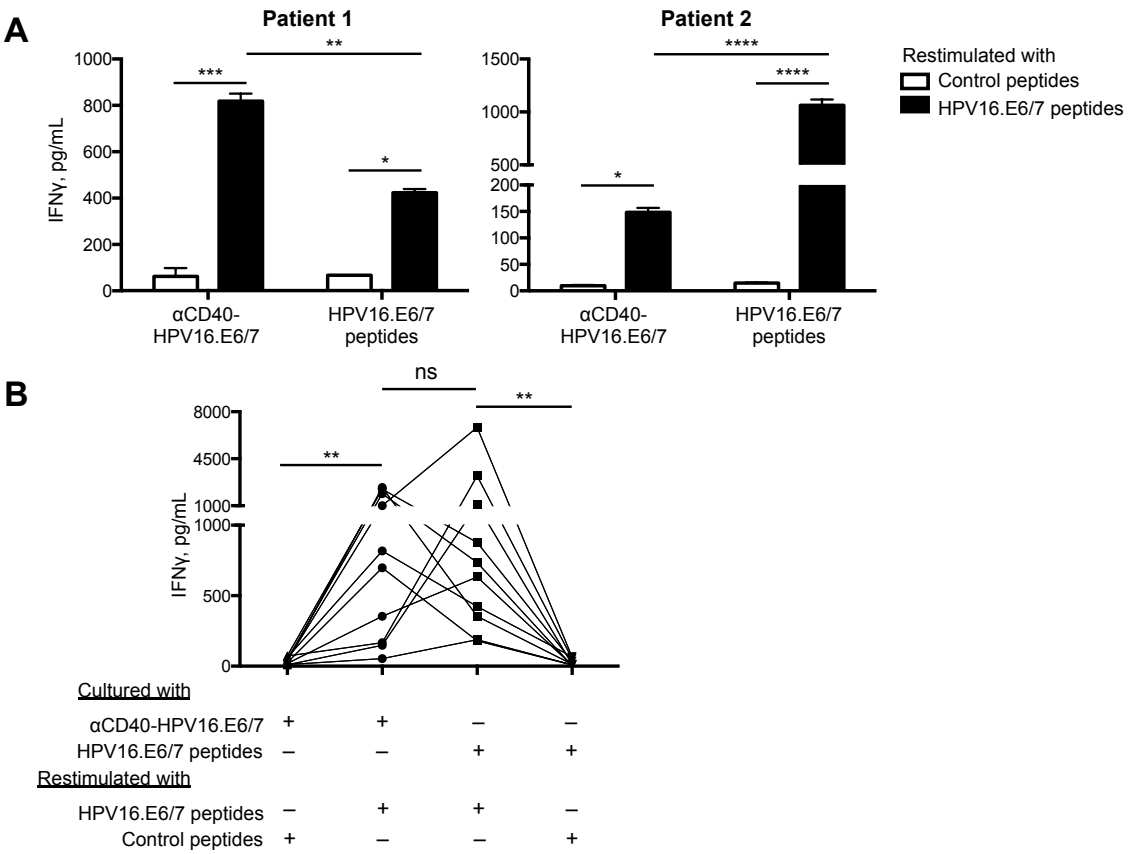

Figure 24. Targeting HPV16.E6/7 to DCs via CD40 elicits IFNγ production from HPV16$^+$ head-and-neck cancer patients *in vitro*. (A and B) PBMCs from HPV16$^+$ head-and-neck cancer patients were cultured for 7 days in the presence of αCD40-HPV16.E6/7 at 0.2 μg/mL or an equivalent amount of HPV16.E6/7 peptides. Cells were then restimulated for 48 h with 1 μM HPV16.E6/7 peptides or control peptides, and IFNγ in the supernatants was quantified by Luminex. (A) Levels of IFNγ from two representative patients. Data are presented as mean ± SD and significance was determined using an ANOVA test. (B) Levels of IFNγ from 10 patients. Dots represent data generated with individual patient samples, and significance was determined using a paired *t* test. *, $P < 0.05$; **, $P < 0.01$; ***, $P < 0.005$; ****, $P < 0.001$; ns, not significant.

delivery. Compared to HPV16.E6/7 whole protein, αCD40-HPV16.E6/7 resulted in increased frequencies of IFNγ$^+$CD8$^+$ and IFNγ$^+$CD4$^+$ T cells, demonstrating that αCD40-HPV16.E6/7 could efficiently activate both E6/7-specific CD8$^+$ and CD4$^+$ T cells. Our data also showed that there was no significant level of HPV16.E6/7-specific CD8$^+$ T cell responses without targeting with protein antigens, although it could elicit minimal levels of E6/7-specific CD4$^+$ T cell responses. It was also of note that αCD40-HPV16.E6/7 was

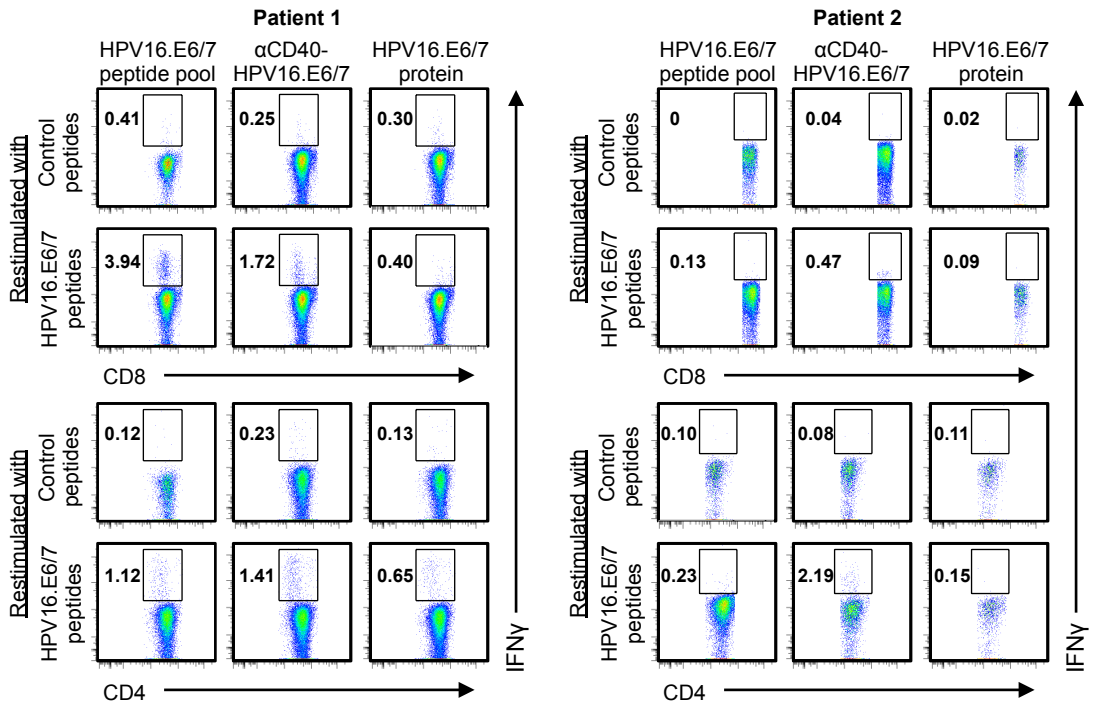

Figure 25. Targeting HPV16.E6/7 to DCs via CD40 can activate memory $CD8^+$ and $CD4^+$ T cells from $HPV16^+$ head-and-neck cancer patients *in vitro*. Purified $CD8^+$ T cells from $HPV16^+$ head-and-neck cancer patients were co-cultured for 7 days with autologous Mo-DCs loaded with αCD40-HPV16.E6/7 at 0.2 μg/mL, or an equivalent amount of HPV16.E6/7 protein or peptides. $CD8^+$ T cells were restimulated with 1 μM HPV16.E6/7 peptides or control peptides. Intracellular IFNγ expression was assessed. Representative flow cytometry data showing $IFN\gamma^+CD8^+$ and $IFN\gamma^+CD4^+$ T cells from two patients are shown.

more efficient than HPV16.E6/7 peptide pool in activating HPV16.E6/7-specific $CD8^+$ and $CD4^+$ T cells in Patient 2, while HPV16.E6/7 peptide pool was more efficient than αCD40-HPV16.E6/7 in eliciting $CD8^+$ T cell responses in Patient 1. Taken together, we conclude that αCD40-HPV16.E6/7 could efficiently activate HPV16.E6/7-specific $CD8^+$ and $CD4^+$ T cells from patients.

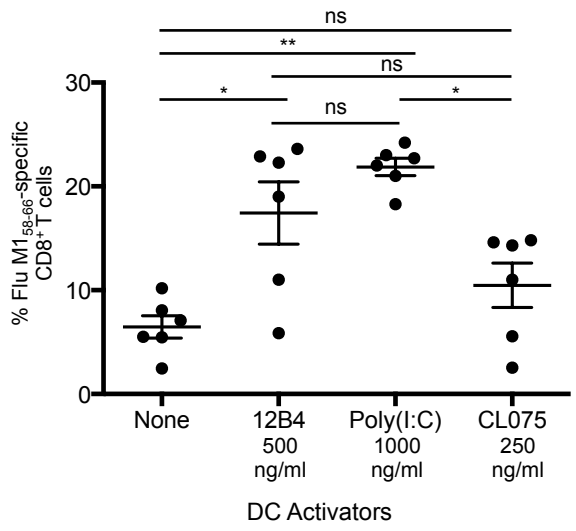

Figure 26. Poly(I:C) effectively enhances antigen-specific $CD8^+$ T cell response *in vitro*. Purified $CD8^+$ T cells from healthy donors (n=6) were co-cultured for 8 days with autologous Mo-DCs loaded with αCD40-Flu.M1 at 0.02 μg/mL either alone or in the presence of αCD40 (12B4), poly(I:C), CL075 at indicated concentrations. $CD8^+$ T cells were stained with HLA-A*A0201-Flu.$M1_{58-66}$ tetramer after 8 days. Data are presented as mean ± SD and significance was determined using an ANOVA test. *, $P < 0.05$; **, $P < 0.01$; ns, not significant.

αCD40-HPV16.E6/7 Can Prime HPV16.E6/7-Specific $CD8^+$ and $CD4^+$ T Cells in hCD40Tg Mice

αCD40 (12E12) was originally a DC agonist (Flamar et al., 2013; Flamar et al., 2012). However, after being fused with HPV16.E6/7, its agonistic effect was greatly diminished. To compensate such loss, we titrated (data not shown) and compared several DC activators, including another αCD40 mAb (12B4), poly(I:C), and CL075 (Figure 26), in targeting experiments in which monocyte-derived dendritic cells (Mo-DCs) were first loaded with a fusion protein αCD40-Flu.$M1_{58-66}$, which was generated from αCD40 (12E12) and the influenza $M1_{58-66}$ peptide (Flu.$M1_{58-66}$), and later co-cultured with autologous $CD8^+$ T cells. The results showed that Mo-DCs incubated with αCD40-Flu.$M1_{58-66}$ plus poly(I:C) activated the highest frequencies of Flu.$M1_{58-66}$-specific $CD8^+$

T cells, suggesting that poly(I:C) was a strong adjuvant in our *in vitro* targeting system. We then proceeded with our *in vivo* immunogenicity test with poly(I:C) as the adjuvant.

In order to assess the immunogenicity of αCD40-HPV16.E6/7, we employed human CD40 transgenic (hCD40Tg) mice. As shown in Figure 27 (left and middle),

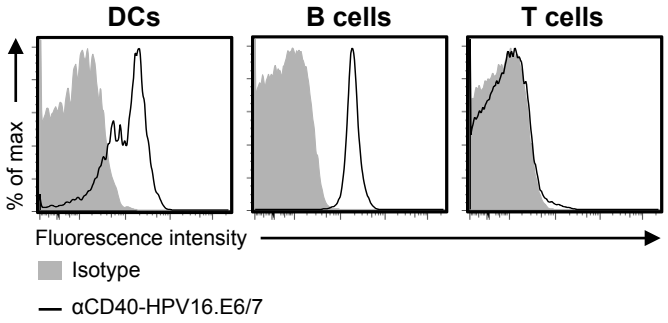

Figure 27. αCD40-HPV16.E6/7 binds mouse DCs. Binding of αCD40-HPV16.E6/7 at 1 μg/mL to splenic $CD11c^+$ DCs, $B220^+$ B cells, and $CD3^+$ T cells of hCD40Tg mouse.

αCD40-HPV16.E6/7 bound to $CD11c^+$ and $B220^+$ cells in the blood of hCD40Tg mice. However, it did not bind to $CD3^+$ cells (Figure 27, right).

αCD40-HPV16.E6/7 was given to mice through subcutaneous (s.c.) injections. The mice were primed and boosted twice at two-week intervals with a combination of 30 μg/dose of aCD40-HPV16.E6/7 plus poly(I:C), administered as an adjuvant, at 50 μg/dose, as previously described (Bonifaz et al., 2002; Gurer et al., 2008). Wild-type (WT) mice were used as controls. One week after the last immunization, IFNγ production by splenic HPV16.E6/7-specific $CD8^+$ and $CD4^+$ T cells was quantified by ELISpot assays (Figures 28A and 28B). Only hCD40Tg mice immunized with αCD40-HPV16.E6/7 had significant amounts of IFNγ-producing $CD8^+$ and $CD4^+$ T cells when restimulated with HPV16.E7 peptide pool, in comparison with the almost non-detectable

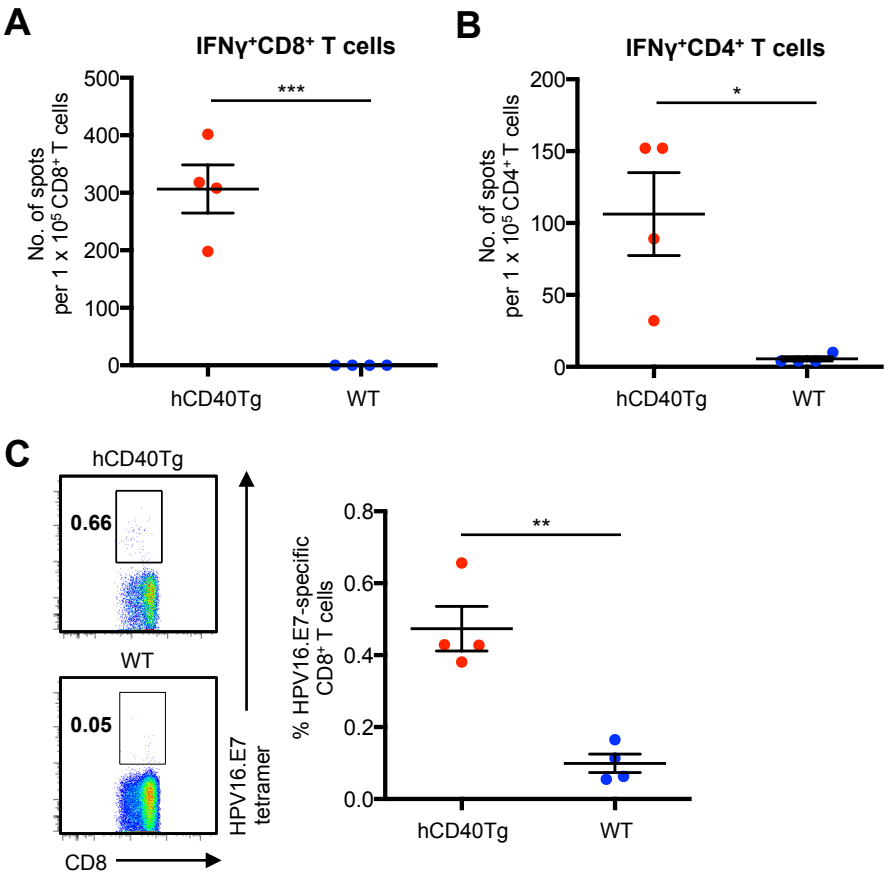

Figure 28. αCD40-HPV16.E6/7 primes HPV16.E6/7-specific $CD8^+$ and $CD4^+$ T cell responses *in vivo*. (A–C) hCD40Tg or WT mice (n=4 per group) were immunized s.c. with a combination of αCD40-HPV16.E6/7 (30 µg/dose) and poly(I:C) (50 µg/dose) in 100 µL PBS. Mice were boosted twice with the same vaccine at two-week intervals and were sacrificed 7 days after the second boost. Spleen and peripheral blood were harvested. (B and C) IFNγ ELISpot assays were performed on (A) $CD8^+$ and (B) $CD4^+$ T cells purified from splenocytes and restimulated for 36 h with 1 µM HPV16.E6/7 peptides. (C) $CD8^+$ T cells in peripheral blood were stained with H-$2D^b$-$HPV16.E7_{RAHYNIVTF}$ tetramer. Left, representative flow cytometry data. Right, summarized data. Data are presented as mean ± SD. Significance was determined using an unpaired *t* test. *, $P < 0.05$; **, $P < 0.01$; ***, $P < 0.005$.

levels of IFNγ in T cells from WT mice. Furthermore, blood staining with H-$2D^b$ HPV16.E7 (RAHYNIVTF) tetramer revealed that αCD40-HPV16.E6/7 elicited increased frequencies of HPV16.E7-specific $CD8^+$ T cells only in hCD40Tg (Figure 28C). Together, these data suggest that αCD40-HPV16.E6/7 was immunogenic and could thus

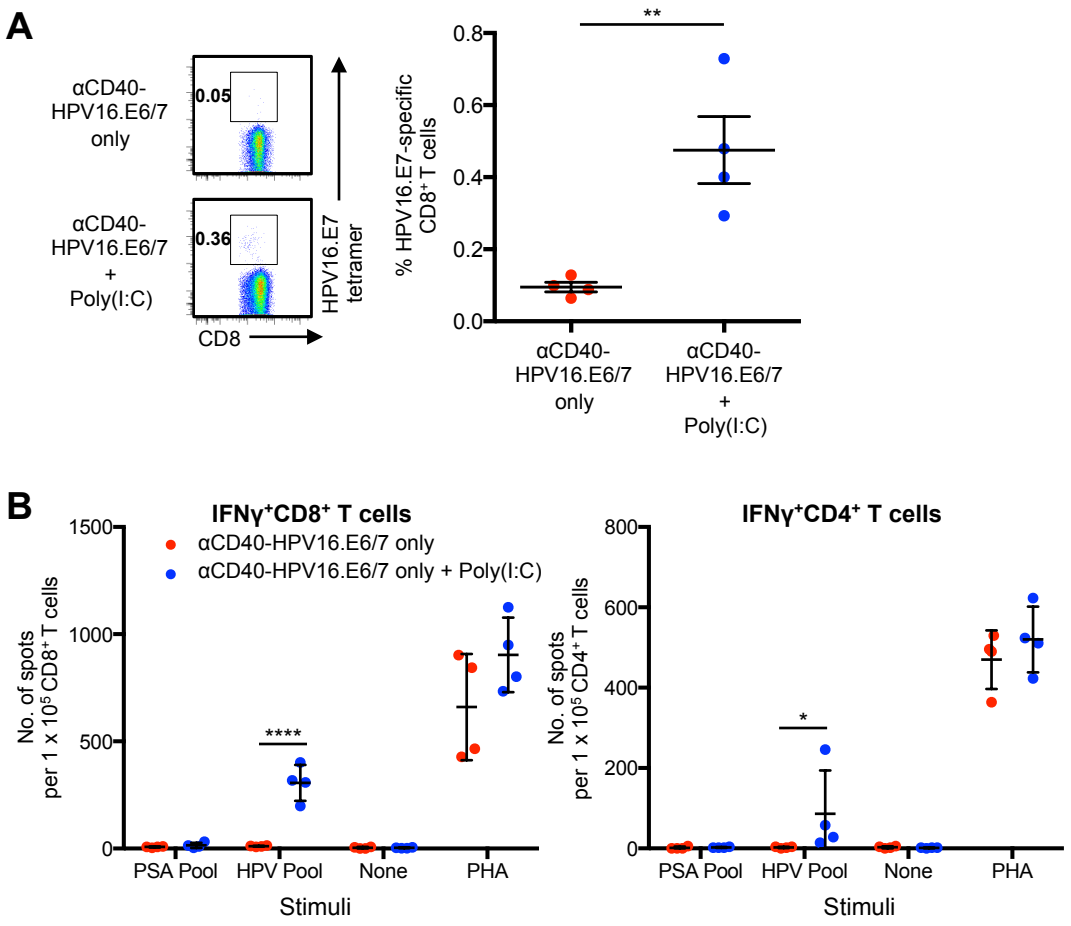

Figure 29. Poly(I:C) effectively enhances both HPV16.E6/7-specific $CD4^+$ and $CD8^+$ T cell response *in vitro*. (A and B) hCD40Tg mice were immunized s.c. with a combination of poly(I:C) (50 µg/dose) and αCD40-HPV16.E6/7 (30 µg/dose) or with αCD40-HPV16.E6/7 alone in 100 µL PBS (n=4 per group). Mice were boosted twice with the same vaccines at two-week intervals and were sacrificed 7 days after the second boost. (A) $CD8^+$ T cells in the blood were stained with H-$2D^b$-HPV16.$E7_{RAHYNIVTF}$ tetramer. Frequencies of HPV16.E7-specific $CD8^+$ T cells are shown. Left, representative flow cytometry data. Right, summarized data. (B) IFNγ ELISpot assays were performed on $CD8^+$ and $CD4^+$ T cells purified from splenocytes. All data are presented as mean (represented by dots) ± SD. Significance was determined using an ANOVA (B) test. *, $P < 0.05$; **, $P < 0.01$; ***, $P < 0.005$; ns, not significant.

prime HPV16.E6/7-specific IFNγ-producing $CD8^+$ and $CD4^+$ T cells in hCD40Tg mice.

To further confirm of the role of poly(I:C) *in vivo*, we similarly immunized the hCD40Tg mice with or without poly(I:C) in a three-dose injection schedule (Figure 29).

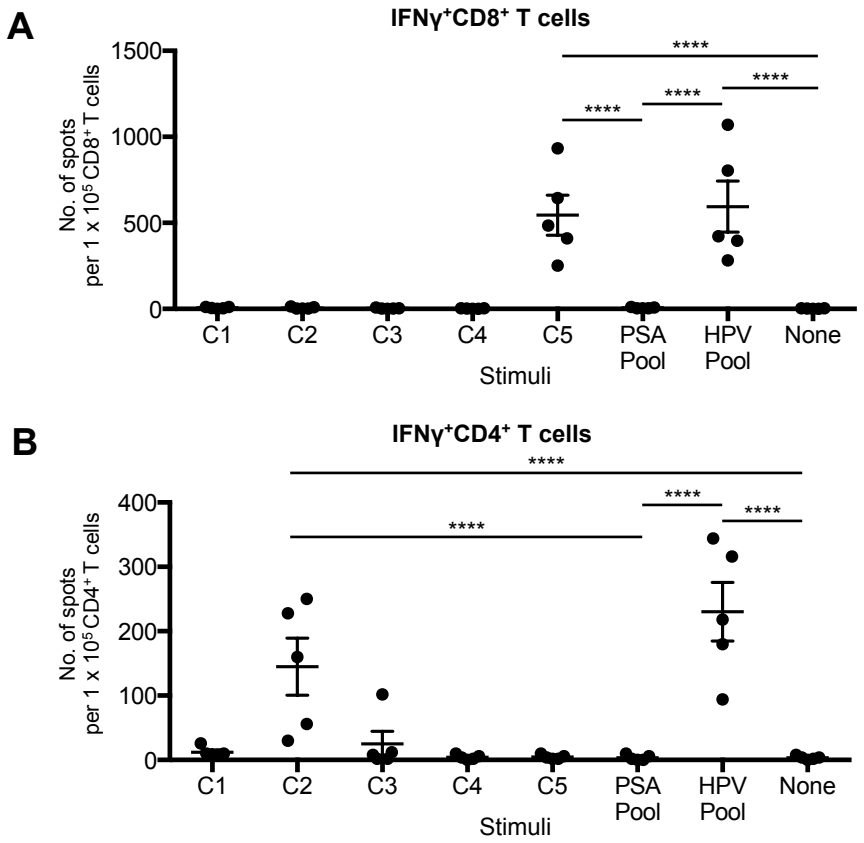

Figure 30. Characterization of HPV16.E6/7-specific $CD8^+$ and $CD4^+$ T cell responses *in vivo*. (A and B) hCD40Tg mice (n=5) were immunized and sacrificed as in Figure 28. $CD8^+$ and $CD4^+$ T cells purified from splenocytes were restimulated with individual HPV16.E6/7 peptides (HPV pool), clusters of HPV16.E6/7 peptides (C1 to C5), or control peptides (PSA pool). IFNγ ELISpot assays performed with (A) $CD8^+$ and (B) $CD4^+$ T cells are shown. Data are presented as mean ± SD. Significance was determined using ANOVA test. PSA, prostate-specific antigen. ****, $P < 0.001$.

Figure 29A shows that the frequencies of HPV16.E7-specific $CD8^+$ T cells from mice immunized with only αCD40-HPV16.E6/7 were significantly lower than those from cells from mice injected with αCD40-HPV16.E6/7 and poly(I:C). Similarly, ELISpot results show that there were no HPV16.E6/7-specific IFNγ-producing splenic $CD4^+$ nor $CD8^+$ T cells in mice inject without poly(I:C) (Figure 29B). These data suggest an indispensible role of poly(I:C) in eliciting HPV16.E6/7-specific $CD8^+$ and $CD4^+$ T cells in hCD40Tg mice.

To further characterize the whole HPV16.E6/7-specific $CD8^+$ and $CD4^+$ T cell responses, we restimulated splenic $CD8^+$ and $CD4^+$ T cells with five partially overlapping peptide clusters (C1–C5) of E6 and E7 (Figure 30). The majority of $CD8^+$ T cells primed with αCD40-HPV16.E6/7 were specific for cluster 5 from E7 protein, while $CD4^+$ T cells primed with αCD40-HPV16.E6/7 were specific for cluster 2 from E6, as previously described (Feltkamp et al., 1993).

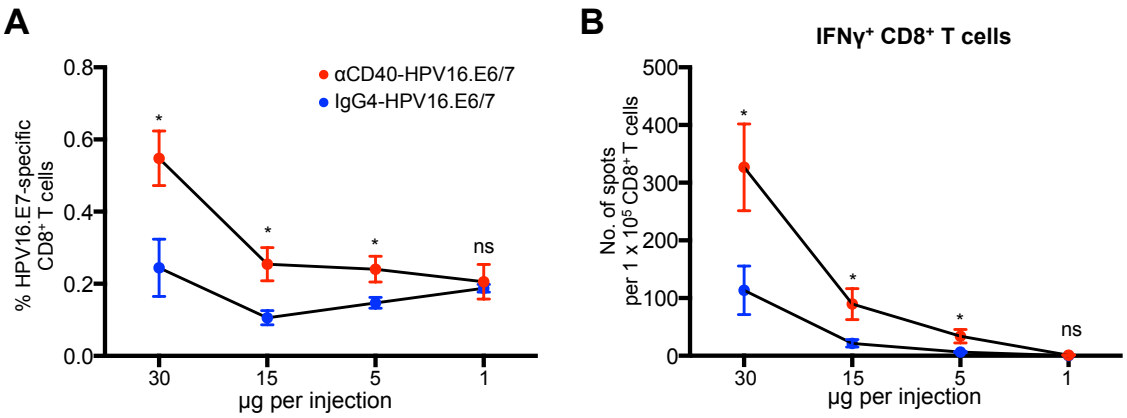

Figure 31. αCD40-HPV16.E6/7 elicits HPV16.E6/7-specific $CD8^+$ and $CD4^+$ T cell in a dose-dependent manner. (A and B) hCD40Tg mice were s.c. immunized with a combination of poly(I:C) (50 µg/dose) and αCD40-HPV16.E6/7 or IgG4-HPV16.E6/7 at indicated doses in 100 µL PBS (n=5 per group). Mice were boosted twice with the same vaccines at two-week intervals and were sacrificed 7 days after the second boost. (A) $CD8^+$ T cells in the blood were stained with H-$2D^b$-HPV16.$E7_{RAHYNIVTF}$ tetramer. Summarized data on the frequencies of HPV16.E7-specific $CD8^+$ T cells are shown. (B) IFNγ ELISpot assays were performed on $CD8^+$ T cells purified from splenocytes. All data are presented as mean (represented by dots) ± SD. Significance was determined using an ANOVA (B) test. *, $P < 0.05$; ns, not significant.

To induce the optimal E6/7-specific $CD8^+$ and $CD4^+$ T cell responses, we performed experiments in which hCD40Tg mice were s.c. immunized with a combination of poly(I:C) at 50 µg/dose and αCD40-HPV16.E6/7 or IgG4-HPV16.E6/7 at 30, 15, 5, or

1 μg/dose (Figure 31). Blood tetramer staining revealed that hCD40Tg immunized with αCD40-HPV16.E6/7 had higher frequencies of HPV16.E7-specific $CD8^+$ T cells at 30,

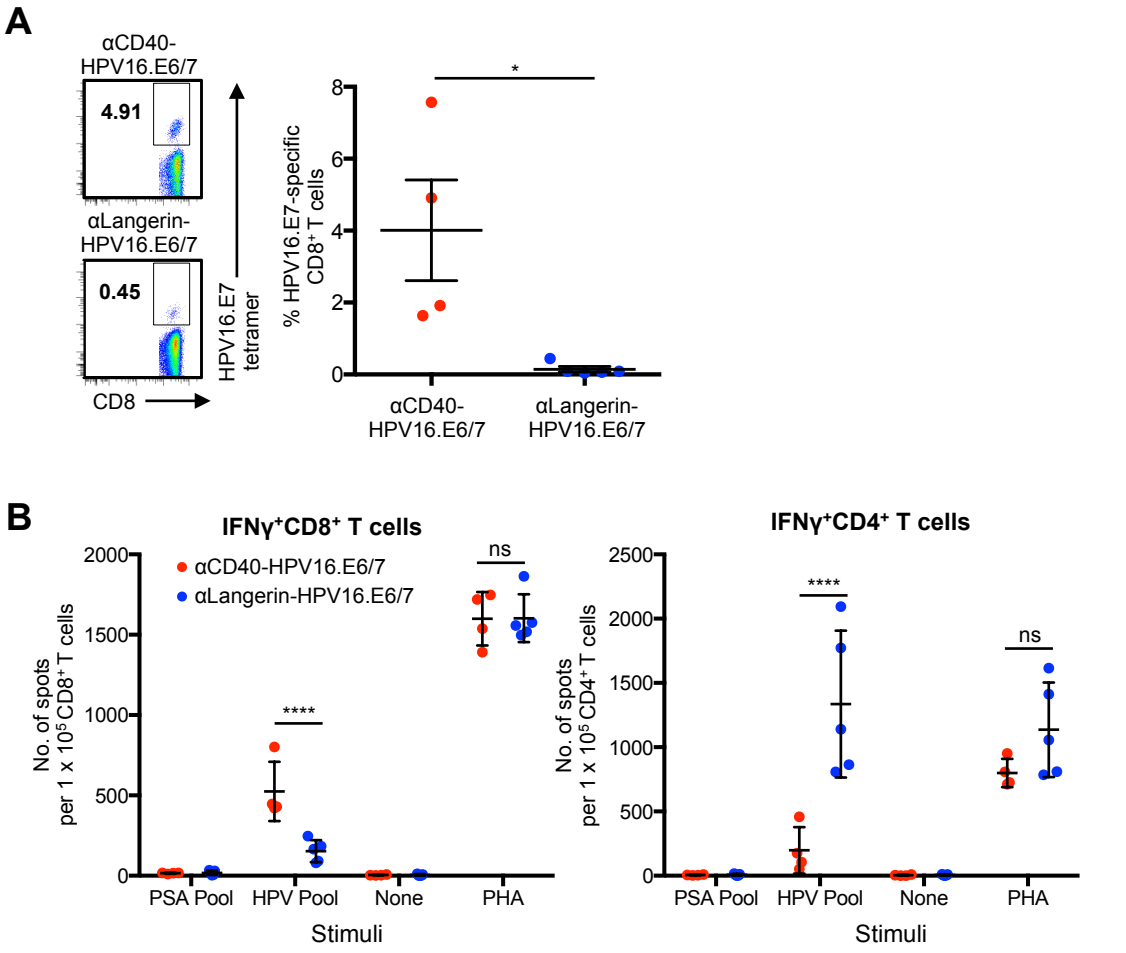

Figure 32. Targeting HPV16.E6/7 to CD40 is more efficient than targeting HPV16.E6/7 to Langerin at priming HPV16.E6/7-specific $CD8^+$ CTLs *in vivo*. (A and B) hCD40Tg mice were immunized i.p. with a combination of poly(I:C) (50 μg/dose) and αCD40-HPV16.E6/7 (30 μg/dose) or αLangerin-HPV16.E6/7 (30 μg/dose) in 100 μL PBS (n=4 per group). Mice were boosted twice with the same vaccines at two-week intervals and were sacrificed 7 days after the second boost. (A) $CD8^+$ T cells in the blood were stained with H-$2D^b$-HPV16.$E7_{RAHYNIVTF}$ tetramer. Left, representative flow cytometry data. Right, data generated with individual mice are summarized. (B) IFNγ ELISpot assays were performed on $CD8^+$ (left) and $CD4^+$(right) T cells purified from splenocytes. Dots represent data generated with individual mice. All data are presented as mean ± SD. Significance was determined using an unpaired *t* test (A) or ANOVA (B) test. PHA, phytohemagglutinin. *, $P < 0.05$; ****, $P < 0.001$; ns, not significant.

15, and 5 μg/dose, in comparison to the mice immunized with the same amount of IgG4-HPV16.E6/7 (Figure 31A). Similarly in ELISpot assays performed on splenic $CD8^+$ T

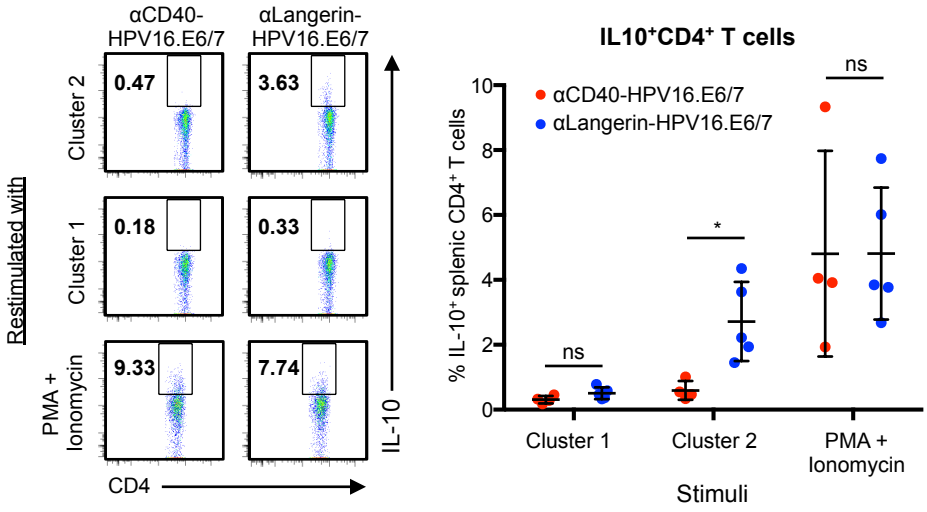

Figure 33. Targeting HPV16.E6/7 to Langerin is more efficient than targeting HPV16.E6/7 to CD40 at priming HPV16.E6/7-specific IL-10-producing $CD4^+$ T cells *in vivo*. Splenic $CD4^+$ T cells from mice immunized in Figure 32 were restimulated with clusters of HPV16.E6 peptides, or PMA and ionomycin in the presence of brefeldin A, and were intracellularly stained for IL-10. Left, representative flow cytometry data. Right, summarized data from individual mice. Dots represent data generated with individual mice. All data are presented as mean ± SD. Significance was determined using an ANOVA test. PHA, phytohemagglutinin. *, $P < 0.05$; ****, $P < 0.001$; ns, not significant.

cells, there were significantly more IFNγ-producing cells from αCD40-HPV16.E6/7-immunized mice than from those injected with IgG4-HPV16.E6/7 at 30, 15, and 5 μg/dose (Figure 31B). Similar results were obtained from experiments in which hCD40Tg mice were i.p. immunized with αCD40-HPV16.E6/7 and IgG4-HPV16.E6/7 at different doses, further indicating that the HPV16.E6/7-specific $CD8^+$ T cell responses were dose-dependent on the amount of αCD40-HPV16.E6/7 injected.

Taken together, we conclude that αCD40-HPV16.E6/7 plus poly(I:C) could prime both HPV16.E6/7-specific $CD8^+$ and $CD4^+$ T cells *in vivo*.

αCD40-HPV16.E6/7 is More Efficient than αLangerin-HPV16.E6/7 at Priming $CD8^+$ T Cell Responses In Vivo

Using hCD40Tg mice, we were able to compare the immunogenicity of αCD40-HPV16.E6/7 and that of αLangerin-HPV16.E6/7. It was previously shown that αLangerin mAb injected i.p. could effectively target $Langerin^+$ cells in mice (Igyarto et al., 2011). hCD40Tg mice were i.p. immunized three times with combinations of poly(I:C) (50 μg) plus either 30 μg αCD40 (12E12)-HPV16.E6/7 or αLangerin (4C7)-HPV16.E6/7 at two-week intervals. Seven days after the second boosting, blood E7-specific $CD8^+$ T cells were assessed for the percentage of $tetramer^+CD8^+$ T cells (Figure 32A). Compared to mice immunized with αLangerin-HPV16.E6/7, those immunized with αCD40-HPV16.E6/7 had a higher percentage of $tetramer^+CD8^+$ T cells. Data from individual mice are shown in Figure 32A (right). IFNγ ELISpot assays using $CD8^+$ and $CD4^+$ T cells purified from splenocytes also showed that mice immunized with αCD40-HPV16.E6/7 had more IFNγ-producing $CD8^+$ T cells than those immunized with αLangerin-HPV16.E6/7 (Figure 32B, left). However, αLangerin-HPV16.E6/7 plus poly(I:C) was more efficient than αCD40-HPV16.E6/7 plus poly(I:C) at eliciting $IFN\gamma^+CD4^+$ T cell responses (Figure 32B, right). In a separate experiment, mice were immunized s.c. and their HPV16.E6/7-specific $CD8^+$ and $CD4^+$ T cell responses were assessed (Figure 34). Figure 34A shows that mice immunized with αCD40-HPV16.E6/7 had a greater percentage of $tetramer^+CD8^+$ T cells in the blood than those immunized with αLangerin-HPV16.E6/7. ELISpot data generated with purified $CD8^+$ and $CD4^+$ T

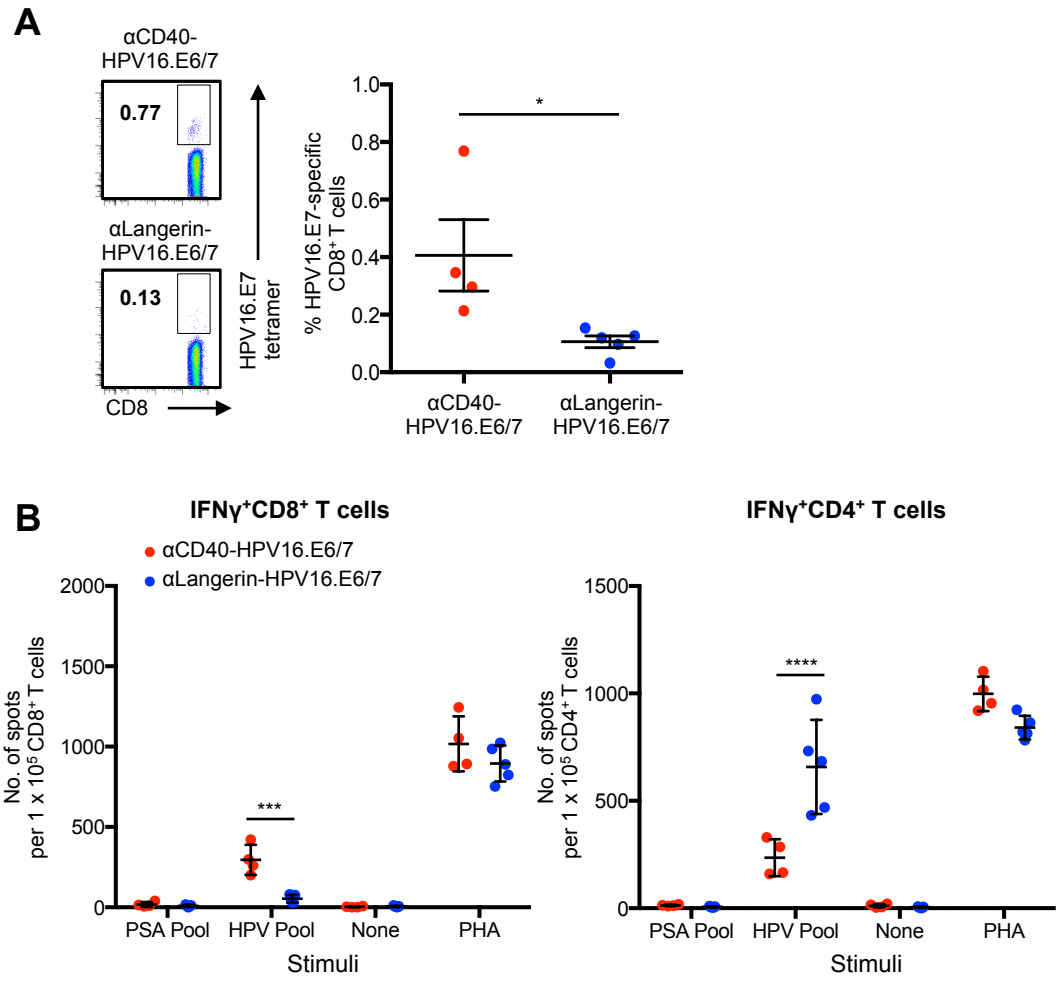

Figure 34. Targeting HPV16.E6/7 to CD40 is more efficient than targeting HPV16.E6/7 to Langerin at priming HPV16.E6/7-specific $CD8^+$ CTLs *in vivo* (s.c.). (A–B) hCD40Tg mice were immunized s.c. with a combination of poly(I:C) (50 µg/dose) and αCD40-HPV16.E6/7 (30 µg/dose) or αLangerin-HPV16.E6/7 (30 µg/dose) in 100 µL PBS (n=4 per group). Mice were boosted twice with the same vaccines at two-week intervals and were sacrificed 7 days after the second boost. (A) $CD8^+$ T cells in the blood were stained with H-$2D^b$-HPV16.$E7_{RAHYNIVTF}$ tetramer. Left, representative flow cytometry data. Right, data generated with individual mice are summarized. (B) IFNγ ELISpot assays were performed on $CD8^+$ (left) and $CD4^+$(right) T cells purified from splenocytes. Dots represent data generated with individual mice. All data are presented as mean ± SD. Significance was determined using an unpaired *t* test (A) or ANOVA (B) test. PHA, phytohemagglutinin. *, $P < 0.05$; ***, $P < 0.005$; ****, $P < 0.001$; ns, not significant.

cells from splenocytes also showed that αCD40-HPV16.E6/7 was more efficient than αLangerin-HPV16.E6/7 at priming HPV16.E6/7-specific IFNγ$^+$CD8$^+$ T cell responses,

while αLangerin-HPV16.E6/7 was more efficient than αCD40-HPV16.E6/7 at eliciting $IFN\gamma^+CD4^+$ T cell responses (Figure 34B). In addition, αLangerin-HPV16.E6/7 resulted in increased $IL\text{-}10^+CD4^+$ T cell responses specific to peptide cluster 2 (Figure 33).

Taken together, we conclude that targeting HPV16.E6/7 to CD40 is more efficient than targeting HPV16.E6/7 to Langerin at priming antigen-specific $IFN\gamma^+CD8^+$ T cells, but not antigen-specific $IFN\gamma^+CD4^+$ T cells.

αCD40-HPV16.E6/7 Can Generate Long-Term HPV16.E6/7-Specific Immunological Memory

To test whether αCD40-HPV16.E6/7 was able to generate long-term immunological memory, two groups of hCD40Tg mice (n=5 per group) were immunized s.c. with a combination of poly(I:C) and αCD40-HPV16.E6/7 for three times at two-week intervals. One group of mice was euthanized one week after the final injection (day 35), and the other was sacrifice nine weeks after the last injection (day 90) (Figure 35). No statistical differences in the frequencies of HPV16.E7-specific $CD8^+$ T cells were found in either peripheral blood or splenocytes between the two groups (Figure 35A). Similarly, frequencies of HPV16.E6/7-specific $IFN\gamma^+CD8^+$ T cells restimulated with HPV16.E6/7 peptide pool were also comparable between groups and were significantly higher than those of their respective controls (Figure 35B). These data indicate that αCD40-HPV16.E6/7 plus poly(I:C) was able to generate long-term HPV16.E6/7-specific immunological memory.

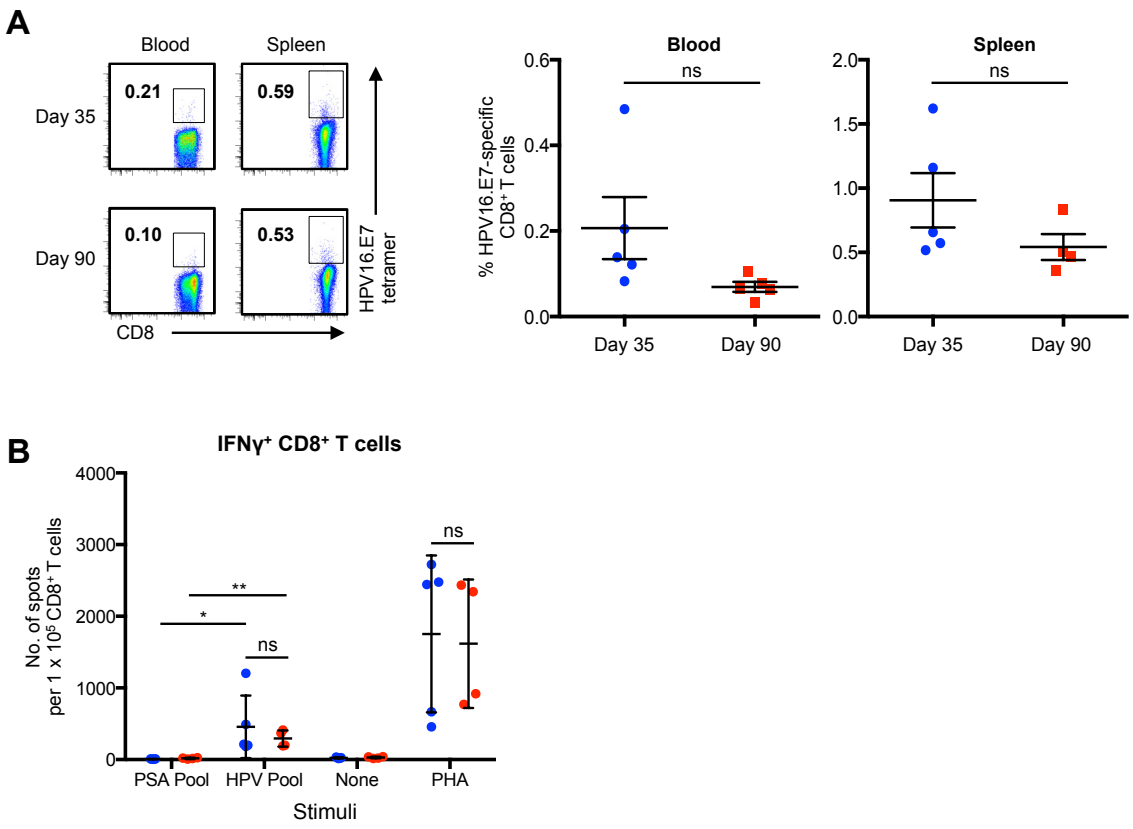

Figure 35. αCD40-HPV16.E6/7 can generate long-term HPV16.E6/7-specific immunological memory. (A–B) Two groups of hCD40Tg mice (5 per group) were immunized s.c. with a combination of poly(I:C) (50 μg/dose) and αCD40-HPV16.E6/7 (30 μg/dose) in 100 μL PBS (n=5 per group). Mice were boosted twice at two-week intervals. One group of mice was euthanized one week after the final injection (day 35), the other nine weeks (day 90). (A) $CD8^+$ T cells in the blood and splenocytes were stained with H-$2D^b$-$HPV16.E7_{RAHYNIVTF}$ tetramer. Left, representative flow cytometry data. Right, data generated with individual mice are summarized. (B) IFNγ ELISpot assays were performed on $CD8^+$ T cells purified from splenocytes. Dots represent data generated with individual mice. All data are presented as mean ± SD. Significance was determined using an unpaired *t* test (A) or ANOVA (B) test. *, $P < 0.05$; **, $P < 0.01$; ns, not significant.

Efficacy of αCD40-HPV16.E6/7 in Preventing TC-1 Tumor Growth

We next aimed to test whether αCD40-HPV16.E6/7 was able to mount protective immunity against implanted TC-1 tumor cells expressing HPV16.E6/7. hCD40Tg mice were first immunized s.c. with a combination of poly(I:C) and αCD40-HPV16.E6/7 for

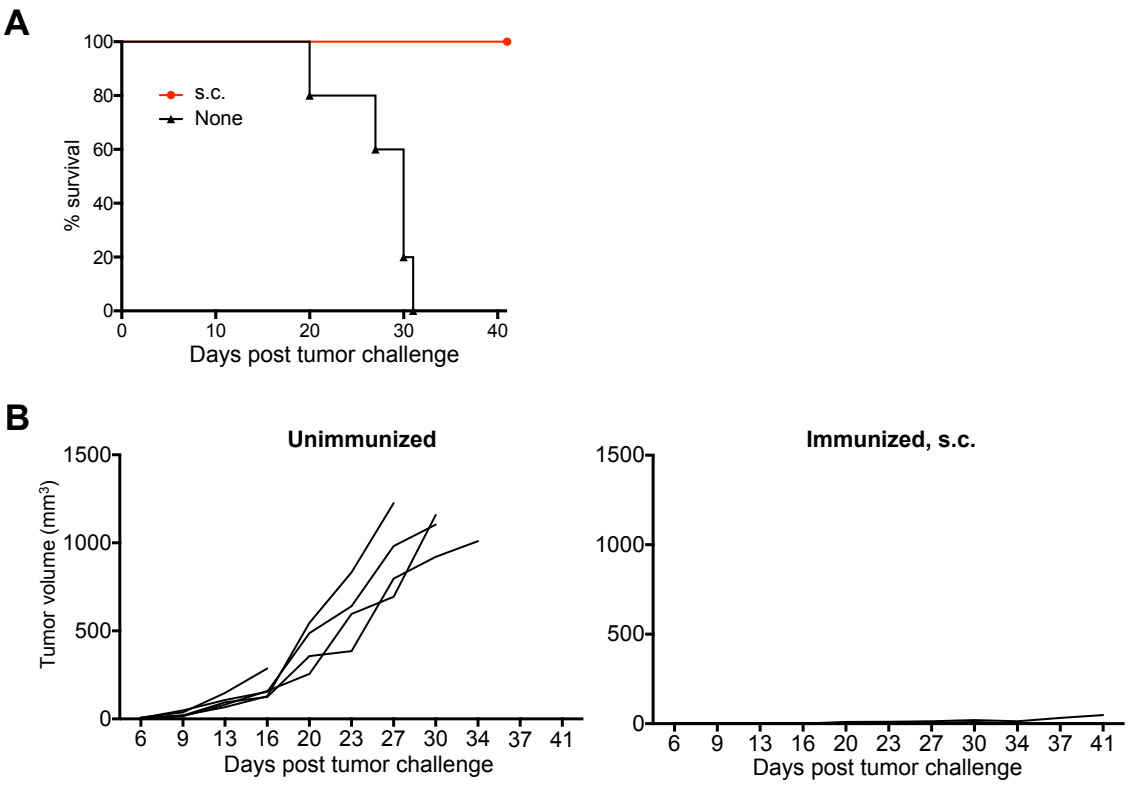

Figure 36. αCD40-HPV16.E6/7 can shape protective immunity to TC-1 tumors. (A and B) hCD40Tg mice were immunized s.c. with a combination of αCD40-HPV16.E6/7 (30 μg/dose) and poly(I:C) (50 μg/dose) in 100 μL PBS (n=5 per group). Mice were boosted twice with the same vaccine at two-week intervals. Seven days after the second boost, immunized mice, along with number-, gender-, and age-matched unimmunized hCD40Tg mice, were implanted with TC-1 cells s.c. on the left flank after shaving. (A) Overall survival curves up to 41 days post tumor implantation. (B) Tumor growth kinetics of individual mice in both groups.

three times at two-weeks intervals at five mice per group. One week after the final immunization, TC-1 cells were implanted s.c. to both immunized and unimmunized mice. On day 31 after tumor implantation, all unimmunized control mice succumbed to death (Figure 36A). In these mice, the TC-1 cells quickly formed a palpable solid tumor around day 6, and continued to grow rapidly (Figure 36B, left). However, all immunized mice remained alive even on day 41 post tumor implantation (Figure 36A). More importantly, nearly all the implanted TC-1 cells failed to form any palpable tumor, even at the end of

the experiment, with the exception of one mouse, which had a tumor of less than 50 mm^3 in volume (Figure 36B, right). These data suggest that αCD40-HPV16.E6/7 was capable of mounting preventive immunity against TC-1 tumor cell.

αCD40-HPV16.E6/7 Can Mount Therapeutic Immunity Against TC-1 Tumor

Since we showed that αCD40-HPV16.E6/7 could induce protective immunity, we therefore investigated whether αCD40-HPV16.E6/7 could also lead to therapeutic immunity. hCD40Tg mice were first implanted s.c. with TC-1 cells, then immunized either s.c., i.p., or intramuscularly (i.m.) with αCD40-HPV16.E6/7 plus poly(I:C) at ten mice per group once every six days for six times starting from day 6 when they had palpable tumors (Figure 37A). Regardless of the injection routes, αCD40-HPV16.E6/7 plus poly(I:C) substantially increased overall survival, with 90% of mice from each immunized group alive at the end of day 41, in comparison to only 10% survival of mice in the unimmunized control group (Figure 37B). Tumor progression in the majority of immunized mice was also suppressed, with some mice showing signs of tumor shrinkage after the fourth, fifth, and sixth immunizations (Figure 37C). Two mice in the i.p. group and one in the i.m. group even rejected the established tumor completely after 4 immunizations of αCD40-HPV16.E6/7 (Figure 37C, bottom). These data suggest that αCD40-HPV16.E6/7 was able to mount therapeutic immunity against established tumors expressing HPV16.E6/7.

To further understand the immune responses elicited by the vaccines in tumor-bearing hCD40Tg mice, we assessed the frequencies of $tetramer^+CD8^+$ T cells in tumor-infiltrating lymphocytes as well as in the peripheral blood from both immunized and

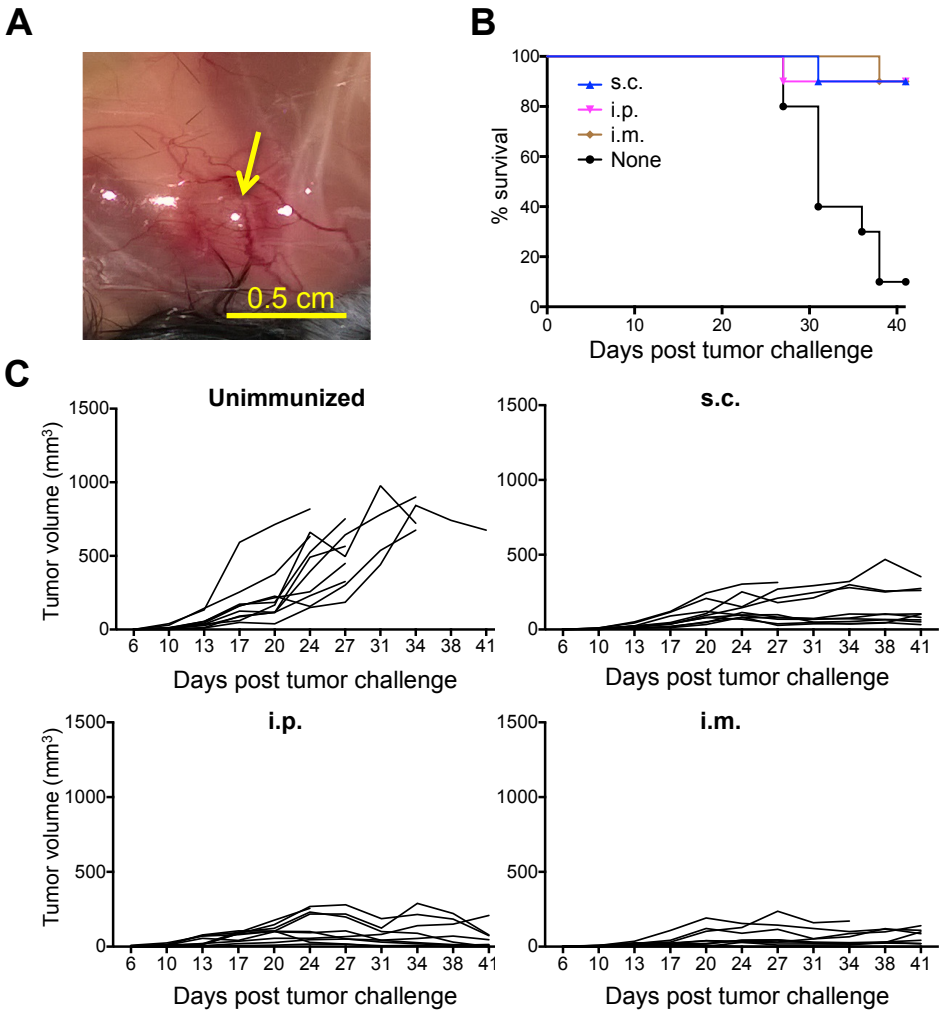

Figure 37. αCD40-HPV16.E6/7 can shape therapeutic immunity to TC-1 tumors. (A) A photo showing the tumor (yellow arrow) 6 days after TC-1 implantation. Scale bar: 0.5 cm. (B and C) hCD40Tg mice were implanted with TC-1 cells s.c. on the left flank after shaving on day 0. On day 6, mice were randomly divided into four groups (n=10 per group). Mice in three groups were injected s.c., i.p., or i.m. with αCD40-HPV16.E6/7 and poly(I:C) in PBS on days 6, 12, 18, 24, 30, and 36 post tumor implantation. Mice in the last group were left unimmunized. (B) Overall survival curves up to 41 days post tumor implantation. (C) Tumor growth kinetics of individual mice in all groups. (D and E) hCD40Tg mice were implanted with TC-1 cells s.c. on the left flank after shaving on day 0. On day 6, mice were randomly divided into two groups (n=12 per group). One group of mice were injected s.c. with αCD40-HPV16.E6/7 and poly(I:C) on days 6, 12, and 18. The other group of mice was not injected. Mice were euthanized 75 days post tumor implantation and $CD8^+$ T cells in tumors were stained with H-$2D^b$-HPV16.$E7_{RAHYNIVTF}$ tetramer and analyzed with flow cytometry.

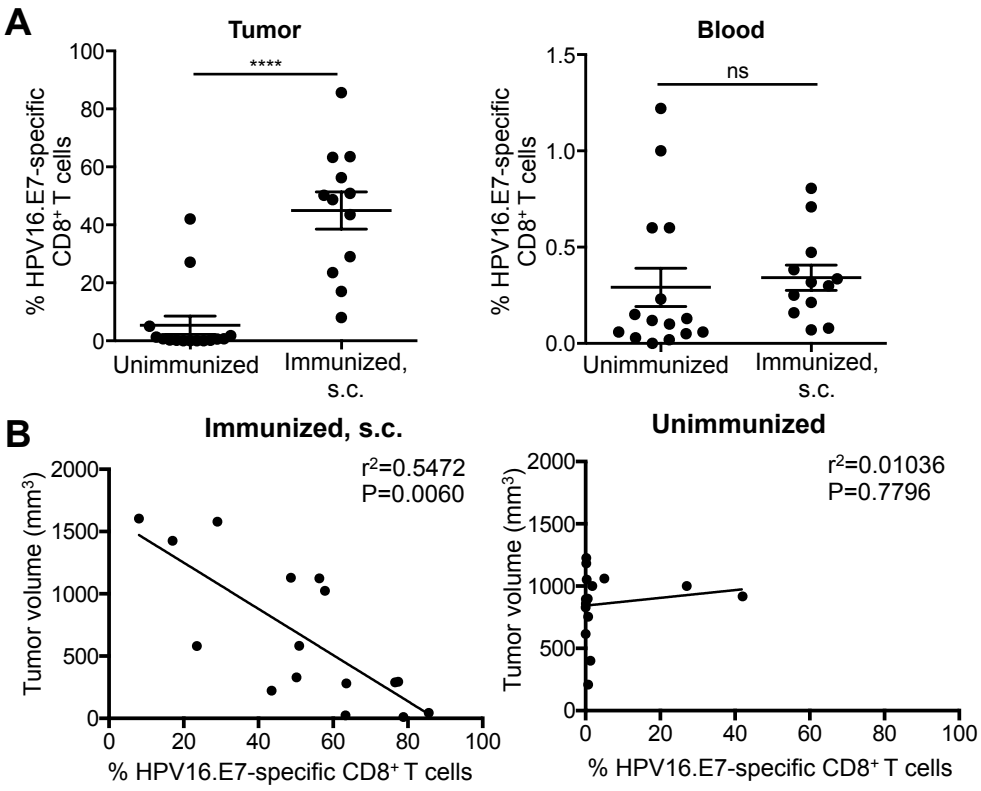

Figure 38. Therapeutic immunity to TC-1 tumors elicited by αCD40-HPV16.E6/7 are mediated by HPV16.E6/7-specific CTLs. (A) Frequencies of tetramer$^+$CD8$^+$ T cells in tumor (left) and blood (right) from the two groups are shown. Data are presented as mean ± SD. Dots represent data generated with individual mice. Significance was determined using an unpaired *t* test. (B) Linear regression of tumor volumes versus the frequencies of tetramer$^+$CD8$^+$ T cells in tumors is shown for the immunized group (left) and the unimmunized group (right). ****, $P < 0.001$; ns, not significant.

unimmunized mice. Immunizations of αCD40-HPV16.E6/7 plus poly(I:C) were performed s.c. once every six days for three times starting from day 6. Mice were euthanized whenever they showed signs of death, including large tumor volume (>1500 mm^3), significant body weight loss (>20%), hunched backs or loss of active movements. Based on these criteria, all mice in the unimmunized group were euthanized within 35 days after TC-1 tumor challenge. In contrast, mice in the immunized group were euthanized between days 35 and 75, with the majority euthanized on day 75. Immunized

mice had significantly higher frequencies of HPV16.E7-specific $CD8^+$ T cells within the tumors than the unimmunized mice (Figure 38A, left). However, there was no statistical difference in the frequencies of blood HPV16.E7-specific $CD8^+$ T cells (Figure 38A, right). In addition, the frequencies of $tetramer^+CD8^+$ T cells in the tumors inversely correlated with the tumor volumes only in the immunized group, but not in the unimmunized group (Figure 38). These data suggest that the high frequencies, with over than half of the mice having the majority of tumor-infiltrating cells tumor-specific $CD8^+$ T cells generated by immunizations of αCD40-HPV16.E6/7 plus poly(I:C), were responsible for the smaller tumor volumes in comparison to those in the unimmunized mice. Collectively, we conclude that αCD40-HPV16.E6/7 plus poly(I:C) could mount HPV16.E6/7-specific $CD8^+$ T cell-mediated immunity to control HPV16.E6/7-expressing TC-1 tumors.

Discussion

Since HPV has become the major causal agent responsible for head and neck cancers and cervical cancers, effective preventive and therapeutic methods are urgently needed. Gardasil and Cervarix, the two FDA-approved HPV vaccines on the market, are only suitable for HPV prevention. Designing and creating a safe, effective, easy-to-use, and low-cost therapeutic HPV vaccine has long been a focal point for treating HPV-related malignancies. Here we reported a new prototype of HPV vaccine, αCD40-HPV16.E6/7, that was able to specifically target DCs to not only activate $CD8^+$ T cells *in vitro*, but also elicit strong $CD8^+$ T cell-mediate protective and therapeutic immunity against TC-1 tumor challenge *in vivo*. Data from this study provide us with sufficient

evidence to move forward to the clinical development of CD40 targeting-based vaccines for cancers.

To maximize the $CD8^+$ T cell responses generated, we specifically selected CD40 as our target DC surface receptor due to its superior cross-priming and cross-activating ability in our previous unpublished work (manuscript in submission). In accordance with our work, previous studies have shown that after receptor-mediated antigen uptake, CD40 mainly localizes to early endosomes and plasma membrane, where the stability of the antigens it carries can be enhanced, leading to prolonged antigen presentation and enhanced $CD8^+$ T cell responses (Chatterjee et al., 2012; Cohn et al., 2013).

In this study, we first demonstrated that αCD40-HPV16.E6/7 was able to bind to blood CD40-expressing DCs and thus activate both HPV16.E6/7-specific $CD4^+$ and $CD8^+$ T cells in $HPV16^+$ cancer patient blood. The experiment platform we used here would be highly useful in routinely identifying and recruiting $HPV16^+$ cancer patients in our follow-up clinical trials.

Next, we showed that αCD40-HPV16.E6/7 plus poly(I:C) was immunogenic in hCD40Tg mice, inducing high frequencies of splenic IFNγ-producing $CD4^+$ and CD8 T^+ cells and blood HPV16.E7-specific $CD8^+$ T cells, the fact of which was consistent with our *in vitro* study. Poly(I:C) has been widely used as an adjuvant in various studies due to its agonistic effects on cell activation through toll-like receptor 3 (TLR3) and has been shown to be more efficient than CL075 at eliciting strong $CD4^+$ Th1 and (CD4-dependent and -independent) $CD8^+$ T cell responses (Caskey et al., 2011; Edwards et al., 2013; Quinn et al., 2013; Schulz et al., 2005), which was also shown in our own experiments.

Interestingly, delivery of HPV16.E6/7 to DCs via CD40 was more efficient than via Langerin at inducing HPV16.E6/7-specific $CD8^+$ T cell responses, but not HPV16.E6/7-specific $CD4^+$ T cell responses. It would seem beneficial to inject both fusion proteins to generate strong $CD8^+$ and $CD4^+$ T cell-mediated immunity. However, one thing to note is that the mouse has two DC populations that express Langerin, with one being Langerhan cells (LCs) in the epidermis and the other being Langerin-expressing dermal DCs (dDCs). While mouse LCs are known to be poor at cross-priming $CD8^+$ T cells (Flacher et al., 2012; Igyarto et al., 2011), mouse $Langerin^+$ dDCs are able to cross-prime $CD8^+$ T cells (Flacher et al., 2012; Flacher et al., 2014a; Igyarto et al., 2011). We demonstrated that αLangerin-HPV16.E6/7 induced HPV16.E6/7-specific $CD8^+$ T cell responses, likely though $Langerin^+$ dDCs, although weaker than the responses elicited by targeting $CD40^+$ DCs. Meanwhile, further dissection of the robust $CD4^+$ T cell responses evoked by αLangerin-HPV16.E6/7 revealed high frequencies of $IL\text{-}10^+CD4^+$ T cells, suggesting HPV16.E6/7 delivered to LCs could likely activate skin-resident regulatory T cells, as previously reported (Seneschal et al., 2012). Therefore, we must take this into consideration when testing dual immunization as a possibility to further enhance the efficacy of αCD40-HPV16.E6/7.

We further demonstrated that αCD40-HPV16.E6/7 was able to generate long-term immunological memory specific to HPV16.E6/7, even 90 days after the initial priming. This is particularly important for a preventive vaccine, as the duration of immunity will effectively determine the frequency of vaccine injections.

Lastly, we tested the therapeutic potential of αCD40-HPV16.E6/7 against established *in vivo* TC-1 tumors; it showed great tumor suppressive function and

significantly promoted overall survival of the immunized mice. In terms of tumor protection, αCD40-HPV16.E6/7-immunized mice were almost completely sheltered from tumor challenge. For tumor treatment, we showed that αCD40-HPV16.E6/7 was able to induce high frequencies of tumor-infiltrating HPV16.E6/7-specific $CD8^+$ T cells, with more than half of the mice showing greater than 50% (up to 90%) of tumor infiltrates being tumor-specific $CD8^+$ T cells. As such, we found that the size of tumor inversely correlated with the frequency of $tetramer^+CD8^+$ T cells within the tumor, indicating that these $CD8^+$ T cells, induced by immunizations of αCD40-HPV16.E6/7 plus poly(I:C), were responsible for tumor shrinking, and in some instances tumor rejection. However, there was no statistical difference in the frequencies of blood HPV16.E7-specific $CD8^+$ T cells between the immunized and the unimmunized mice. These data demonstrated that tumor existence alone induced HPV16.E7-specific $CD8^+$ T cells; however, these $CD8^+$ T cells did not efficiently infiltrate the tumor, implying an inhibitory mechanism, whereby tumor cells silence the tumoricidal effector $CD8^+$ T cells (Yee et al., 2002). Collectively, our data suggested that the potency of vaccine to elicit $CD8^+$ T cells able to migrate into the tumors is a critical factor for enhanced therapeutic immunity of the vaccine, although additional strategies to overcome immunosuppressive tumor microenvironments could further promote the efficacy of this vaccine in patients.

In our *in vivo* tumor models, the detectable immune responses mediated by $CD8^+$ T cells were dependent mainly on the E6 and E7 epitopes, while in the actual cases of HPV16-related malignancies in human, the situation is much more complicated. However, E6 and E7 are present in all virus-infected and transformed tumor cells. It is thus essential to elicit a broad anti-tumor response repertoire that will effectively cover

multiple E6 and E7 epitopes recognized by $CD8^+$, and even $CD4^+$, T cells. In comparison to peptide vaccines that only carry limited amount of immunodominant epitopes, we anticipate that αCD40-HPV16.E6/7, with the inclusion of the majority of both E6 and E7 sequences, is capable of mounting immune responses sufficient to provide both protective and therapeutic immunity against HPV-related malignancies. In addition, αCD40-HPV16.E6/7 is safer than DNA or viral vector vaccines since it does not engage the human genome. Furthermore, CD40-targeting vaccines may even replace current *ex vivo* DC-based cancer vaccines that are safe, but result in durable clinical responses in only a small percentage of cancer patients (Anguille et al., 2014).

CHAPTER FIVE

Preclinical Assessment of CD40 Targeting Vaccine for Prostate Cancer

Abstract

Prostate cancer (CaP) is one of the most prevalent cancers in males worldwide. Development of a safe and effective vaccine that can provide better benefit to patients is therefore urgently needed. Herein, we report a new prototype vaccine, αCD40-PSA, in the form of a recombinant fusion protein of humanized αCD40 monoclonal antibody with prostate-specific antigen (PSA). αCD40-PSA was able to target and activate human $CD40^+$ dendritic cells (DCs), promoting the expansion of PSA-specific $CD8^+$ and $CD4^+$ T cells. Specifically, αCD40-PSA-loaded DCs primed PSA-specific $CD8^+$ and $CD4^+$ T cells in the blood of healthy donors, and activated PSA-specific $CD8^+$ T cells in CaP patient blood. We also demonstrated that the combination of αCD40-PSA and poly(I:C) primed and activated PSA-specific T cells in human CD40 transgenic mice. This study shows the potency of DC-targeting vaccines and sheds light on the design of therapeutic vaccines against CaP.

Introduction

Prostate cancer (CaP) is one of the less aggressive cancers, and generally slower to progress than most other cancers. However, annual deaths due to prostate cancer still amount to almost 30,000. Currently, nearly 3 million men in the United States are living with prostate cancer (National Cancer Institute, 2015). Radical prostatectomy and radiotherapy have been proven to be effective curative treatment methods for CaP

patients. However, in approximately 30% patients, the disease eventually recurs and becomes castration-resistant prostate cancer (CRPC) that is refractory to standard androgen deprivation therapy (Han et al., 2003).

Sipuleucel-T (Provenge) is a cell-based cancer immunotherapy for CaP that has been approved by the U.S. Food and Drug Administration (FDA) for the treatment of asymptomatic, or minimally symptomatic CRPC. Sipuleucel-T is a novel cancer vaccine developed from autologous DCs loaded with engineered fusion protein of prostatic acid phosphatase (PAP) specifically expressed in 95% of prostate tissue and prostate tumors, and GM-CSF (Thara et al., 2011). The resulting *ex vivo* activated DCs are then infused back into the original donor. Although a phase III clinical trial concluded that sipuleucel-T increased median patient survival by 4.1 months, it had no anti-tumor effect (Small et al., 2006; Thara et al., 2011). Moreover, the costly and labor-intensive nature of this immunotherapy becomes its own obstacle against widespread use. It is therefore of crucial importance to develop a therapeutic strategy that can specifically and efficiently target and eliminate CaP cells in a low-cost and easy-to-use fashion.

Prostate-specific antigen (PSA) is a protein of the kallikrein-related peptidase family and is secreted by the epithelial cells of the prostate gland. Serum PSA levels are often elevated in the presence of CaP (Catalona et al., 1994) and have been used as a common target tumor antigen for experimental CaP due to its restricted prostate tissue distribution and widespread expression in most prostate tumor cells.

Dendritic cells (DCs) are the major professional antigen-presenting cells (APCs) that are able to efficiently prime $CD8^+$ T cells. Extracellular or intracellular antigens, both endogenous and exogenous, can be captured and presented by DCs in the form of

major histocompatibility class I (MHC I)-peptide complex. Among various types of APCs, DCs are the most efficient at cross-presenting antigens to prime and boost naïve and memory $CD8^+$ T cells, respectively (Delamarre and Mellman, 2011; Jung et al., 2002; Segura and Villadangos, 2009). In addition, both effector and memory $CD8^+$ T cells are the key components of the therapeutic immunity against cancers and viral infections. Therefore, the potent ability of DCs to cross-present antigens to $CD8^+$ T cells effectively makes them ideal cellular targets for the rational design of cancer vaccines (Bonifaz et al., 2002; Bonifaz et al., 2004).

In this study, we generated a recombinant fusion protein of αCD40 antibody and PSA (αCD40-PSA) that targeted CD40-expressing DCs and induced both PSA-specific $CD4^+$ and $CD8^+$ T cells in the blood of normal donors, and activated PSA-specific $CD8^+$ in CaP patient blood. Furthermore, the immunogenicity of αCD40-PSA was assessed in the human CD40 transgenic mice.

Materials and Methods

Antibodies, Peptides, Tetramer and Other Reagents

Fluorescent dye-labeled αCD8, αCD4, and αIFNγ were purchased from BioLegend. αCD3, αCD80, αCD83, and αCD86 were purchased from BD Biosciences. Live/Dead fixable dead cell stain kit was from Invitrogen. HLA-A*02:01-$PSA_{KLQCVDLHV}$ tetramer labeled with fluorescent dye was from MBL International. Overlapping 15-mer peptides spanning human $PSA_{1\text{-}244}$, $HPV16.E6_{1\text{-}120}$ and $HPV16.E7_{1\text{-}60}$ proteins, and gear-bound peptide library for the ectodomain of CD40 were purchased from Mimotopes. IL-2 and IL-7 used in cell cultures were from PeproTech. Poly(I:C) was purchased from

Invivogen. Mouse $CD8^+$ T cell (negative) enrichment kit and $CD4^+$ T cell (positive) enrichment kit were both purchased from StemCell Technologies.

DC-Targeting mAbs

αCD40 (12E12) specific for the ectodomains of human CD40 was previously described (Flamar et al., 2013). Cloned mAbs were purified by HPLC using MabSelect resin (GE Healthcare). The specificities of mAbs were verified by their specific binding to corresponding receptors expressed on 293F cells transfected with the full-length receptors. The specificities of the mAbs were also confirmed with ELISA by comparing with their corresponding recombinant receptor-Fc and hIgG-Fc fusion proteins (Ni et al., 2010). Chimeric mAbs containing human IgG4 heavy chain with two site mutations (S228P and L235E) were made (Reddy et al., 2000).

Recombinant Fusion Proteins of mAb-PSA

Fusion protein bearing PSA fused to the heavy chain C-terminus was produced using methods previously described(Flamar et al., 2013; Li et al., 2012; Ni et al., 2010), and are exemplified in the GenBank sequences of a humanized αCD40 (12E12) derivative αCD40VH2-PSA paired with the corresponding light chain αCD40VK2-hIgGK sequence within KM660792.

Human Cells, Cell Culture Medium, and In Vitro Experiments

All human samples were from donors who provided a written informed consent prior to inclusion in the study in accordance to the approval by the Institutional Review

Boards at Baylor Research Institute, Baylor University Medical Center. PBMCs were enriched from peripheral blood of healthy donor or CaP patients by density gradient centrifugation with Ficoll Paque PLUS (GE Healthcare). Monocytes, $CD4^+$ and $CD8^+$ T cells were further purified using cell enrichment kits (StemCell Technologies). RPMI 1640 medium (Gibco), supplemented with 10% heat-inactivated human AB serum (Gemini), 50 unit/mL penicillin, 50 μg/mL streptomycin, 2 mM L-glutamate, 1X non-essential amino acids (Sigma), 25 mM HEPES (Life Technologies), and 1 mM sodium pyruvate (Sigma), was used as cell culture medium for human *in vitro* experiments. For DC-T cell coculture experiments, a total of 5 x 10^3 Mo-DCs, differentiated from monocytes in the presence of GM-CSF and IFNα, were cultured for 24 h with αCD40-PSA at 3.2 μg/mL, and later co-cocultured with autologous 2 x 10^5 $CD4^+$ or $CD8^+$ T cells in a 37°C incubator with 5% CO_2. IL-2 (50 units/mL) and IL-7 (50 units/mL) were supplemented on day two. Cells were recovered and restimulated with PSA peptides. Cells were restimulated for either 6 h to be further intracellularly stained for IFNγ production, or 48 h and IFNγ levels in cell cultures were detected by Luminex analysis. For patient samples, $CD8^+$ T cells were stained with HLA-A*02:01-$PSA_{KLQCVDLHV}$ tetramer on day eight. In DC activation assays, 1 x 10^5 Mo-DCs were cultured in the presence of αCD40-PSA at 3.2 μg/mL and were stained for activation marker expression 24 h later. In proliferation assays, CFSE-stained T cells were recovered on day six. All flow cytometry data were collected on FACSCanto II (BD Biosciences) and analyzed with FlowJo v9 (Tree Star).

Epitope Determination

Gear-bound peptide library of CD40 (15-mers over lapping by 11 amino acids) was incubated with αCD40-PSA and later with a secondary antibody conjugated with horseradish peroxidase (HRP). Substrate 3,3',5,5'-tetramethylbenzidine (TMB) was added to induce colorimetric change. ODs were measured on SpectraMax M2 (Molecular Devices).

Mice, Immunization, and Sample Collection

hCD40Tg mice (ImmuRx) used were 6-to-10-week-old males. Mouse experiments were conducted with the approval of the Institutional Animal Care and Use Committee at Baylor Research Institute. In experiments testing the immunogenicity of αCD40-PSA recombinant fusion protein, hCD40Tg or wild-type mice were immunized s.c on days 0, 14 and 28, with 100 μL of vaccine composed of 30 μg αCD40-PSA and 50 μg poly(I:C) in PBS. Mice were sacrificed on day 35. Spleen was collected from all the mice and processed into single-cell suspension with frosted-end glass slides (Fisher Scientific).

ELISpot Assays

Mouse IFNγ ELISpot^{Plus} pre-coated plates and reagents were obtained from Mabtech. Briefly, purified splenic $CD4^+$ and $CD8^+$ T cells from immunized mice were stimulated with γ-irradiated wild-type splenocytes loaded with the indicated peptide pools at 1 μM. After a 40-h incubation, plates were washed and incubated with biotinylated rat anti-mouse IFNγ for 2 h. After washing plates, streptavidin-HRP was added and

incubated for 1 h. IFNγ was detected using TMB. The reaction was terminated once the formation of discrete purple-colored spots was detected. Spots were counted using ELISpot services (Zellnet Consulting).

Statistical Analysis

Primary methods of data analysis included descriptive statistics (means and SD). Differences between two groups were detected using Student's *t* test or analysis of variance, as indicated in figure legends. Significance was set at $P < 0.05$. Data are presented as the mean ± SD. All data sets were calculated and analyzed with Prism 6 (GraphPad Software).

Results

Generation and Characterization of αCD40-PSA

Recombinant fusion protein of humanized αCD40 antibody (12E12) and PSA was generated as previously described (Flamar et al., 2013; Joo et al., 2014; Li et al., 2012). As shown in Figure 39A, αCD40-PSA carries PSA_{1-244}. The PSA sequence was conjugated to αCD40 via a linker sequence. Figure 39B (left) further illustrates the structure of the αCD40-PSA fusion protein. Results from SDS-PAGE analysis of the parental humanized αCD40 antibody and αCD40-PSA are shown in Figure 39B (right).

We next tested whether αCD40-PSA retained its ability to bind to human CD40. Human CD40 transfected CHO cell was stained with different amounts (0.01 to 10 μg/ml) of αCD40-PSA or IgG4-PSA. As shown in Figure 40A, αCD40-PSA bound to CHO-hCD40 line in a dose-dependent manner, while IgG4-PSA did not. Neither

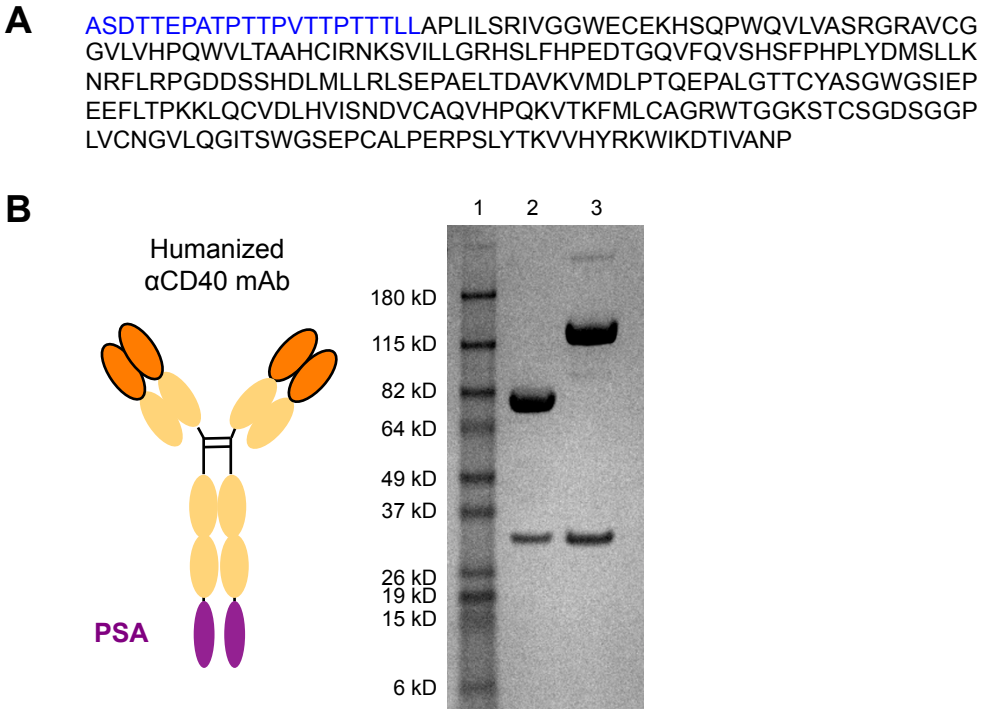

Figure 39. Composition of recombinant fusion protein αCD40-PSA. (A) Amino acid sequence of PSA. Linker sequence (blue) and PSA_{1-244} (black) are shown. (B) Left, schematic representation of αCD40-PSA. Right, reducing SDS-PAGE analysis of purified recombinant fusion proteins. Lane 1, molecular weight ladder; Lane 2, αCD40; Lane 3, αCD40-PSA.

nor IgG4-PSA bound to CHO cells transfected with a mock plasmid (Figure 40A, bottom). αCD40-PSA was also able to efficiently bind to monocyte-derived DCs (Mo-DCs) even at a concentration of 0.125 μg/mL, while IgG4-PSA did not (Figure 40B, left). Summarized data from two experiments are shown in (Figure 40B, right). Taken together, we conclude that αCD40-PSA could efficiently bind to CD40 and could thus target CD40-expressing DCs.

We further characterized αCD40-PSA binding sites using gear-bound peptides (41 15-mers over lapping by 11 amino acids) derived from the ectodomain of CD40 (Table 1). Figure 41A shows that αCD40-PSA mainly recognized three regions, all of which are

part of the tumor necrosis factor receptor cysteine-rich regions (TNFR Cys), as shown in Figure 41B, which are largely overlapping with the binding sites of CD40L.

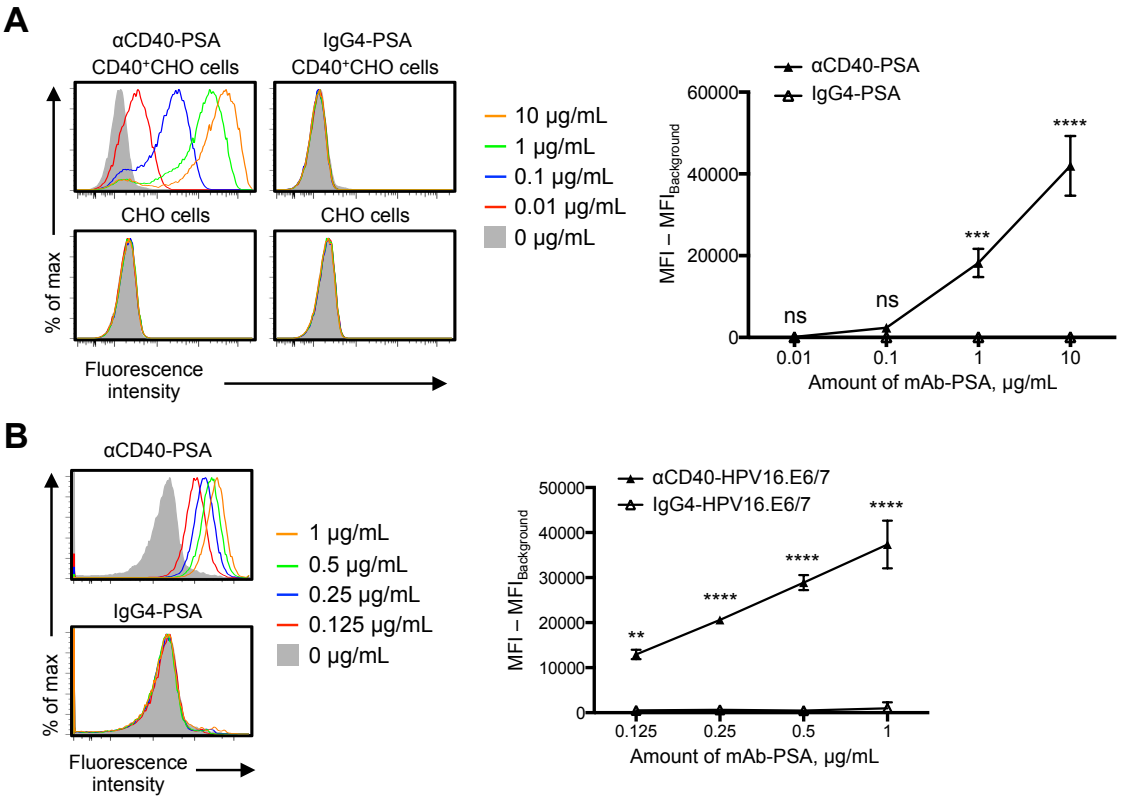

Figure 40. Binding of αCD40-PSA. (A) Binding of αCD40-PSA or control IgG4-PSA to CHO cells transfected with CD40 or a mock plasmid. Left, histogram overlays showing distributions of fluorescence intensities of CHO cells incubated with fusion proteins at 10, 1, 0.1, 0.01 and 0 μg/mL. Right, mean fluorescence intensity (MFI) comparisons between fusion proteins on CD40-expressing CHO cells. (B) Binding of αCD40-PSA or control IgG4-PSA to Mo-DCs. Left, histogram overlays showing distributions of MFIs of fusion proteins at 1, 0.5, 0.25, 0.125 and 0 μg/mL. Right, MFI comparison between fusion proteins. Data are presented as mean ± SD and significance was calculated using an ANOVA test. **, $P < 0.01$; ****, $P < 0.001$; ns, not significant.

αCD40-PSA Can Activate DCs and Promote T Cell Proliferation

Since the parental αCD40 is agonistic (Flamar et al., 2013), we tested whether the fusion protein αCD40-PSA retained its activating effect on Mo-DCs. Figure 42A shows

Table 1. Gear-bound peptide library of ectodomain of CD40

No.	Position	Sequence	No.	Position	Sequence
1	1-15	PPTACREKQYLINSQ	22	85-99	EEGWHCTSEACESCV
2	5-19	CREKQYLINSQCCSL	23	89-103	HCTSEACESCVLHRS
3	9-23	QYLINSQCCSLCQPG	24	93-107	EACESCVLHRSCSPG
4	13-27	NSQCCSLCQPGQKLV	25	97-111	SCVLHRSCSPGFGVK
5	17-31	CSLCQPGQKLVSDCT	26	101-115	HRSCSPGFGVKQIAT
6	21-35	QPGQKLVSDCTEFTE	27	105-119	SPGFGVKQIATGVSD
7	25-39	KLVSDCTEFTETECL	28	109-123	GVKQIATGVSDTICE
8	29-43	DCTEFTETECLPCGE	29	113-127	IATGVSDTICEPCPV
9	33-47	FTETECLPCGESEFL	30	117-131	VSDTICEPCPVGFFS
10	37-51	ECLPCGESEFLDTWN	31	121-135	ICEPCPVGFFSNVSS
11	41-55	CGESEFLDTWNRETH	32	125-139	CPVGFFSNVSSAFEK
12	45-59	EFLDTWNRETHCHQH	33	129-143	FFSNVSSAFEKCHPW
13	49-63	TWNRETHCHQHKYCD	34	133-147	VSSAFEKCHPWTSCE
14	53-67	ETHCHQHKYCDPNLG	35	137-151	FEKCHPWTSCETKDL
15	57-71	HQHKYCDPNLGLRVQ	36	141-155	HPWTSCETKDLVVQQ
16	61-75	YCDPNLGLRVQQKGT	37	145-159	SCETKDLVVQQAGTN
17	65-79	NLGLRVQQKGTSETD	38	149-163	KDLVVQQAGTNKTDV
18	69-83	RVQQKGTSETDTICT	39	153-167	VQQAGTNKTDVVCGP
19	73-87	KGTSETDTICTCEEG	40	157-171	GTNKTDVVCGPQDRL
20	77-91	ETDTICTCEEGWHCT	41	158-172	TNKTDVVCGPQDRLR
21	81-95	ICTCEEGWHCTSEAC			

that αCD40-PSA induced the expression of CD80, CD83, and CD86 on DCs. However, comparing to αCD40, the agonistic effect of αCD40-PSA was significantly weaker. Summarized data from four donors are shown in Figure 42B. These data suggest that αCD40-PSA could activate DCs.

We then co-cultured autologous CFSE-stained $CD4^+$ and $CD8^+$ T cells with Mo-DCs that were pre-incubated with αCD40-PSA (Figures 42C and 42D). αCD40-PSA-loaded Mo-DCs were able to induce the most significant expansion of both $CD4^+$ and $CD8^+$ T cells, compared to the IgG4-PSA-loaded or untreated Mo-DCs. In conclusion, αCD40-PSA could activate DCs, which in turn could further promote T cell proliferation.

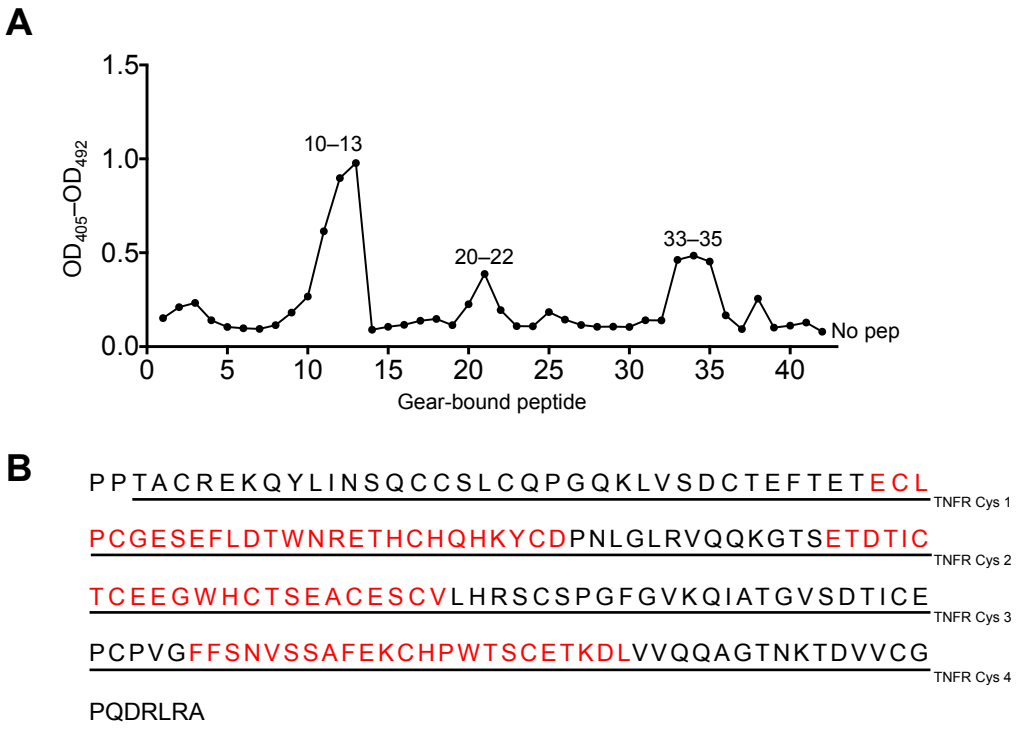

Figure 41. Binding epitopes of αCD40-PSA on CD40. (A and B) Gear-bound peptide library of CD40 (15-mers over lapping by 11 amino acids) was incubated with αCD40-PSA and later with a secondary antibody conjugated with horseradish peroxidase. Substrate was added to induce colorimetric change. Optical density at 450 nm (OD_{450}) minus the background at OD_{492} was measured on a spectrophotometer. (A) OD for all 41 peptides. Data are representative of three independent experiments. (B) Sequence of the ectodomain of CD40. TNFR Cys sequences are underlined and binding epitopes of αCD40-PSA are in red.

αCD40-PSA-Loaded DCs Are Able to Prime PSA-Specific $CD4^+$ and $CD8^+$ T Cells

To test the immunogenicity of αCD40-PSA, CFSE-labeled $CD4^+$ and $CD8^+$ T cells purified from PBMCs of healthy donors were co-cultured with αCD40-PSA-loaded DCs, and then restimulated with individual peptides or peptide pool derived from PSA (Table 2). Figure 43 shows representative flow cytometric data on PSA-specific $CD4^+$ and $CD8^+$ T cells primed by αCD40-PSA-loaded DCs. Figures 44 and 45 show the

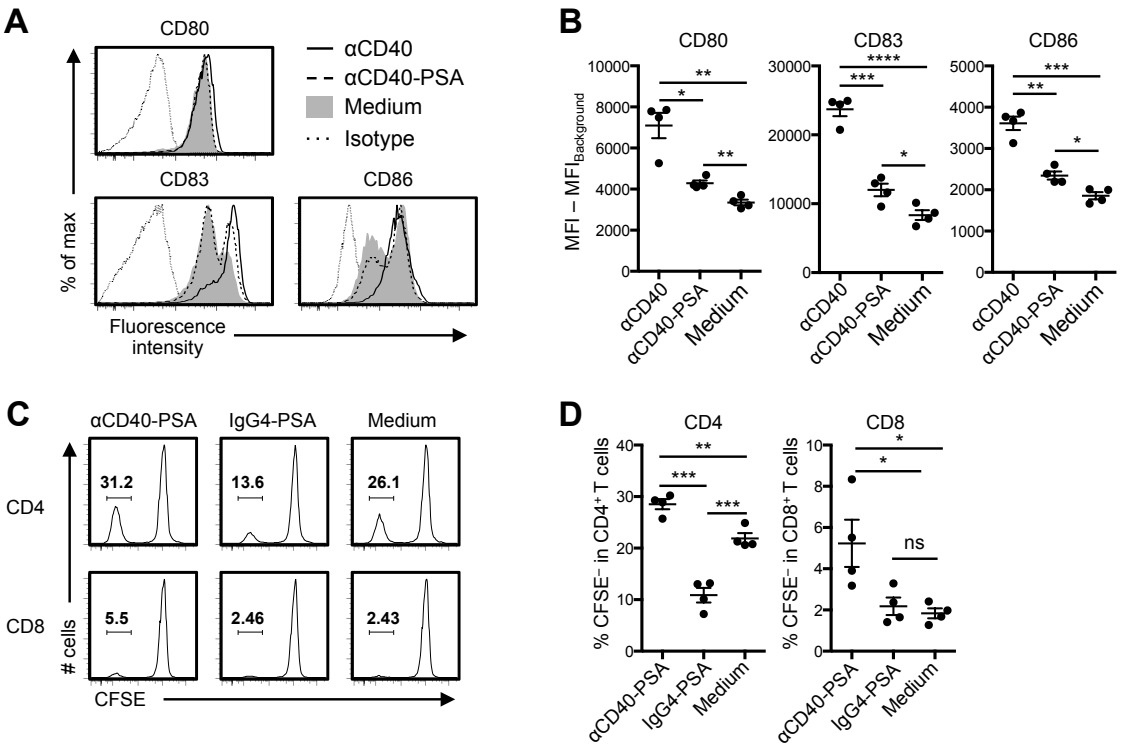

Figure 42. αCD40-PSA can activate DCs. (A and B) Mo-DCs were cultured in the presence of αCD40-PSA at 3.2 μg/mL or equimolar αCD40, isotype control, or left untreated. Surface expression of CD80, CD83 and CD86 was determined 24 h later. (A) Representative histogram overlays showing the distributions of fluorescence intensities of each marker. (B) Summarized data on MFIs of markers from differentially treated DCs from six healthy donors. (C–D) Purified CFSE-stained $CD4^+$ and $CD8^+$ T cells were co-cultured for six days with autologous Mo-DCs pre-incubated with αCD40-PSA, IgG4-PSA or left treated. (C) Representative histograms showing the frequencies of proliferated T cells. (D) Summarized data from four donors. Dots represent data generated with individual healthy donor samples and are presented as mean ± SD. Significance was determined using a paired *t* test. *, $P < 0.05$; **, $P < 0.01$; ***, $P < 0.005$; ****, $P < 0.001$; ns, not significant.

frequencies of IFNγ-producing cells and the IFNγ levels in cell cultures of $CD4^+$ and $CD8^+$ T cells, respectively, in response to restimulation by all the peptides and peptide pool. Taken together, these data indicate that αCD40-PSA was able to prime both PSA-specific $CD4^+$ and $CD8^+$ T cells.

Table 2. Peptide library of prostate-specific antigen

No.	Position	Sequence	No.	Position	Sequence
1	1-15	APLILSRIVGGWECE	31	121-135	VMDLPTQEPALGTTC
2	5-19	LSRIVGGWECEKHSQ	32	125-139	PTQEPALGTTCYASG
3	9-23	VGGWECEKHSQPWQV	33	129-143	PALGTTCYASGWGSI
4	13-27	ECEKHSQPWQVLVAS	34	133-147	TTCYASGWGSIEPEE
5	17-31	HSQPWQVLVASRGRA	35	137-151	ASGWGSIEPEEFLTP
6	21-35	WQVLVASRGRAVCGG	36	141-155	GSIEPEEFLTPKKLQ
7	25-39	VASRGRAVCGGVLVH	37	145-159	PEEFLTPKKLQCVDL
8	29-43	GRAVCGGVLVHPQWV	38	149-163	LTPKKLQCVDLHVIS
9	33-47	CGGVLVHPQWVLTAA	39	153-167	KLQCVDLHVISNDVC
10	37-51	LVHPQWVLTAAHCIR	40	157-171	VDLHVISNDVCAQVH
11	41-55	QWVLTAAHCIRNKSV	41	161-175	VISNDVCAQVHPQKV
12	45-59	TAAHCIRNKSVILLG	42	165-179	DVCAQVHPQKVTKFM
13	49-63	CIRNKSVILLGRHSL	43	169-183	QVHPQKVTKFMLCAG
14	53-67	KSVILLGRHSLFHPE	44	173-187	QKVTKFMLCAGRWTG
15	57-71	LLGRHSLFHPEDTGQ	45	177-191	KFMLCAGRWTGGKST
16	61-75	HSLFHPEDTGQVFQV	46	181-195	CAGRWTGGKSTCSGD
17	65-79	HPEDTGQVFQVSHSF	47	185-199	WTGGKSTCSGDSGGP
18	69-83	TGQVFQVSHSFPHPL	48	189-203	KSTCSGDSGGPLVCN
19	73-87	FQVSHSFPHPLYDMS	49	193-207	SGDSGGPLVCNGVLQ
20	77-91	HSFPHPLYDMSLLKN	50	197-211	GGPLVCNGVLQGITS
21	81-95	HPLYDMSLLKNRFLR	51	201-215	VCNGVLQGITSWGSE
22	85-99	DMSLLKNRFLRPGDD	52	205-219	VLQGITSWGSEPCAL
23	89-103	LKNRFLRPGDDSSHD	53	209-223	ITSWGSEPCALPERP
24	93-107	FLRPGDDSSHDLMLL	54	213-227	GSEPCALPERPSLYT
25	97-111	GDDSSHDLMLLRLSE	55	217-231	CALPERPSLYTKVVH
26	101-115	SHDLMLLRLSEPAEL	56	221-235	ERPSLYTKVVHYRKW
27	105-119	MLLRLSEPAELTDAV	57	225-239	LYTKVVHYRKWIKDT
28	109-123	LSEPAELTDAVKVMD	58	229-243	VVHYRKWIKDTIVAN
29	113-127	AELTDAVKVMDLPTQ	59	230-244	VHYRKWIKDTIVANP
30	117-131	DAVKVMDLPTQEPAL			

αCD40-PSA-Loaded DCs Efficiently Activate PSA-Specific CD8$^+$ T Cells

We next tested whether αCD40-PSA could activate PSA-specific T cells from PBMCs of patients with stage III CaP. Patient CD8$^+$ T cells were enriched and co-cultured with Mo-DCs, which were differentiated from autologous monocytes, in the presence of equimolar amounts of αCD40-PSA, αCD40 mAb plus PSA protein, PSA protein only, or αCD40 mAb only. CD8$^+$ T cells were then stained with tetramer

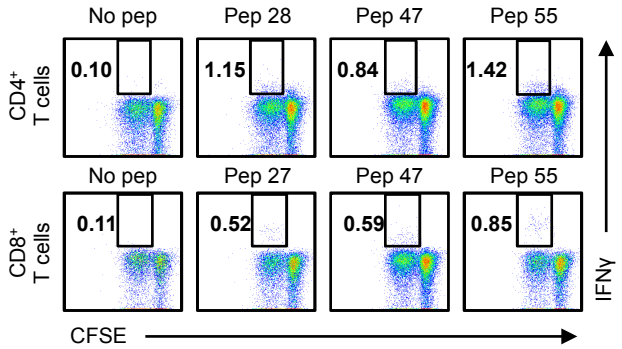

Figure 43. DCs loaded with αCD40-PSA can prime PSA-specific $CD4^+$ and $CD8^+$ T cells (staining). Purified CFSE-stained $CD4^+$ and $CD8^+$ T cells were co-cultured with autologous Mo-DCs pre-incubated with αCD40-PSA at 3.2 μg/mL. Cells were restimulated on day eight with individual peptides or peptide pool at 1 μM. Shown are representative flow cytometric data on intracellular expressions of IFNγ by proliferated $CD4^+$ T cells in response to Pep 28 (LSEPAELTDAVKVMD), Pep 47 (WTGGKSTCSGDSGGP), and Pep 55 (CALPERPSLYTKVVH) and $CD8^+$ T cells to Pep 27 (MLLRLSEPAELTDAV), Pep 47, and Pep 55.

containing $PSA_{153\text{-}161}$ (KLQCVDLHV) (Alexander et al., 1998). Figure 46 shows that Mo-DCs loaded with αCD40-PSA activated the highest frequencies of tetramer$^+$$CD8^+$ T cells, compared to PSA protein alone, or PSA protein plus αCD40 plus PSA protein, suggesting that αCD40-PSA was able to activate PSA-specific $CD8^+$ T cells.

αCD40-PSA Can Prime PSA-Specific $CD4^+$ and $CD8^+$ T Cells In Vivo

We then tested the *in vivo* immunogenicity of αCD40-PSA in human CD40-trangenic (hCD40Tg) mice. Figure 47A shows that αCD40-PSA bound to $CD11c^+$ and $CD19^+$, but not $CD3^+$ cells, in the spleen of the hCD40Tg mice. hCD40Tg or wild-type (WT) mice were immunized with a combination of αCD40-PSA at 30 μg/dose and poly(I:C) at 50 μg/dose through subcutaneous injection, as previously described (Bonifaz et al., 2002; Gurer et al., 2008), for a total of three times in two-week intervals. One week after the final injection, IFNγ production by splenic PSA-specific $CD8^+$ and $CD4^+$ T cells

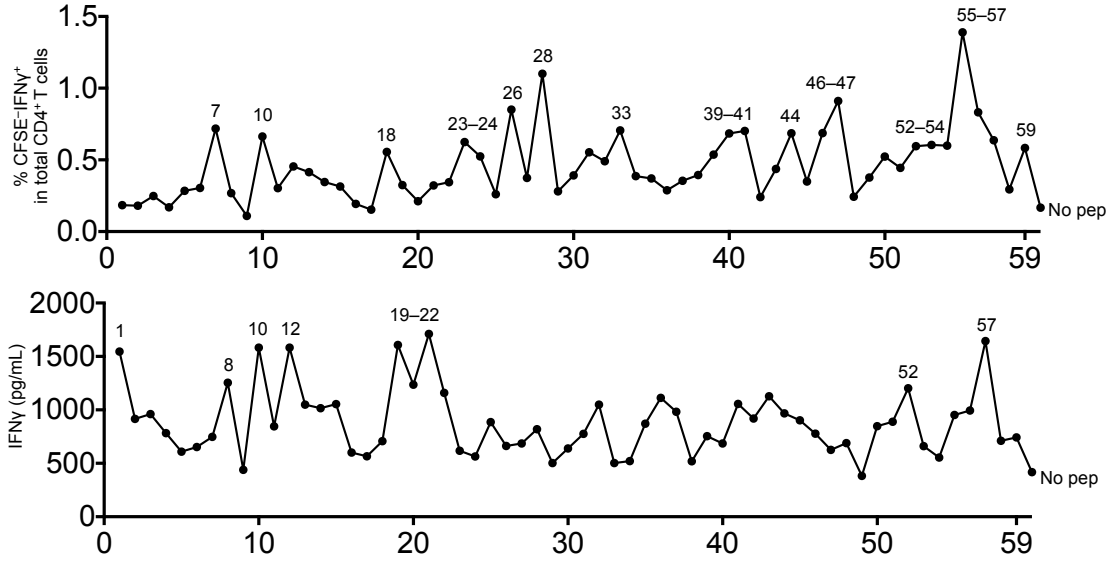

Figure 44. DCs loaded with αCD40-PSA can prime PSA-specific $CD4^+$ T cells (staining and Luminex). Cells were cultured as in Figure 43. Top, frequencies of $CFSE^-$ $IFN\gamma^+CD4^+$ T cells in response to individual peptides and peptide pool. Bottom, $IFN\gamma^+$ expression levels in $CD4^+$ T-cell culture supernatant 48 h after restimulation. Similar data were obtained in three independent experiments.

were quantified by ELISpot assays (Figure 47B). hCD40Tg mice immunized with αCD40-PSA had significantly more IFNγ-producing $CD8^+$ and $CD4^+$ T cells in response to restimulation with PSA peptide pool, compared with WT mice immunized with the same combination. These data demonstrate that αCD40-PSA plus poly(I:C) was immunogenic and could thus prime PSA-specific $CD8^+$ and $CD4^+$ T cells in hCD40Tg mice.

To further characterize the PSA-specific $CD8^+$ and $CD4^+$ T cell responses, we restimulated splenic $CD8^+$ and $CD4^+$ T cells with six partially overlapping peptide clusters (C1–C6) covering the whole sequence of PSA (Figures 48A and 48B). The

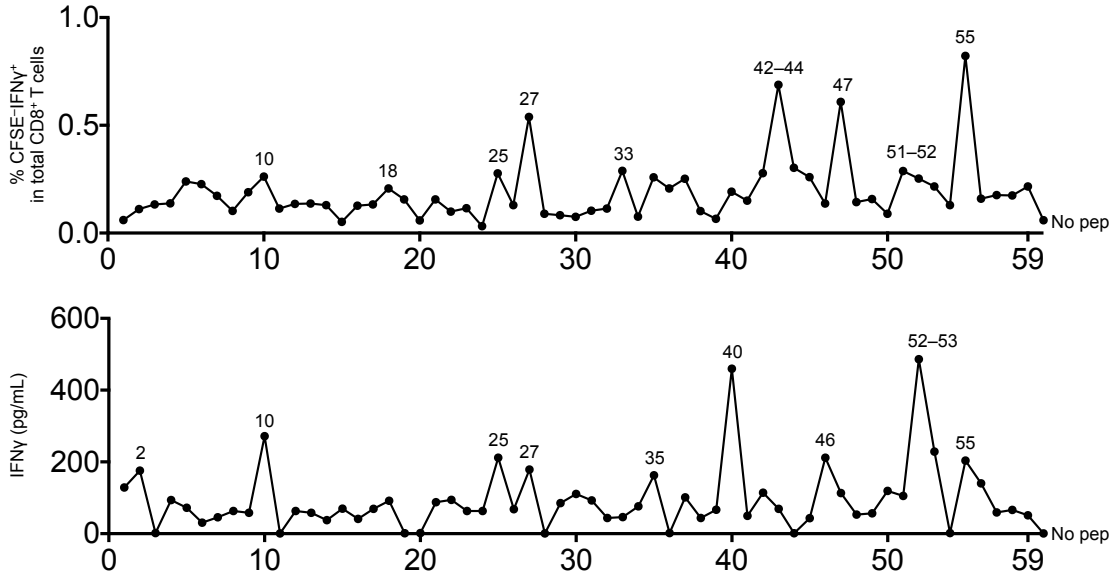

Figure 45. DCs loaded with αCD40-PSA can prime PSA-specific $CD8^+$ T cells (staining and Luminex). Cells were cultured as in Figure 43. Top, frequencies of $CFSE^-$ $IFN\gamma^+CD8^+$ T cells in response to individual peptides and peptide pool. Bottom, $IFN\gamma^+$ expression levels in $CD8^+$ T-cell culture supernatant 48 h after restimulation. Similar data were obtained in three independent experiments.

majority of responding $CD8^+$ T cells primed with αCD40-PSA were specific to C2, while the responding $CD4^+$ T cells primed with αCD40-PSA were specific to both C2 and C4, as previously described (Hural et al., 2002; Klyushnenkova et al., 2012; Lemke et al., 2011). Taken together, we concluded that αCD40-PSA plus poly(I:C) could prime both PSA-specific $CD8^+$ and $CD4^+$ T cells *in vivo*.

Discussion

CaP is becoming one of the major cancers in males worldwide. Although common and less aggressive than most other types of cancers, affordable and easy-to-use therapeutic methods are needed to improve the quality of life of CaP patients. Sipuleucel-

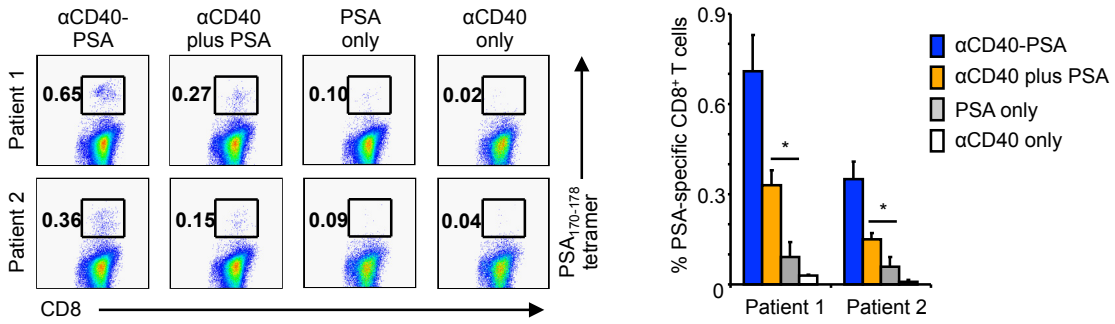

Figure 46. DCs loaded with αCD40-PSA activate PSA-specific $CD8^+$ T cells. Purified CaP patient $CD8^+$ T cells were co-cultured with autologous Mo-DCs pre-incubated with equimolar αCD40-PSA, αCD40 mAb plus PSA protein, PSA protein only, or αCD40 mAb only. On day eight, cells were stained with tetramer containing $PSA_{153-161}$ (KLQCVDLHV). Left, representative flow cytometric data on $tetramer^+CD8^+$ T cells. Right, summarized data on the frequencies of $tetramer^+CD8^+$ T cells from two CaP patients. Data are presented as mean ± SD. Significance was determined using an ANOVA test. *, $P < 0.05$.

T, as the only FDA-approved CaP vaccine on the market, is only minimally effective at treating CaP. Here we reported that a novel CaP vaccine, αCD40-PSA, was able to specifically target DCs to not only prime and activate naïve and memory $CD8^+$ T cells *in vitro*, respectively, but also could elicit strong $CD4^+$ and $CD8^+$ T cell responses *in vivo* when combined with poly(I:C).

CD40 is expressed mainly on APCs, including DCs, and has been known as a co-stimulatory receptor that interacts with CD40L expressed on activated T cells. We have previously reported that targeting antigens through CD40 on DCs could more efficiently cross-prime and cross-activate antigen-specific $CD8^+$ T cells than targeting antigens via lectins, including Dectin-1 and LOX-1 (manuscript in submission).

In this study, we first demonstrated that αCD40-PSA was able to specifically target CD40-expressing DCs by binding to the four TNFR Cys regions of CD40. Since the parental αCD40 mAb is agonistic (Flamar et al., 2013), we tested to confirm whether

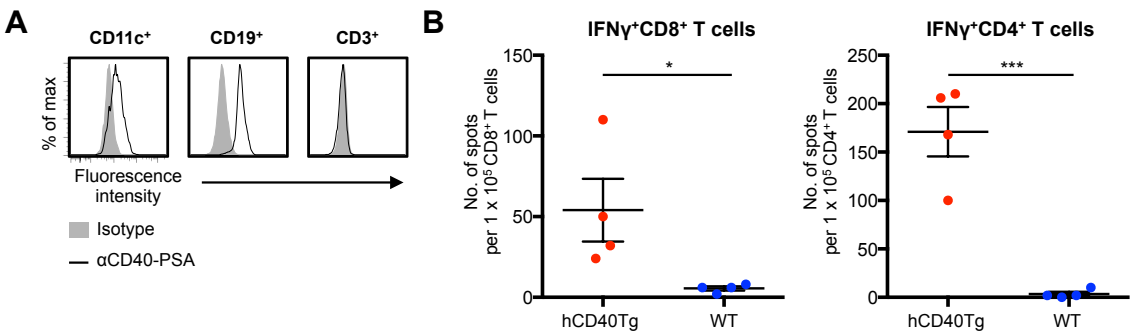

Figure 47. αCD40-PSA can prime PSA-specific $CD4^+$ and $CD8^+$ T cell *in vivo*. (A) Binding of αCD40-PSA at 2 μg/mL to splenic $CD11c^+$ DCs, $CD19^+$ B cells, and $CD3^+$ T cells of hCD40Tg mouse. (B–D) hCD40Tg or WT mice (n=4 per group) were immunized s.c. with a combination of αCD40-PSA (30 μg/dose) and poly(I:C) (50 μg/dose) in 100 μL PBS. Mice were boosted twice with the same vaccine at two-week intervals and were sacrificed 7 days after the second boost. Spleen was harvested. (B) IFNγ ELISpot assays were performed on $CD8^+$ (left) and $CD4^+$ (right) T cells purified from splenocytes and restimulated for 36 h with PSA peptide pool at 1 μM. Dots represent data generated with individual mice and are presented as mean ± SD Significance was determined using an unpaired *t* test. *, $P < 0.05$; ***, $P < 0.005$.

αCD40-PSA was still agonistic. Although αCD40-PSA activated DCs by increasing the expression levels of CD80, CD83, and CD86, the agonistic effect was significantly decreased. One possible explanation is that PSA itself can inhibit DC activation, as previously reported (Aalamian et al., 2003). However, the remaining stimulating signals by αCD40-PSA were still able to promote the proliferation of both $CD4^+$ and $CD8^+$ T cells *in vitro*.

Next, we found that Mo-DCs loaded with αCD40-PSA efficiently primed PSA-specific $CD4^+$ and $CD8^+$ T cells in the blood of healthy donors, and activated PSA-specific memory $CD8^+$ T cells in CaP patient blood. These data suggest that αCD40-PSA was immunogenic *in vitro*.

Lastly, we showed that αCD40-PSA plus poly(I:C) was also highly immunogenic in hCD40Tg mice, inducing high frequencies of splenic IFNγ-producing $CD4^+$ and $CD8^+$

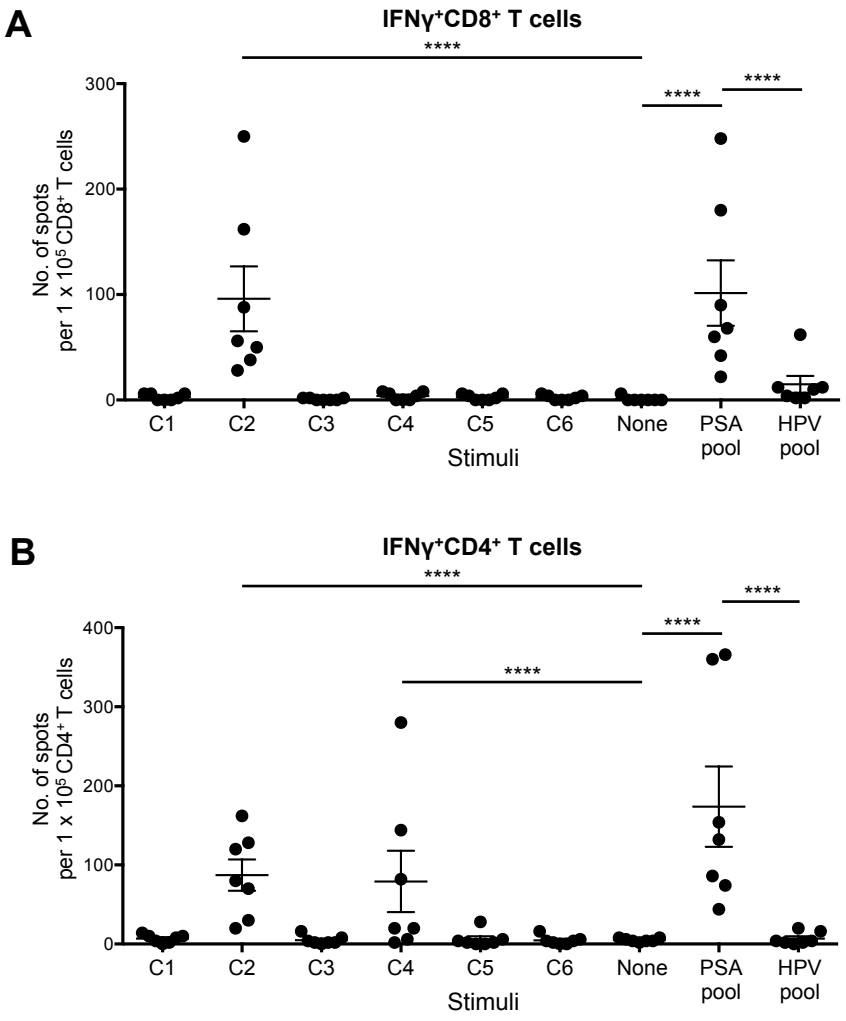

Figure 48. Characterization of PSA-specific T cell responses elicited by αCD40-PSA. (A and B) hCD40Tg mice (n=7) were immunized as in Figure 47. Purified splenic $CD8^+$ and $CD4^+$ T cells were restimulated with individual PSA peptide pool, clusters of PSA peptides (C1 to C6), or control peptide pool (HPV pool). IFNγ ELISpot assays performed with (A) $CD8^+$ and (B) $CD4^+$ T cells are shown. Dots represent data generated with individual mice and are presented as mean ± SD. Significance was determined using an unpaired *t* test (B) or ANOVA test (C and D). HPV, human papillomavirus. *, $P < 0.05$; ***, $P < 0.005$; ****, $P < 0.001$.

T cells, in accordance with our *in vitro* study. Poly(I:C) has been widely used as an adjuvant in various studies and has been shown to be more efficient than CL075 at eliciting $CD8^+$ T cell responses (Caskey et al., 2011; Quinn et al., 2013; Schulz et al., 2005).

In conclusion, targeting DCs with αCD40-PSA elicited PSA-specific T cell responses both *in vitro* and *in vivo*. Comparing to the current vaccines carrying PSA peptides, we anticipate that αCD40-PSA will be more effective against CaP due to the broad anti-CaP response repertoire elicited by the whole protein sequence of PSA that covers multiple $CD8^+$, and even $CD4^+$, T-cell epitopes. We hypothesize that αCD40-PSA is capable of mounting potent immune responses sufficient to provide therapeutic immunity against CaP. Furthermore, CD40-targeting vaccines against CaP are likely to be an alternative immunotherapy to the current *ex vivo* DC-based cancer vaccine, Sipuleucel-T.

CHAPTER SIX

Conclusions

Based on the studies presented, we conclude:

- Antigen targeting to DCs via CD40 is an efficient strategy for enhancing antigen cross-presentation to $CD8^+$ T cells.
- Targeting antigens to DCs via lectins (e.g., LOX-1 and Dectin-1) can efficiently activate antigen-specific $CD4^+$ T cells.
- αCD40-HPV16.E6/7 is able to prime and activate HPV-specific $CD4^+$ and $CD8^+$ T cells both *in vitro* and *in vivo*.
- αCD40-HPV16.E6/7 can elicit preventive and therapeutic immunity to HPV16.E6/7-expressing tumors in mice.
- αCD40-PSA primes and activates PSA-specific $CD4^+$ and $CD8^+$ T cells both *in vitro* and *in vivo*.

APPENDICES

APPENDIX A

List of Current and Future Publications

Publications Related to the Topics of Dissertation

Yin, W., L. Gorvel, D. Li, L. Ni, H. Joo, D. Duluc, K.C. Upchurch, C. Gu, Y. Xue, Z. Wang, S. Zurawski, J.-P. Gorvel, G. Zurawski, and S. Oh. Specialized functions of human dendritic cell surface receptors that enhance antigen cross-presentation to either $CD8^+$ or $CD4^+$ T cells (manuscript in revision).

Yin, W., D. Duluc, H. Joo, Y. Xue, C. Gu, Z. Wang, R. Ouedraogo, S. Zurawski, L. Oxford, A. Clark, F. Parikh, M. Posner, A. Sikora, G. Zurawski, and S. Oh. Preclinical assessment of CD40 targeting vaccine for HPV16-associated malignancies (manuscript in preparation).

Yin, W., D. Duluc, D. Li, H. Joo, Y. Xue, C. Gu, Z. Wang, R. Ouedraogo, S. Zurawski, G. Zurawski, and S. Oh. Preclinical assessment of CD40 targeting vaccine for prostate cancer (manuscript in preparation).

Additional Publications

Duluc, D., H. Joo, L. Ni, **W. Yin**, K. Upchurch, D. Li, Y. Xue, P. Klucar, S. Zurawski, G. Zurawski, and S. Oh. 2014. Induction and activation of human Th17 by targeting antigens to dendritic cells via dectin-1. *Journal of immunology* 192:5776-5788.

Upchurch, K.C., J.R. Boquin, **W. Yin**, Y. Xue, H. Joo, R.R. Kane, and S. Oh. 2015. New TLR7 agonists with improved humoral and cellular immune responses. *Immunology letters* 168:89-97.

APPENDIX B

Author Contributions

Chapter Three

W.Y. performed experiments in Figures 4, 5, 7, 8, 9, 11, 12, 14, 15, 16 and 20, analyzed the data, and wrote the manuscript. L.G. and J.-P.G. performed experiments in Figures 18 and 19, and analyzed the data. D.L. helped the experiments in Figures 5, 6, 13, 14 and 15, and analyzed the data. L.N. helped the experiments in Figures 8, 9, 10, 12, 14 and 15. D.D., H.J., K.C.U., Y.X., and C.G performed experiments in Figures 14, 15 and 17, and analyzed the data. Z.W., S.Z., and G.Z. made the fusion proteins and the protein conjugates. S.O. supervised the project, analyzed the data, and wrote the manuscript.

Chapter Four

W.Y. performed experiments in Figures 22, 23 and 26–38, analyzed the data, and wrote the manuscript. D.D. performed experiments in Figures 22, 24, 28, 29, 30 and 35–38, and analyzed the data. H.J., Y.X., C.G., and R.O provided general technical assistance. Z.W. and S.Z. performed the experiment in Figure 21, and made the fusion proteins and the protein conjugates. L.O, A.C., F.P., M.P., A.S. provided $HPV16^{+}$ patient samples. G.Z. made fusion proteins and helped the project. S.O. supervised the project, analyzed the data, and wrote the manuscript.

Chapter Five

W.Y. performed experiments in Figures 40, 41, 42, 43, 44, 45, 47 and 48, analyzed the data, and wrote the manuscript. D.D. helped the experiments in Figures 47 and 48. D.L. performed experiment in Figure 46 and analyzed the data. H.J., Y.X., C.G., and R.O provided general technical assistance. Z.W. and S.Z. performed the experiment in Figure 39, and made the fusion proteins and the protein conjugates. G.Z. made the fusion proteins. S.O. supervised the project, analyzed the data, and wrote the manuscript.

BIBLIOGRAPHY

Aalamian, M., I.L. Tourkova, G.S. Chatta, H. Lilja, E. Huland, H. Huland, G.V. Shurin, and M.R. Shurin. 2003. Inhibition of Dendropoiesis by Tumor Derived and Purified Prostate Specific Antigen. *The Journal of urology* 170:2026-2030.

Alexander, R.B., F. Brady, M.S. Leffell, V. Tsai, and E. Celis. 1998. Specific T cell recognition of peptides derived from prostate-specific antigen in patients with prostate cancer. *Urology* 51:150-157.

Angel, C.E., E. George, A.E.S. Brooks, L.L. Ostrovsky, T.L.H. Brown, and P.R. Dunbar. 2006. Cutting edge: CD1a+ antigen-presenting cells in human dermis respond rapidly to CCR7 ligands. *Journal of Immunology* 176:5730-5734.

Anguille, S., E.L. Smits, E. Lion, V.F. van Tendeloo, and Z.N. Berneman. 2014. Clinical use of dendritic cells for cancer therapy. *The Lancet. Oncology* 15:e257-267.

Annacker, O., J.L. Coombes, V. Malmstrom, H.H. Uhlig, T. Bourne, B. Johansson-Lindbom, W.W. Agace, C.M. Parker, and F. Powrie. 2005. Essential role for CD103 in the T cell-mediated regulation of experimental colitis. *Journal of Experimental Medicine* 202:1051-1061.

Bachem, A., S. Güttler, E. Hartung, F. Ebstein, M. Schaefer, A. Tannert, A. Salama, K. Movassaghi, C. Opitz, H.W. Mages, V. Henn, P.M. Kloetzel, S. Gurka, and R.A. Kroczek. 2010. Superior antigen cross-presentation and XCR1 expression define human CD11c+CD141+ cells as homologues of mouse CD8+ dendritic cells. *Journal of Experimental Medicine* 207:1273-1281.

Belizaire, R., and E.R. Unanue. 2009. Targeting proteins to distinct subcellular compartments reveals unique requirements for MHC class I and II presentation. *Proceedings of the National Academy of Sciences of the United States of America* 106:17463-17468.

Blasius, A.L., and B. Beutler. 2010. Intracellular toll-like receptors. *Immunity* 32:305-315.

Blot, W.J., J.K. McLaughlin, S.S. Devesa, and J.F.J. Fraumeni. 1996. Cancers of the oral cavity and pharynx. . In Cancer epidemiology and prevention. D. Schottenfeld, and J.F.J. Fraumeni, editors. Oxford University Press, New York. 666-680.

Bonifaz, L., D. Bonnyay, K. Mahnke, M. Rivera, M.C. Nussenzweig, and R.M. Steinman. 2002. Efficient targeting of protein antigen to the dendritic cell receptor DEC-205 in the steady state leads to antigen presentation on major histocompatibility complex class I products and peripheral CD8+ T cell tolerance. *The Journal of experimental medicine* 196:1627-1638.

Bonifaz, L.C., D.P. Bonnyay, A. Charalambous, D.I. Darguste, S. Fujii, H. Soares, M.K. Brimnes, B. Moltedo, T.M. Moran, and R.M. Steinman. 2004. In vivo targeting of antigens to maturing dendritic cells via the DEC-205 receptor improves T cell vaccination. *The Journal of experimental medicine* 199:815-824.

Burgdorf, S., A. Kautz, V. Bohnert, P.A. Knolle, and C. Kurts. 2007. Distinct pathways of antigen uptake and intracellular routing in CD4 and CD8 T cell activation. *Science (New York, N.Y.)* 316:612-616.

Burgdorf, S., C. Scholz, A. Kautz, R. Tampe, and C. Kurts. 2008. Spatial and mechanistic separation of cross-presentation and endogenous antigen presentation. *Nature immunology* 9:558-566.

Caminschi, I., A.I. Proietto, F. Ahmet, S. Kitsoulis, J. Shin Teh, J.C. Lo, A. Rizzitelli, L. Wu, D. Vremec, S.L. van Dommelen, I.K. Campbell, E. Maraskovsky, H. Braley, G.M. Davey, P. Mottram, N. van de Velde, K. Jensen, A.M. Lew, M.D. Wright, W.R. Heath, K. Shortman, and M.H. Lahoud. 2008. The dendritic cell subtype-restricted C-type lectin Clec9A is a target for vaccine enhancement. *Blood* 112:3264-3273.

Carter, R.W., C. Thompson, D.M. Reid, S.Y. Wong, and D.F. Tough. 2006. Preferential induction of CD4+ T cell responses through in vivo targeting of antigen to dendritic cell-associated C-type lectin-1. *Journal of immunology (Baltimore, Md. : 1950)* 177:2276-2284.

Caskey, M., F. Lefebvre, A. Filali-Mouhim, M.J. Cameron, J.P. Goulet, E.K. Haddad, G. Breton, C. Trumpfheller, S. Pollak, I. Shimeliovich, A. Duque-Alarcon, L. Pan, A. Nelkenbaum, A.M. Salazar, S.J. Schlesinger, R.M. Steinman, and R.P. Sekaly. 2011. Synthetic double-stranded RNA induces innate immune responses similar to a live viral vaccine in humans. *The Journal of experimental medicine* 208:2357-2366.

Castro, F.V., A.L. Tutt, A.L. White, J.L. Teeling, S. James, R.R. French, and M.J. Glennie. 2008. CD11c provides an effective immunotarget for the generation of both CD4 and CD8 T cell responses. *European journal of immunology* 38:2263-2273.

Catalona, W.J., J.P. Richie, F.R. Ahmann, M.A. Hudson, P.T. Scardino, R.C. Flanigan, J.B. deKernion, T.L. Ratliff, L.R. Kavoussi, B.L. Dalkin, and et al. 1994. Comparison of digital rectal examination and serum prostate specific antigen in the early detection of prostate cancer: results of a multicenter clinical trial of 6,630 men. *The Journal of urology* 151:1283-1290.

Cella, M., D. Jarrossay, F. Facchetti, O. Alebardi, H. Nakajima, A. Lanzavecchia, and M. Colonna. 1999. Plasmacytoid monocytes migrate to inflamed lymph nodes and produce large amounts of type I interferon. *Nat Med* 5:919-923.

Cerovic, V., S.A. Houston, C.L. Scott, A. Aumeunier, U. Yrlid, A.M. Mowat, and S.W.F. Milling. 2013. Intestinal CD103- dendritic cells migrate in lymph and prime effector T cells. *Mucosal Immunology* 6:104-113.

Cervantes-Barragan, L., K.L. Lewis, S. Firner, V. Thiel, S. Hugues, W. Reith, B. Ludewig, and B. Reizis. 2012. Plasmacytoid dendritic cells control T-cell response to chronic viral infection. *Proceedings of the National Academy of Sciences of the United States of America* 109:3012-3017.

Chatterjee, B., A. Smed-Sorensen, L. Cohn, C. Chalouni, R. Vandlen, B.C. Lee, J. Widger, T. Keler, L. Delamarre, and I. Mellman. 2012. Internalization and endosomal degradation of receptor-bound antigens regulate the efficiency of cross presentation by human dendritic cells. *Blood* 120:2011-2020.

Cohn, L., B. Chatterjee, F. Esselborn, A. Smed-Sorensen, N. Nakamura, C. Chalouni, B.C. Lee, R. Vandlen, T. Keler, P. Lauer, D. Brockstedt, I. Mellman, and L. Delamarre. 2013. Antigen delivery to early endosomes eliminates the superiority of human blood BDCA3+ dendritic cells at cross presentation. *The Journal of experimental medicine* 210:1049-1063.

Conry, S.J., K.A. Milkovich, N.L. Yonkers, B. Rodriguez, H.B. Bernstein, R. Asaad, F.P. Heinzel, M. Tary-Lehmann, M.M. Lederman, and D.D. Anthony. 2009. Impaired Plasmacytoid Dendritic Cell (PDC)-NK Cell Activity in Viremic Human Immunodeficiency Virus Infection Attributable to Impairments in both PDC and NK Cell Function. *Journal of virology* 83:11175-11187.

Crowley, M., K. Inaba, M. Witmer-Pack, and R.M. Steinman. 1989. The cell surface of mouse dendritic cells: FACS analyses of dendritic cells from different tissues including thymus. *Cellular Immunology* 118:108-125.

de Sanjose, S., M. Diaz, X. Castellsague, G. Clifford, L. Bruni, N. Munoz, and F.X. Bosch. 2007. Worldwide prevalence and genotype distribution of cervical human papillomavirus DNA in women with normal cytology: a meta-analysis. *Lancet Infect Dis* 7:453-459.

de Vos van Steenwijk, P.J., T.H. Ramwadhdoebe, M.J. Lowik, C.E. van der Minne, D.M. Berends-van der Meer, L.M. Fathers, A.R. Valentijn, J. Oostendorp, G.J. Fleuren, B.W. Hellebrekers, M.J. Welters, M.I. van Poelgeest, C.J. Melief, G.G. Kenter, and S.H. van der Burg. 2012. A placebo-controlled randomized HPV16 synthetic long-peptide vaccination study in women with high-grade cervical squamous intraepithelial lesions. *Cancer Immunol Immunother* 61:1485-1492.

Del Rio, M.-L., G. Bernhardt, J.-I. Rodriguez-Barbosa, and R. Förster. 2010. Development and functional specialization of CD103+ dendritic cells. *Immunological Reviews* 234:268-281.

Delamarre, L., H. Holcombe, and I. Mellman. 2003. Presentation of exogenous antigens on major histocompatibility complex (MHC) class I and MHC class II molecules is differentially regulated during dendritic cell maturation. *J Exp Med* 198:111-122.

Delamarre, L., and I. Mellman. 2011. Harnessing dendritic cells for immunotherapy. *Seminars in immunology* 23:2-11.

Delneste, Y. 2004. Scavenger receptors and heat-shock protein-mediated antigen cross-presentation. *Biochem Soc Trans* 32:633-635.

Delneste, Y., G. Magistrelli, J. Gauchat, J. Haeuw, J. Aubry, K. Nakamura, N. Kawakami-Honda, L. Goetsch, T. Sawamura, J. Bonnefoy, and P. Jeannin. 2002. Involvement of LOX-1 in dendritic cell-mediated antigen cross-presentation. *Immunity* 17:353-362.

Desch, A.N., G.J. Randolph, K. Murphy, E.L. Gautier, R.M. Kedl, M.H. Lahoud, I. Caminschi, K. Shortman, P.M. Henson, and C.V. Jakubzick. 2011. CD103+ pulmonary dendritic cells preferentially acquire and present apoptotic cell–associated antigen. *The Journal of experimental medicine* 208:1789-1797.

Dudziak, D., A.O. Kamphorst, G.F. Heidkamp, V.R. Buchholz, C. Trumpfheller, S. Yamazaki, C. Cheong, K. Liu, H.W. Lee, C.G. Park, R.M. Steinman, and M.C. Nussenzweig. 2007. Differential antigen processing by dendritic cell subsets in vivo. *Science (New York, N.Y.)* 315:107-111.

Duluc, D., H. Joo, L. Ni, W. Yin, K. Upchurch, D. Li, Y. Xue, P. Klucar, S. Zurawski, G. Zurawski, and S. Oh. 2014. Induction and activation of human Th17 by targeting antigens to dendritic cells via dectin-1. *Journal of immunology (Baltimore, Md. : 1950)* 192:5776-5788.

Dunne, E.F., C.M. Nielson, K.M. Stone, L.E. Markowitz, and A.R. Giuliano. 2006. Prevalence of HPV infection among men: A systematic review of the literature. *J Infect Dis* 194:1044-1057.

Edelson, B.T., K.C. Wumesh, R. Juang, M. Kohyama, L.A. Benoit, P.A. Klekotka, C. Moon, J.C. Albring, W. Ise, D.G. Michael, D. Bhattacharya, T.S. Stappenbeck, M.J. Holtzman, S.S.J. Sung, T.L. Murphy, K. Hildner, and K.M. Murphy. 2010. Peripheral CD103+ dendritic cells form a unified subset developmentally related to CD8α+ conventional dendritic cells. *Journal of Experimental Medicine* 207:823-836.

Edwards, L.E., C. Haluszczak, and R.M. Kedl. 2013. Phenotype and function of protective, CD4-independent CD8 T cell memory. *Immunologic research* 55:135-145.

Fausch, S.C., D.M. Da Silva, G.L. Eiben, I.C. Le Poole, and W.M. Kast. 2003. HPV protein/peptide vaccines: from animal models to clinical trials. *Front Biosci* 8:s81-91.

Feltkamp, M.C., H.L. Smits, M.P. Vierboom, R.P. Minnaar, B.M. de Jongh, J.W. Drijfhout, J. ter Schegget, C.J. Melief, and W.M. Kast. 1993. Vaccination with cytotoxic T lymphocyte epitope-containing peptide protects against a tumor induced by human papillomavirus type 16-transformed cells. *European journal of immunology* 23:2242-2249.

Figdor, C.G., I.J. de Vries, W.J. Lesterhuis, and C.J. Melief. 2004. Dendritic cell immunotherapy: mapping the way. *Nat Med* 10:475-480.

Fithian, E., P. Kung, G. Goldstein, M. Rubenfeld, C. Fenoglio, and R. Edelson. 1981. Reactivity of Langerhans cells with hybridoma antibody. *Proceedings of the National Academy of Sciences* 78:2541-2544.

Flacher, V., C.H. Tripp, B. Haid, A. Kissenpfennig, B. Malissen, P. Stoitzner, J. Idoyaga, and N. Romani. 2012. Skin langerin+ dendritic cells transport intradermally injected anti-DEC-205 antibodies but are not essential for subsequent cytotoxic CD8+ T cell responses. *Journal of immunology (Baltimore, Md. : 1950)* 188:2146-2155.

Flacher, V., C.H. Tripp, D.G. Mairhofer, R.M. Steinman, P. Stoitzner, J. Idoyaga, and N. Romani. 2014a. Murine Langerin+ dermal dendritic cells prime CD8+ T cells while Langerhans cells induce cross-tolerance. *EMBO molecular medicine* 6:1191-1204.

Flacher, V., C.H. Tripp, D.G. Mairhofer, R.M. Steinman, P. Stoitzner, J. Idoyaga, and N. Romani. 2014b. Murine Langerin+ dermal dendritic cells prime CD8+ T cells while Langerhans cells induce cross-tolerance. *EMBO molecular medicine* 6:1638.

Flamar, A.L., Y. Xue, S.M. Zurawski, M. Montes, B. King, L. Sloan, S. Oh, J. Banchereau, Y. Levy, and G. Zurawski. 2013. Targeting concatenated HIV antigens to human CD40 expands a broad repertoire of multifunctional CD4+ and CD8+ T cells. *AIDS (London, England)* 27:2041-2051.

Flamar, A.L., S. Zurawski, F. Scholz, I. Gayet, L. Ni, X.H. Li, E. Klechevsky, J. Quinn, S. Oh, D.H. Kaplan, J. Banchereau, and G. Zurawski. 2012. Noncovalent assembly of anti-dendritic cell antibodies and antigens for evoking immune responses in vitro and in vivo. *Journal of immunology (Baltimore, Md. : 1950)* 189:2645-2655.

Forster, R., A.C. Davalos-Misslitz, and A. Rot. 2008. CCR7 and its ligands: balancing immunity and tolerance. *Nature reviews. Immunology* 8:362-371.

Fujikado, N., S. Saijo, T. Yonezawa, K. Shimamori, A. Ishii, S. Sugai, H. Kotaki, K. Sudo, M. Nose, and Y. Iwakura. 2008. Dcir deficiency causes development of autoimmune diseases in mice due to excess expansion of dendritic cells. *Nat Med* 14:176-180.

Geijtenbeek, T.B., and S.I. Gringhuis. 2009. Signalling through C-type lectin receptors: shaping immune responses. *Nat Rev Immunol* 9:465-479.

Gerard, C.M., N. Baudson, K. Kraemer, C. Bruck, N. Garcon, Y. Paterson, Z.K. Pan, and D. Pardoll. 2001. Therapeutic potential of protein and adjuvant vaccinations on tumour growth. *Vaccine* 19:2583-2589.

Gilliet, M., W. Cao, and Y.J. Liu. 2008. Plasmacytoid dendritic cells: sensing nucleic acids in viral infection and autoimmune diseases. *Nature reviews. Immunology* 8:594-606.

Ginhoux, F., K. Liu, J. Helft, M. Bogunovic, M. Greter, D. Hashimoto, J. Price, N. Yin, J. Bromberg, S.A. Lira, E.R. Stanley, M. Nussenzweig, and M. Merad. 2009. The origin and development of nonlymphoid tissue CD103+ DCs. *The Journal of experimental medicine* 206:3115-3130.

Ginhoux, F., and M. Merad. 2010. Ontogeny and homeostasis of Langerhans cells. *Immunology and Cell Biology* 88:387-392.

Guéry, L., and S. Hugues. 2013. Tolerogenic and Activatory Plasmacytoid Dendritic Cells in Autoimmunity. *Frontiers in Immunology* 4:59.

Gunn, G.R., A. Zubair, C. Peters, Z.K. Pan, T.C. Wu, and Y. Paterson. 2001. Two Listeria monocytogenes vaccine vectors that express different molecular forms of human papilloma virus-16 (HPV-16) E7 induce qualitatively different T cell immunity that correlates with their ability to induce regression of established tumors immortalized by HPV-16. *J Immunol* 167:6471-6479.

Gurer, C., T. Strowig, F. Brilot, M. Pack, C. Trumpfheller, F. Arrey, C.G. Park, R.M. Steinman, and C. Munz. 2008. Targeting the nuclear antigen 1 of Epstein-Barr virus to the human endocytic receptor DEC-205 stimulates protective T-cell responses. *Blood* 112:1231-1239.

Han, M., A.W. Partin, M. Zahurak, S. Piantadosi, J.I. Epstein, and P.C. Walsh. 2003. Biochemical (prostate specific antigen) recurrence probability following radical prostatectomy for clinically localized prostate cancer. *The Journal of urology* 169:517-523.

Haniffa, M., A. Shin, V. Bigley, N. McGovern, P. Teo, P. See, P.S. Wasan, X.N. Wang, F. Malinarich, B. Malleret, A. Larbi, P. Tan, H. Zhao, M. Poidinger, S. Pagan, S. Cookson, R. Dickinson, I. Dimmick, R.F. Jarrett, L. Renia, J. Tam, C. Song, J. Connolly, J.K.Y. Chan, A. Gehring, A. Bertoletti, M. Collin, and F. Ginhoux. 2012. Human Tissues Contain CD141 hi Cross-Presenting Dendritic Cells with Functional Homology to Mouse CD103 + Nonlymphoid Dendritic Cells. *Immunity* 37:60-73.

Harding, C.V., D.S. Collins, J.W. Slot, H.J. Geuze, and E.R. Unanue. 1991. Liposome-encapsulated antigens are processed in lysosomes, recycled, and presented to T cells. *Cell* 64:393-401.

Harman, A.N., C.R. Bye, N. Nasr, K.J. Sandgren, M. Kim, S.K. Mercier, R.A. Botting, S.R. Lewin, A.L. Cunningham, and P.U. Cameronx. 2013. Identification of lineage relationships and novel markers of blood and skin human dendritic cells. *Journal of Immunology* 190:66-79.

Helft, J., F. Ginhoux, M. Bogunovic, and M. Merad. 2010. Origin and functional heterogeneity of non-lymphoid tissue dendritic cells in mice. *Immunological Reviews* 234:55-75.

Helft, J., B. Manicassamy, P. Guermonprez, D. Hashimoto, A. Silvin, J. Agudo, B.D. Brown, M. Schmolke, J.C. Miller, M. Leboeuf, K.M. Murphy, A. García-Sastre, and M. Merad. 2012. Cross-presenting CD103+ dendritic cells are protected from influenza virus infection. *Journal of Clinical Investigation* 122:4037-4047.

Hieronymus, T., T.C. Gust, R.D. Kirsch, T. Jorgas, G. Blendinger, M. Goncharenko, K. Supplitt, S. Rose-John, A.M. Müller, and M. Zenke. 2005. Progressive and Controlled Development of Mouse Dendritic Cells from Flt3+CD11b+ Progenitors In Vitro. *The Journal of Immunology* 174:2552-2562.

Hildner, K., B.T. Edelson, W.E. Purtha, M. Diamond, H. Matsushita, M. Kohyama, B. Calderon, B.U. Schraml, E.R. Unanue, M.S. Diamond, R.D. Schreiber, T.L. Murphy, and K.M. Murphy. 2008. Batf3 deficiency reveals a critical role for CD8α+ dendritic cells in cytotoxic T cell immunity. *Science (New York, N.Y.)* 322:1097-1100.

Hochrein, H., M. O'Keeffe, and H. Wagner. 2002. Human and mouse plasmacytoid dendritic cells. *Human Immunology* 63:1103-1110.

Hural, J.A., R.S. Friedman, A. McNabb, S.S. Steen, R.A. Henderson, and M. Kalos. 2002. Identification of Naturally Processed CD4 T Cell Epitopes from the Prostate-Specific Antigen Kallikrein 4 Using Peptide-Based In Vitro Stimulation. *The Journal of Immunology* 169:557-565.

Idoyaga, J., C. Cheong, K. Suda, N. Suda, J.Y. Kim, H. Lee, C.G. Park, and R.M. Steinman. 2008. Cutting edge: langerin/CD207 receptor on dendritic cells mediates efficient antigen presentation on MHC I and II products in vivo. *Journal of immunology (Baltimore, Md. : 1950)* 180:3647-3650.

Idoyaga, J., A. Lubkin, C. Fiorese, M.H. Lahoud, I. Caminschi, Y. Huang, A. Rodriguez, B.E. Clausen, C.G. Park, C. Trumpfheller, and R.M. Steinman. 2011. Comparable T helper 1 (Th1) and CD8 T-cell immunity by targeting HIV gag p24 to CD8 dendritic cells within antibodies to Langerin, DEC205, and Clec9A. *Proceedings of the National Academy of Sciences of the United States of America* 108:2384-2389.

Igyártó, B., K. Haley, D. Ortner, A. Bobr, M. Gerami-Nejad, B. Edelson, S. Zurawski, B. Malissen, G. Zurawski, J. Berman, and D. Kaplan. 2011. Skin-Resident Murine Dendritic Cell Subsets Promote Distinct and Opposing Antigen-Specific T Helper Cell Responses. *Immunity* 35:260-272.

Igyarto, B.Z., K. Haley, D. Ortner, A. Bobr, M. Gerami-Nejad, B.T. Edelson, S.M. Zurawski, B. Malissen, G. Zurawski, J. Berman, and D.H. Kaplan. 2011. Skin-resident murine dendritic cell subsets promote distinct and opposing antigen-specific T helper cell responses. *Immunity* 35:260-272.

Jabbar, I.A., G.J. Fernando, N. Saunders, A. Aldovini, R. Young, K. Malcolm, and I.H. Frazer. 2000. Immune responses induced by BCG recombinant for human papillomavirus L1 and E7 proteins. *Vaccine* 18:2444-2453.

Janssen, E.M., E.E. Lemmens, T. Wolfe, U. Christen, M.G. von Herrath, and S.P. Schoenberger. 2003. CD4+ T cells are required for secondary expansion and memory in CD8+ T lymphocytes. *Nature* 421:852-856.

Jeannin, P., B. Bottazzi, M. Sironi, A. Doni, M. Rusnati, M. Presta, V. Maina, G. Magistrelli, J.F. Haeuw, G. Hoeffel, N. Thieblemont, N. Corvaia, C. Garlanda, Y. Delneste, and A. Mantovani. 2005. Complexity and complementarity of outer membrane protein A recognition by cellular and humoral innate immunity receptors. *Immunity* 22:551-560.

Jego, G., A.K. Palucka, J.-P. Blanck, C. Chalouni, V. Pascual, and J. Banchereau. 2003. Plasmacytoid Dendritic Cells Induce Plasma Cell Differentiation through Type I Interferon and Interleukin 6. *Immunity* 19:225-234.

Jiang, W., W.J. Swiggard, C. Heufler, M. Peng, A. Mirza, R.M. Steinman, and M.C. Nussenzweig. 1995. The receptor DEC-205 expressed by dendritic cells and thymic epithelial cells is involved in antigen processing. *Nature* 375:151-155.

Jongbloed, S.L., A.J. Kassianos, K.J. McDonald, G.J. Clark, X. Ju, C.E. Angel, C.-J.J. Chen, P.R. Dunbar, R.B. Wadley, V. Jeet, A.J.E. Vulink, D.N.J. Hart, and K.J. Radford. 2010. Human CD141+ (BDCA-3)+ dendritic cells (DCs) represent a unique myeloid DC subset that cross-presents necrotic cell antigens. *The Journal of experimental medicine* 207:1247-1260.

Joo, H., D. Li, M. Dullaers, T.W. Kim, D. Duluc, K. Upchurch, Y. Xue, S. Zurawski, R. Le Grand, Y.J. Liu, M. Kuroda, G. Zurawski, and S. Oh. 2014. C-Type Lectin-like Receptor LOX-1 Promotes Dendritic Cell-Mediated Class-Switched B Cell Responses. *Immunity* 41:592-604.

Joo, H., K. Upchurch, W. Zhang, L. Ni, D. Li, Y. Xue, X.H. Li, T. Hori, S. Zurawski, Y.J. Liu, G. Zurawski, and S. Oh. 2015. Opposing Roles of Dectin-1 Expressed on Human Plasmacytoid Dendritic Cells and Myeloid Dendritic Cells in Th2 Polarization. *J Immunol* 195:1723-1731.

Jung, S., D. Unutmaz, P. Wong, G. Sano, K. De los Santos, T. Sparwasser, S. Wu, S. Vuthoori, K. Ko, F. Zavala, E.G. Pamer, D.R. Littman, and R.A. Lang. 2002. In vivo depletion of CD11c+ dendritic cells abrogates priming of CD8+ T cells by exogenous cell-associated antigens. *Immunity* 17:211-220.

Kanitakis, J., E. Morelon, P. Petruzzo, L. Badet, and J.M. Dubernard. 2011. Self-renewal capacity of human epidermal Langerhans cells: Observations made on a composite tissue allograft. *Experimental Dermatology* 20:145-146.

Karsunky, H., M. Merad, A. Cozzio, I.L. Weissman, and M.G. Manz. 2003. Flt3 Ligand Regulates Dendritic Cell Development from Flt3(+) Lymphoid and Myeloid-committed Progenitors to Flt3(+) Dendritic Cells In Vivo. *The Journal of experimental medicine* 198:305-313.

Kastenmuller, W., K. Kastenmuller, C. Kurts, and R.A. Seder. 2014. Dendritic cell-targeted vaccines--hope or hype? *Nature reviews. Immunology* 14:705-711.

Kenter, G.G., M.J. Welters, A.R. Valentijn, M.J. Lowik, D.M. Berends-van der Meer, A.P. Vloon, J.W. Drijfhout, A.R. Wafelman, J. Oostendorp, G.J. Fleuren, R. Offringa, S.H. van der Burg, and C.J. Melief. 2008. Phase I immunotherapeutic trial with long peptides spanning the E6 and E7 sequences of high-risk human papillomavirus 16 in end-stage cervical cancer patients shows low toxicity and robust immunogenicity. *Clin Cancer Res* 14:169-177.

Kenter, G.G., M.J. Welters, A.R. Valentijn, M.J. Lowik, D.M. Berends-van der Meer, A.P. Vloon, F. Essahsah, L.M. Fathers, R. Offringa, J.W. Drijfhout, A.R. Wafelman, J. Oostendorp, G.J. Fleuren, S.H. van der Burg, and C.J. Melief. 2009. Vaccination against HPV-16 oncoproteins for vulvar intraepithelial neoplasia. *N Engl J Med* 361:1838-1847.

Kinnebrew, M.A., C.G. Buffie, G.E. Diehl, L.A. Zenewicz, I. Leiner, T.M. Hohl, R.A. Flavell, D.R. Littman, and E.G. Pamer. 2012. Interleukin 23 production by intestinal CD103(+)CD11b(+) dendritic cells in response to bacterial flagellin enhances mucosal innate immune defense. *Immunity* 36:276-287.

Klechevsky, E., A.L. Flamar, Y. Cao, J.P. Blanck, M. Liu, A. O'Bar, O. Agouna-Deciat, P. Klucar, L. Thompson-Snipes, S. Zurawski, Y. Reiter, A.K. Palucka, G. Zurawski, and J. Banchereau. 2010. Cross-priming CD8+ T cells by targeting antigens to human dendritic cells through DCIR. *Blood* 116:1685-1697.

Klechevsky, E., R. Morita, M. Liu, Y. Cao, S. Coquery, L. Thompson-Snipes, F. Briere, D. Chaussabel, G. Zurawski, A.K. Palucka, Y. Reiter, J. Banchereau, and H. Ueno. 2008. Functional Specializations of Human Epidermal Langerhans Cells and CD14+ Dermal Dendritic Cells. *Immunity* 29:497-510.

Klyushnenkova, E.N., D.V. Kouiavskaia, C.J. Parkins, P. Caposio, S. Botto, R.B. Alexander, and M.A. Jarvis. 2012. A cytomegalovirus-based vaccine expressing a single tumor-specific CD8+ T-cell epitope delays tumor growth in a murine model of prostate cancer. *Journal of immunotherapy (Hagerstown, Md. : 1997)* 35:390-399.

Kreimer, A.R., G.M. Clifford, P. Boyle, and S. Franceschi. 2005. Human papillomavirus types in head and neck squamous cell carcinomas worldwide: a systematic review. *Cancer epidemiology, biomarkers & prevention : a publication of the American Association for Cancer Research, cosponsored by the American Society of Preventive Oncology* 14:467-475.

Krug, A., A. Towarowski, S. Britsch, S. Rothenfusser, V. Hornung, R. Bals, T. Giese, H. Engelmann, S. Endres, A.M. Krieg, and G. Hartmann. 2001. Toll-like receptor expression reveals CpG DNA as a unique microbial stimulus for plasmacytoid dendritic cells which synergizes with CD40 ligand to induce high amounts of IL-12. *European journal of immunology* 31:3026-3037.

Lahoud, M.H., A.I. Proietto, F. Ahmet, S. Kitsoulis, L. Eidsmo, L. Wu, P. Sathe, S. Pietersz, H.W. Chang, I.D. Walker, E. Maraskovsky, H. Braley, A.M. Lew, M.D. Wright, W.R. Heath, K. Shortman, and I. Caminschi. 2009. The C-type lectin Clec12A present on mouse and human dendritic cells can serve as a target for antigen delivery and enhancement of antibody responses. *Journal of immunology (Baltimore, Md. : 1950)* 182:7587-7594.

Le, D.T., J.N. Uram, H. Wang, B.R. Bartlett, H. Kemberling, A.D. Eyring, A.D. Skora, B.S. Luber, N.S. Azad, D. Laheru, B. Biedrzycki, R.C. Donehower, A. Zaheer, G.A. Fisher, T.S. Crocenzi, J.J. Lee, S.M. Duffy, R.M. Goldberg, A. de la Chapelle, M. Koshiji, F. Bhaijee, T. Huebner, R.H. Hruban, L.D. Wood, N. Cuka, D.M. Pardoll, N. Papadopoulos, K.W. Kinzler, S. Zhou, T.C. Cornish, J.M. Taube, R.A. Anders, J.R. Eshleman, B. Vogelstein, and L.A. Diaz, Jr. 2015. PD-1 Blockade in Tumors with Mismatch-Repair Deficiency. *The New England journal of medicine* 372:2509-2520.

Lee, L.Y., L.A. Ha do, C. Simmons, M.D. de Jong, N.V. Chau, R. Schumacher, Y.C. Peng, A.J. McMichael, J.J. Farrar, G.L. Smith, A.R. Townsend, B.A. Askonas, S. Rowland-Jones, and T. Dong. 2008. Memory T cells established by seasonal human influenza A infection cross-react with avian influenza A (H5N1) in healthy individuals. *J Clin Invest* 118:3478-3490.

LeibundGut-Landmann, S., O. Gross, M.J. Robinson, F. Osorio, E.C. Slack, S.V. Tsoni, E. Schweighoffer, V. Tybulewicz, G.D. Brown, J. Ruland, and C. Reis e Sousa. 2007. Syk- and CARD9-dependent coupling of innate immunity to the induction of T helper cells that produce interleukin 17. *Nat Immunol* 8:630-638.

Lemke, C.D., J.B. Graham, D.M. Lubaroff, and A.K. Salem. 2011. Development of an MHC class I L(d)-restricted PSA peptide-loaded tetramer for detection of PSA-specific CD8+ T cells in the mouse. *Prostate cancer and prostatic diseases* 14:118-121.

Lewis, K.L., M.L. Caton, M. Bogunovic, M. Greter, L.T. Grajkowska, D. Ng, A. Klinakis, I.F. Charo, S. Jung, J.L. Gommerman, Ivanov, II, K. Liu, M. Merad, and B. Reizis. 2011. Notch2 receptor signaling controls functional differentiation of dendritic cells in the spleen and intestine. *Immunity* 35:780-791.

Li, D., G. Romain, A.L. Flamar, D. Duluc, M. Dullaers, X.H. Li, S. Zurawski, N. Bosquet, A.K. Palucka, R. Le Grand, A. O'Garra, G. Zurawski, J. Banchereau, and S. Oh. 2012. Targeting self- and foreign antigens to dendritic cells via DC-ASGPR generates IL-10-producing suppressive CD4+ T cells. *The Journal of experimental medicine* 209:109-121.

Lin, C.W., J.Y. Lee, Y.P. Tsao, C.P. Shen, H.C. Lai, and S.L. Chen. 2002. Oral vaccination with recombinant Listeria monocytogenes expressing human papillomavirus type 16 E7 can cause tumor growth in mice to regress. *Int J Cancer* 102:629-637.

Lin, K., E. Roosinovich, B. Ma, C.F. Hung, and T.C. Wu. 2010. Therapeutic HPV DNA vaccines. *Immunol Res* 47:86-112.

Lote, H., C. Cafferkey, and I. Chau. 2015. PD-1 and PD-L1 blockade in gastrointestinal malignancies. *Cancer treatment reviews*

Lundberg, K., A.-S. Albrekt, I. Nelissen, S. Santegoets, T.D. de Gruijl, S. Gibbs, and M. Lindstedt. 2013. Transcriptional Profiling of Human Dendritic Cell Populations and Models - Unique Profiles of In Vitro Dendritic Cells and Implications on Functionality and Applicability. *PLoS ONE* 8:e52875.

Maciag, P.C., S. Radulovic, and J. Rothman. 2009. The first clinical use of a live-attenuated Listeria monocytogenes vaccine: a Phase I safety study of Lm-LLO-E7 in patients with advanced carcinoma of the cervix. *Vaccine* 27:3975-3983.

Mashayekhi, M., M.M. Sandau, I.R. Dunay, E.M. Frickel, A. Khan, R.S. Goldszmid, A. Sher, H.L. Ploegh, T.L. Murphy, L.D. Sibley, and K.M. Murphy. 2011. CD8α+ Dendritic Cells Are the Critical Source of Interleukin-12 that Controls Acute Infection by Toxoplasma gondii Tachyzoites. *Immunity* 35:249-259.

Matthews, K., N.P.Y. Chung, P.J. Klasse, J.P. Moore, and R.W. Sanders. 2012. Potent induction of antibody-secreting B cells by human dermal-derived CD14+ dendritic cells triggered by dual TLR ligation. *Journal of Immunology* 189:5729-5744.

McGovern, N., A. Schlitzer, M. Gunawan, L. Jardine, A. Shin, E. Poyner, K. Green, R. Dickinson, X.-n. Wang, D. Low, K. Best, S. Covins, P. Milne, S. Pagan, K. Aljefri, M. Windebank, D. Miranda-Saavedra, A. Larbi, Pavandip S. Wasan, K. Duan, M. Poidinger, V. Bigley, F. Ginhoux, M. Collin, and M. Haniffa. 2014. Human Dermal CD14+ Cells Are a Transient Population of Monocyte-Derived Macrophages. *Immunity* 41:465-477.

McMichael, A.J., C.A. Michie, F.M. Gotch, G.L. Smith, and B. Moss. 1986. Recognition of influenza A virus nucleoprotein by human cytotoxic T lymphocytes. *J Gen Virol* 67 (Pt 4):719-726.

Merad, M., F. Ginhoux, and M. Collin. 2008. Origin, homeostasis and function of Langerhans cells and other langerin-expressing dendritic cells. *Nature reviews. Immunology* 8:935-947.

Merad, M., P. Sathe, J. Helft, J. Miller, and A. Mortha. 2013. The dendritic cell lineage: Ontogeny and function of dendritic cells and their subsets in the steady state and the inflamed setting. In Annual review of immunology. 563-604.

Mestas, J., and C.C.W. Hughes. 2004. Of Mice and Not Men: Differences between Mouse and Human Immunology. *The Journal of Immunology* 172:2731-2738.

Meyer-Wentrup, F., D. Benitez-Ribas, P.J. Tacken, C.J. Punt, C.G. Figdor, I.J. de Vries, and G.J. Adema. 2008. Targeting DCIR on human plasmacytoid dendritic cells results in antigen presentation and inhibits IFN-alpha production. *Blood* 111:4245-4253.

Miller, J.C., B.D. Brown, T. Shay, E.L. Gautier, V. Jojic, A. Cohain, G. Pandey, M. Leboeuf, K.G. Elpek, J. Helft, D. Hashimoto, A. Chow, J. Price, M. Greter, M. Bogunovic, A. Bellemare-Pelletier, P.S. Frenette, G.J. Randolph, S.J. Turley, and M. Merad. 2012. Deciphering the transcriptional network of the dendritic cell lineage. *Nature immunology* 13:888-899.

Munger, K., M. Scheffner, J.M. Huibregtse, and P.M. Howley. 1992. Interactions of HPV E6 and E7 oncoproteins with tumour suppressor gene products. *Cancer surveys* 12:197-217.

Nakajima, S., B.Z. Igyarto, T. Honda, G. Egawa, A. Otsuka, M. Hara-Chikuma, N. Watanabe, S.F. Ziegler, M. Tomura, K. Inaba, Y. Miyachi, D.H. Kaplan, and K. Kabashima. 2012. Langerhans cells are critical in epicutaneous sensitization with protein antigen via thymic stromal lymphopoietin receptor signaling. *The Journal of allergy and clinical immunology* 129:1048-1055.e1046.

National Cancer Institute. 2015. SEER Cancer Statistics Factsheets: Prostate Cancer. In Bethesda, MD.

Newall, A.T., J.M. Brotherton, H.E. Quinn, P.B. McIntyre, J. Backhouse, L. Gilbert, M.T. Esser, J. Erick, J. Bryan, N. Formica, and C.R. MacIntyre. 2008. Population seroprevalence of human papillomavirus types 6, 11, 16, and 18 in men, women, and children in Australia. *Clin Infect Dis* 46:1647-1655.

Ni, L., I. Gayet, S. Zurawski, D. Duluc, A.L. Flamar, X.H. Li, A. O'Bar, S. Clayton, A.K. Palucka, G. Zurawski, J. Banchereau, and S. Oh. 2010. Concomitant activation and antigen uptake via human dectin-1 results in potent antigen-specific CD8+ T cell responses. *Journal of immunology (Baltimore, Md. : 1950)* 185:3504-3513.

Nizzoli, G., J. Krietsch, A. Weick, S. Steinfelder, F. Facciotti, P. Gruarin, A. Bianco, B. Steckel, M. Moro, M. Crosti, C. Romagnani, K. Stölzel, S. Torretta, L. Pignataro, C. Scheibenbogen, P. Neddermann, R. De Francesco, S. Abrignani, and J. Geginat. 2013. Human CD1c+ dendritic cells secrete high levels of IL-12 and potently prime cytotoxic T-cell responses. 932-942 pp.

Ohl, L., M. Mohaupt, N. Czeloth, G. Hintzen, Z. Kiafard, J. Zwirner, T. Blankenstein, G. Henning, and R. Förster. 2004. CCR7 Governs Skin Dendritic Cell Migration under Inflammatory and Steady-State Conditions. *Immunity* 21:279-288.

Palucka, K., and J. Banchereau. 2012. Cancer immunotherapy via dendritic cells. *Nature reviews. Cancer* 12:265-277.

Penel-Sotirakis, K., E. Simonazzi, J. Péguet-Navarro, and A. Rozières. 2012. Differential Capacity of Human Skin Dendritic Cells to Polarize CD4⁺T Cells into IL-17, IL-21 and IL-22 Producing Cells. *PLoS ONE* 7:e45680.

Peng, S., S. Lyford-Pike, B. Akpeng, A. Wu, C.F. Hung, D. Hannaman, J.R. Saunders, T.C. Wu, and S.I. Pai. 2013. Low-dose cyclophosphamide administered as daily or single dose enhances the antitumor effects of a therapeutic HPV vaccine. *Cancer Immunol Immunother* 62:171-182.

Persson, C.M., and B.J. Chambers. 2010. Plasmacytoid dendritic cell-induced migration and activation of NK cells in vivo. *European journal of immunology* 40:2155-2164.

Plantinga, M., M. Guilliams, M. Vanheerswynghels, K. Deswarte, F. Branco-Madeira, W. Toussaint, L. Vanhoutte, K. Neyt, N. Killeen, B. Malissen, H. Hammad, and B. Lambrecht. 2013. Conventional and Monocyte-Derived CD11b+ Dendritic Cells Initiate and Maintain T Helper 2 Cell-Mediated Immunity to House Dust Mite Allergen. *Immunity* 38:322-335.

Quinn, K.M., A. Yamamoto, A. Costa, P.A. Darrah, R.W. Lindsay, S.T. Hegde, T.R. Johnson, B.J. Flynn, K. Lore, and R.A. Seder. 2013. Coadministration of polyinosinic:polycytidylic acid and immunostimulatory complexes modifies antigen processing in dendritic cell subsets and enhances HIV gag-specific T cell immunity. *Journal of immunology (Baltimore, Md. : 1950)* 191:5085-5096.

Reddy, M.P., C.A. Kinney, M.A. Chaikin, A. Payne, J. Fishman-Lobell, P. Tsui, P.R. Dal Monte, M.L. Doyle, M.R. Brigham-Burke, D. Anderson, M. Reff, R. Newman, N. Hanna, R.W. Sweet, and A. Truneh. 2000. Elimination of Fc receptor-dependent effector functions of a modified IgG4 monoclonal antibody to human CD4. *Journal of immunology (Baltimore, Md. : 1950)* 164:1925-1933.

Reis e Sousa, C. 2006. Dendritic cells in a mature age. *Nature reviews. Immunology* 6:476-483.

Reuter, A., S.E. Panozza, C. Macri, C. Dumont, J. Li, H. Liu, E. Segura, J. Vega-Ramos, N. Gupta, I. Caminschi, J.A. Villadangos, A.P. Johnston, and J.D. Mintern. 2015. Criteria for dendritic cell receptor selection for efficient antibody-targeted vaccination. *J Immunol* 194:2696-2705.

Rydnert, F., K. Lundberg, L. Greiff, and M. Lindstedt. 2014. Circulating CD1c+ DCs are superior at activating Th2 responses upon Phl p stimulation compared with basophils and pDCs. *Immunol Cell Biol* 92:557-560.

Sancho, D., D. Mourao-Sa, O.P. Joffre, O. Schulz, N.C. Rogers, D.J. Pennington, J.R. Carlyle, and C. Reis e Sousa. 2008. Tumor therapy in mice via antigen targeting to a novel, DC-restricted C-type lectin. *The Journal of clinical investigation* 118:2098-2110.

Sanderson, R.J., and J.A. Ironside. 2002. Squamous cell carcinomas of the head and neck. *BMJ (Clinical research ed.)* 325:822-827.

Sangro, B., C. Gomez-Martin, M. de la Mata, M. Inarrairaegui, E. Garralda, P. Barrera, J.I. Riezu-Boj, E. Larrea, C. Alfaro, P. Sarobe, J.J. Lasarte, J.L. Perez-Gracia, I. Melero, and J. Prieto. 2013. A clinical trial of CTLA-4 blockade with tremelimumab in patients with hepatocellular carcinoma and chronic hepatitis C. *Journal of hepatology* 59:81-88.

Santegoets, S.J.A.M., S. Gibbs, K. Kroeze, R. van de Ven, R.J. Scheper, C.A. Borrebaeck, T.D. de Gruijl, and M. Lindstedt. 2008. Transcriptional profiling of human skin-resident Langerhans cells and CD1a+ dermal dendritic cells: differential activation states suggest distinct functions. *Journal of Leukocyte Biology* 84:143-151.

Schiller, J.T., X. Castellsague, L.L. Villa, and A. Hildesheim. 2008. An update of prophylactic human papillomavirus L1 virus-like particle vaccine clinical trial results. *Vaccine* 26 Suppl 10:K53-61.

Schlitzer, A., and F. Ginhoux. 2014. Organization of the mouse and human DC network. *Current opinion in immunology* 26:90-99.

Schlitzer, A., N. McGovern, P. Teo, T. Zelante, K. Atarashi, D. Low, A. Ho, P. See, A. Shin, P. Wasan, G. Hoeffel, B. Malleret, A. Heiseke, S. Chew, L. Jardine, H. Purvis, C. Hilkens, J. Tam, M. Poidinger, E. Stanley, A. Krug, L. Renia, B. Sivasankar, L. Ng, M. Collin, P. Ricciardi-Castagnoli, K. Honda, M. Haniffa, and F. Ginhoux. 2013. IRF4 Transcription Factor-Dependent CD11b+ Dendritic Cells in Human and Mouse Control Mucosal IL-17 Cytokine Responses. *Immunity* 38:970-983.

Schulz, O., S.S. Diebold, M. Chen, T.I. Naslund, M.A. Nolte, L. Alexopoulou, Y.T. Azuma, R.A. Flavell, P. Liljestrom, and C. Reis e Sousa. 2005. Toll-like receptor 3 promotes cross-priming to virus-infected cells. *Nature* 433:887-892.

Segura, E., J. Valladeau-Guilemond, M.H. Donnadieu, X. Sastre-Garau, V. Soumelis, and S. Amigorena. 2012. Characterization of resident and migratory dendritic cells in human lymph nodes. *Journal of Experimental Medicine* 209:653-660.

Segura, E., and J.A. Villadangos. 2009. Antigen presentation by dendritic cells in vivo. *Current opinion in immunology* 21:105-110.

Seneschal, J., R.A. Clark, A. Gehad, C.M. Baecher-Allan, and T.S. Kupper. 2012. Human epidermal Langerhans cells maintain immune homeostasis in skin by activating skin resident regulatory T cells. *Immunity* 36:873-884.

Siegal, F.P., N. Kadowaki, M. Shodell, P.A. Fitzgerald-Bocarsly, K. Shah, S. Ho, S. Antonenko, and Y.J. Liu. 1999. The nature of the principal type 1 interferon-producing cells in human blood. *Science (New York, N.Y.)* 284:1835-1837.

Silk, K.M., J.D. Silk, N. Ichiryu, T.J. Davies, K.F. Nolan, A.J. Leishman, L. Carpenter, S.M. Watt, V. Cerundolo, and P.J. Fairchild. 2012. Cross-presentation of tumour antigens by human induced pluripotent stem cell-derived CD141(+)XCR1+ dendritic cells. *Gene therapy* 19:1035-1040.

Skinner, J.A., S.M. Zurawski, C. Sugimoto, H. Vinet-Oliphant, P. Vinod, Y. Xue, K. Russel-Lodrigue, R.A. Albrecht, A. Garcia-Sastre, A.M. Salazar, C.J. Roy, M.J. Kuroda, S. Oh, and G. Zurawski. 2014. Immunologic Characterization of a Rhesus Macaque H1N1 Challenge Model for Candidate Influenza Vaccine Assessment. *Clin Vaccine Immunol*

Small, E.J., P.F. Schellhammer, C.S. Higano, C.H. Redfern, J.J. Nemunaitis, F.H. Valone, S.S. Verjee, L.A. Jones, and R.M. Hershberg. 2006. Placebo-controlled phase III trial of immunologic therapy with sipuleucel-T (APC8015) in patients with metastatic, asymptomatic hormone refractory prostate cancer. *Journal of clinical oncology : official journal of the American Society of Clinical Oncology* 24:3089-3094.

Stanley, M. 2008. Immunobiology of HPV and HPV vaccines. *Gynecol Oncol* 109:S15-21.

Stein, A.P., S. Saha, J.L. Kraninger, A.D. Swick, M. Yu, P.F. Lambert, and R.J. Kimple. 2015. Prevalence of Human Papillomavirus in Oropharyngeal Cancer: A Systematic Review. *Cancer journal (Sudbury, Mass.)* 21:138-146.

Steinman, R.M., and M.C. Nussenzweig. 2002. Avoiding horror autotoxicus: the importance of dendritic cells in peripheral T cell tolerance. *Proceedings of the National Academy of Sciences of the United States of America* 99:351-358.

Steller, M.A., K.J. Gurski, M. Murakami, R.W. Daniel, K.V. Shah, E. Celis, A. Sette, E.L. Trimble, R.C. Park, and F.M. Marincola. 1998. Cell-mediated immunological responses in cervical and vaginal cancer patients immunized with a lipidated epitope of human papillomavirus type 16 E7. *Clin Cancer Res* 4:2103-2109.

Tacken, P.J., I.J. de Vries, K. Gijzen, B. Joosten, D. Wu, R.P. Rother, S.J. Faas, C.J. Punt, R. Torensma, G.J. Adema, and C.G. Figdor. 2005. Effective induction of naive and recall T-cell responses by targeting antigen to human dendritic cells via a humanized anti-DC-SIGN antibody. *Blood* 106:1278-1285.

Tacken, P.J., I.J. de Vries, R. Torensma, and C.G. Figdor. 2007. Dendritic-cell immunotherapy: from ex vivo loading to in vivo targeting. *Nature reviews. Immunology* 7:790-802.

Tacken, P.J., W. Ginter, L. Berod, L.J. Cruz, B. Joosten, T. Sparwasser, C.G. Figdor, and A. Cambi. 2011. Targeting DC-SIGN via its neck region leads to prolonged antigen residence in early endosomes, delayed lysosomal degradation, and cross-presentation. *Blood* 118:4111-4119.

Thara, E., T.B. Dorff, J.K. Pinski, and D.I. Quinn. 2011. Vaccine therapy with sipuleucel-T (Provenge) for prostate cancer. *Maturitas* 69:296-303.

Thompson, E.A., F. Liang, G. Lindgren, K.J. Sandgren, K.M. Quinn, P.A. Darrah, R.A. Koup, R.A. Seder, R.M. Kedl, and K. Loré. 2015. Human Anti-CD40 Antibody and Poly IC:LC Adjuvant Combination Induces Potent T Cell Responses in the Lung of Nonhuman Primates. *The Journal of Immunology* 195:1015-1024.

Tommasino, M., and L. Crawford. 1995. Human papillomavirus E6 and E7: proteins which deregulate the cell cycle. *BioEssays : news and reviews in molecular, cellular and developmental biology* 17:509-518.

Townsend, A.R., and J.J. Skehel. 1982. Influenza A specific cytotoxic T-cell clones that do not recognize viral glycoproteins. *Nature* 300:655-657.

Tsuji, T., J. Matsuzaki, M.P. Kelly, V. Ramakrishna, L. Vitale, L.Z. He, T. Keler, K. Odunsi, L.J. Old, G. Ritter, and S. Gnjatic. 2011. Antibody-targeted NY-ESO-1 to mannose receptor or DEC-205 in vitro elicits dual human CD8+ and CD4+ T cell responses with broad antigen specificity. *Journal of immunology (Baltimore, Md. : 1950)* 186:1218-1227.

U.S. FDA. 2006. Approval Letter - Human Papillomavirus Quadrivalent (Types 6, 11, 16, 18) Vaccine, Recombinant. In U.S. FDA.

U.S. FDA. 2009. Approval Letter - Cervarix. In U.S. FDA.

Valladeau, J., V. Duvert-Frances, J.-J. Pin, C. Dezutter-Dambuyant, C. Vincent, C. Massacrier, J. Vincent, K. Yoneda, J. Banchereau, C. Caux, J. Davoust, and S. Saeland. 1999. The monoclonal antibody DCGM4 recognizes Langerin, a protein specific of Langerhans cells, and is rapidly internalized from the cell surface. *European journal of immunology* 29:2695-2704.

Villadangos, J.A., and K. Shortman. 2010. Found in translation: the human equivalent of mouse CD8(+) dendritic cells. *The Journal of experimental medicine* 207:1131-1134.

Villadangos, J.A., and L. Young. 2008. Antigen-presentation properties of plasmacytoid dendritic cells. *Immunity* 29:352-361.

Ville, S., N. Poirier, G. Blancho, and B. Vanhove. 2015. Co-Stimulatory Blockade of the CD28/CD80-86/CTLA-4 Balance in Transplantation: Impact on Memory T Cells? *Front Immunol* 6:411.

Voskens, C.J., D. Sewell, R. Hertzano, J. DeSanto, S. Rollins, M. Lee, R. Taylor, J. Wolf, M. Suntharalingam, B. Gastman, J.C. Papadimitriou, C. Lu, M. Tan, R. Morales, K. Cullen, E. Celis, D. Mann, and S.E. Strome. 2012. Induction of MAGE-A3 and HPV-16 immunity by Trojan vaccines in patients with head and neck carcinoma. *Head & neck* 34:1734-1746.

Walboomers, J.M., M.V. Jacobs, M.M. Manos, F.X. Bosch, J.A. Kummer, K.V. Shah, P.J. Snijders, J. Peto, C.J. Meijer, and N. Munoz. 1999. Human papillomavirus is a necessary cause of invasive cervical cancer worldwide. *The Journal of pathology* 189:12-19.

Weck, M.M., S. Appel, D. Werth, C. Sinzger, A. Bringmann, F. Grunebach, and P. Brossart. 2008. hDectin-1 is involved in uptake and cross-presentation of cellular antigens. *Blood* 111:4264-4272.

Welters, M.J., G.G. Kenter, S.J. Piersma, A.P. Vloon, M.J. Lowik, D.M. Berends-van der Meer, J.W. Drijfhout, A.R. Valentijn, A.R. Wafelman, J. Oostendorp, G.J. Fleuren, R. Offringa, C.J. Melief, and S.H. van der Burg. 2008. Induction of tumor-specific CD4+ and CD8+ T-cell immunity in cervical cancer patients by a human papillomavirus type 16 E6 and E7 long peptides vaccine. *Clin Cancer Res* 14:178-187.

Witz, I.P. 2009. The Tumor Microenvironment: The Making of a Paradigm. *Cancer Microenvironment* 2:9-17.

Woodman, C.B., S. Collins, H. Winter, A. Bailey, J. Ellis, P. Prior, M. Yates, T.P. Rollason, and L.S. Young. 2001. Natural history of cervical human papillomavirus infection in young women: a longitudinal cohort study. *Lancet* 357:1831-1836.

Yee, C., J.A. Thompson, D. Byrd, S.R. Riddell, P. Roche, E. Celis, and P.D. Greenberg. 2002. Adoptive T cell therapy using antigen-specific CD8(+) T cell clones for the treatment of patients with metastatic melanoma: In vivo persistence, migration, and antitumor effect of transferred T cells. *Proceedings of the National Academy of Sciences of the United States of America* 99:16168-16173.

Young, D., C.C. Xiao, B. Murphy, M. Moore, C. Fakhry, and T.A. Day. 2015. Increase in head and neck cancer in younger patients due to human papillomavirus (HPV). *Oral oncology*

Yu, Chun I., C. Becker, Y. Wang, F. Marches, J. Helft, M. Leboeuf, E. Anguiano, S. Pourpe, K. Goller, V. Pascual, J. Banchereau, M. Merad, and K. Palucka. 2013. Human CD1c+ Dendritic Cells Drive the Differentiation of CD103+ CD8+ Mucosal Effector T Cells via the Cytokine TGF-β. *Immunity* 38:818-830.

Zehner, M., A.I. Chasan, V. Schuette, M. Embgenbroich, T. Quast, W. Kolanus, and S. Burgdorf. 2011. Mannose receptor polyubiquitination regulates endosomal recruitment of p97 and cytosolic antigen translocation for cross-presentation. *Proceedings of the National Academy of Sciences of the United States of America* 108:9933-9938.

Zelenay, S., A.M. Keller, P.G. Whitney, B.U. Schraml, S. Deddouche, N.C. Rogers, O. Schulz, D. Sancho, and C. Reis E Sousa. 2012. The dendritic cell receptor DNGR-1 controls endocytic handling of necrotic cell antigens to favor cross-priming of CTLs in virus-infected mice. *Journal of Clinical Investigation* 122:1615-1627.